

AD-A021 266

AN ENERGY METHOD FOR PREDICTION OF HELICOPTER
MANEUVERABILITY

T. L. Wood, et al

Bell Helicopter Company
Fort Worth, Texas

December 1971

DISTRIBUTED BY:

NTIS

National Technical Information Service
U. S. DEPARTMENT OF COMMERCE

065083

1

ADA021266

An Energy Method For Prediction Of Helicopter Maneuverability

REPORT 299-099-557

December 1971

DDC
RECEIVED
JAN 21 1976
A



BELL
HELICOPTER COMPANY

POST OFFICE BOX 482 • FORT WORTH TEXAS 76101 A **Textron** COMPANY

APPROVED FOR PUBLIC RELEASE; DISTRIBUTION UNLIMITED

Reproduced by
NATIONAL TECHNICAL
INFORMATION SERVICE

U S Department of Commerce
Springfield VA 22151

114



BELL HELICOPTER COMPANY

POST OFFICE BOX 482 • FORT WORTH TEXAS 76101

A DIVISION OF BELL AEROSPACE CORPORATION A  COMPANY

TECHNICAL DATA

BY T. L. Wood / C. L. Livingston DATE 1/6/72
CHECKED C. L. Livingston DATE 1/6/72
APPROVED J. M. Drees DATE 1/8/72
APPROVED R. L. Stuart DATE 1/8/72

MODEL

NO. OF PAGES 111

REPORT NO. 299-099-557 ' DATE 12/28/71

TITLE AN ENERGY METHOD FOR PREDICTION
OF HELICOPTER MANEUVERABILITY

PREPARED UNDER
CONTRACT F33615-70-C-1052

REPORT SEQUENCE NUMBER

PERIOD COVERED

DDC
RECEIVED
JAN 21 1972
A

Approved for Release by NSA
Distribution Unlimited

SUMMARY

In response to Phase III of Contract F33615-70-C-1052, the necessary methodology has been developed to provide an independent analysis capability to Air Force Studies Analysis (AFSA) for accurately simulating the flight paths of single main rotor helicopters. The equations developed under Phase I of this contract have been generalized to represent other single main rotor helicopters that are currently operational and those designed for the near future.

This report reviews the necessary equations for the determination of power required in accelerated flight and a method for determining the input coefficients based on the helicopter's physical parameters and power required in one g flight. The impact of the type of rotor system on the maximum thrust which can be produced is examined in light of the available flight test data. The concepts of energy maneuverability for a helicopter are examined using the AH-1G helicopter as an example. Several applications of these equations are considered including terrain following, decelerating turns, and low speed maneuvering.

DATE		PAGE	
1		1	

TABLE OF CONTENTS

	Page
LIST OF FIGURES	iv
LIST OF TABLES	vii
NOMENCLATURE	viii
INTRODUCTION	1
ENERGY MANEUVERABILITY	2
Concepts	2
Energy Diagram	6
Maneuver Diagram	6
DERIVATION OF EQUATIONS	15
Technical Approach	15
Power Equation - Pure Helicopter	15
Power Equation - Compound Helicopter	20
Acceleration and Deceleration	25
Alpha Equation - Pure Helicopter	27
Alpha Equation - Compound Helicopter	29
Maneuverability Limits	31
Simplified Maximum Thrust Model	38
DETERMINATION OF INPUT COEFFICIENTS	42
Sensitivity of Parameters	42
Methodology	50
Results	55
Example Problem	55
APPLICATIONS	66
Terrain Following	66
Decelerating Turns	66



BELL HELICOPTER COMPANY

TABLE OF CONTENTS

	Page
Low Speed Maneuvering	69
Survivability	76
Flight Test	81
RECOMMENDATIONS	82
REFERENCES	83
APPENDIX A	85
APPENDIX B	93
APPENDIX C	98

LIST OF FIGURES

No.	Page
1. Bank Angle Versus Normal Load Factor for AH-1G Helicopter	4
2. Comparison of Theory and Flight Test Data for Bank Angle versus Normal Load Factor	5
3. Energy Diagram for AH-1G Helicopter at 7500 Pounds and 1 g	7
4. Energy Diagram for AH-1G Helicopter at 9000 Pounds and 1 g	8
5. Energy Diagram for AH-1G Helicopter at 9000 Pounds and 1.5 g	9
6. Maneuver Diagram for AH-1G Helicopter at 7500 Pounds and 2000 Feet	11
7. Maneuver Diagram for AH-1G Helicopter at 9000 Pounds and 2000 Feet	12
8. Normal Acceleration versus Velocity for AH-1G Helicopter at 7500 Pounds	13
9. Normal Acceleration versus Velocity for AH-1G Helicopter at 9000 Pounds	14
10. Wing Lift versus Normal Acceleration at 17000 Pounds and Sea Level	19
11. Minimum Equivalent Power Required in Maneuvering Flight for the AH-1G Helicopter	21
12. Equivalent Flat-Plate Drag Area versus True Airspeed	23
13. Acceleration Performance for AH-1G Helicopter	26
14. Deceleration Performance for AH-1G Helicopter	28
15. Fuselage Angle of Attack versus True Airspeed for Symmetrical Pullups and Pushovers at 7500 Pounds and Sea Level	30
16. Rotor Thrust Limits for HH-2C Helicopter	33
17. Rotor Thrust Limits for CH-3C Helicopter	34
18. Rotor Thrust Limits for CH-53A Helicopter	35

LIST OF FIGURES

No.	Page
19. Rotor Thrust Limits for OH-6A Helicopter	36
20. Rotor Thrust Capability for AH-1G/J Helicopter	37
21. Analytical Model for Maximum Rotor Thrust	39
22. Maximum Thrust Predicted by Simplified Analytical Model for AH-1J Helicopter	40
23. Maximum Thrust Predicted by Simplified Analytical Model for CH-3C Helicopter	41
24. Variation of Parasite Power with True Airspeed and Fuselage Drag, f	43
25. Variation of Profile Power with True Airspeed and Blade Profile Drag, t_0	44
26. Variation of Profile Power with True Airspeed and Blade Profile Drag, t_2	46
27. Variation of Induced Power with True Airspeed and Weighting Factor, K_1	47
28. Variation of Compressibility Power with True Airspeed and Critical Mach Number	48
29. Stall Power versus Δt_c	49
30. Flow Diagram of Input Program	51
31. Typical Values of K_3 and K_6 for Various Helicopters	53
32. Divergent Rotor Thrust Coefficient versus Advance Ratio	54
33. Level Flight Performance for OH-58A Helicopter	58
34. Level Flight Performance for OH-6A Helicopter	59
35. Level Flight Performance for YUH-1H Helicopter	60
36. Level Flight Performance for CH-3C Helicopter	61
37. Level Flight Performance for HH-53C Helicopter	62
38. Level Flight Performance for AH-1G Helicopter	63

LIST OF FIGURES

No.		Page
39.	Example of Input and Output from Input Coefficient Program	64
40.	Pilot Logic for Terrain Following Model	67
41.	Terrain Following Flight Profile	68
42.	180-Degree Turning Performance for the AH-1G Helicopter	70
43.	Thrust Vectoring for Linear Acceleration	71
44.	Power Required in Accelerated Flight	73
45.	Linear Acceleration Produced by Excess Power	74
46.	Approximate Combined Normal and Linear Acceleration Capability	75
47.	Technique for Matching Power and Geometric Constraints	77
48.	Normal and Linear Acceleration Capability	78
49.	Effect of Speed on Normal and Linear Acceleration at Constant Power	79
50.	Constant Energy Acceleration Capability from Hover to Maximum Speed	80



BELL HELICOPTER COMPANY

LIST OF TABLES

	Page
I. Dimensional Data for Various Helicopters	56
II. Input Coefficients for Various Helicopters	57

NOMENCLATURE

Symbol		Unit
A	Disk area (πR^2)	ft ²
A _w	Wing area	ft ²
a	Blade section lift curve slope	/rad
a _w	Wing lift curve slope	/rad
b	Number of blades or wing span	-- or ft
C _T	Thrust coefficient $[T/A(\pi R)^2]$	--
C _p	Power coefficient $[P/A(\pi R)^3]$	--
c	Rotor chord	ft
D	Parasite drag ($0.5\rho V^2$)	lb
E	Total aircraft energy ($GW h + 0.5mV^2 + 0.5I \dot{\theta}^2$)	ft - lb
E _s	Specific aircraft energy ($h + V^2/2g$)	ft
e	Wing efficiency factor	--
f	Equivalent flat-plate drag area ($C_D = 1.0$ so that drag = $0.5cfV^2$)	ft ²
f ₀	Initial value of f schedule for compound helicopter or initial approximation for input coefficient program	ft ²
GW	Gross weight	lb
HP _{avail}	Power available at the throttle position set	hp
HP _{reqd}	Power required to maintain flight	hp
I	Total rotor inertia	slug - ft ²
i _w	Wing incidence	rad
K ₃	Induced velocity weighting factor ($K_1 = 1 - (\mu - 0.14)K_3$)	--
K ₆	Rotor angle of attack factor ($K_6 C_T / ca$)	rad
L _w	Wing lift	lb

NOMENCLATURE

Symbol		Unit
M_{cr}	Drag divergent Mach number	--
m	Mass of helicopter	Slugs
ΔM	Amount by which advancing blade tip Mach number exceeds M_{cr}	--
n	Normal acceleration ($\sqrt{(n_{ })^2 + (n_{\perp})^2}$)	g
$n_{ }$	Acceleration parallel to flight path (linear acceleration)	g
n_{\perp}	Normal acceleration perpendicular to flight path	g
P_s	Energy rat. ($\frac{\partial E_s}{\partial t}$)	ft/sec
q	Dynamic pressure ($0.5\rho v^2$)	lb/ft ²
R	Rotor radius or turn radius ($v^2/g\sqrt{n^2 - 1}$)	ft
T	Rotor thrust ($\sqrt{D^2 + (nGW - L_w)^2}$)	lb
ΔT_{aux}	Change in auxiliary thrust $\left(\frac{(HP_{avail} - HP_{reqd})(550)(\tau_{prop})}{V} \right)$	lb
t_c	Thrust coefficient ($2C_T/c$)	--
t_{cdiv}	Thrust coefficient at which stall power occurs	--
v	Flight path velocity	ft/sec
\dot{v}	Flight path acceleration or deceleration	ft/sec ²
v_i	Induced velocity	ft/sec
v_{MAX}	Maximum velocity desired for input coefficient program	Kt
v_{MIN}	Velocity for minimum power	Kt
v_{ne}	Never exceed velocity (structural limit)	Kt
v_p	Velocity parallel to thrust vector	ft/sec

NOMENCLATURE

Symbol		Unit
V_s	Speed of sound	ft/sec
V_T	True airspeed	Kt
V_v	Vertical velocity (positive upward)	ft/sec
α	Angle of attack	deg
β	Sideslip angle	deg
δ_0	Constant part of blade C_D	--
δ_1	α - varying part of blade C_D	/rad
δ_2	α^2 - varying part of blade C_D	/rad ²
η	Efficiency factor	<div> <div> If $V_v > 0$, $\eta = 0.85$ If $V_v < 0$, $\eta = 0.8$ If $P_s < 0$, $\eta = 0.8$ If $P_s > 0$, $\eta = 1.0$ </div> <div> -- -- -- -- </div> </div>
η_{prop}	Propeller efficiency factor ($\eta = 0.85$)	--
θ	Pitch attitude	deg
μ	Advance ratio ($V/\omega R$)	--
π	Pi	3.141592
ρ	Air Density	slug/ft ³
σ	Rotor solidity ($bc/\pi R$)	--
σ'	Air density ratio ($\rho/0.002378$)	--
ϕ	Roll angle	deg
ω	Rotor rotational speed	rad/sec



INTRODUCTION

Combat simulations of aircraft require knowledge of the flight path trajectories which the aircraft may follow. The flight path trajectory is normally described in terms of the Euler angles (ϕ , θ , ψ) which give the orientation (direction) of the aircraft in space relative to some inertial reference frame and the velocity vector of the center of gravity. The flight path trajectories which the aircraft may describe are dependent on the performance and maneuver capabilities of the aircraft which must be known.

There are two basic types of accelerated flight conditions which must be considered: constant energy maneuvers and maneuvers involving a loss of airspeed (kinetic energy), altitude (potential energy), or both. Constant energy maneuvers result in flight at constant speed and altitude. This g-capability is power limited and is primarily a function of excess power available and rotor disc loading. The maximum normal acceleration which can be attained with constant energy flights is referred to as the sustained g-capability. For definition of this capability, power required must be computed based on speed, altitude, and type of maneuver. Transient g-capability refers to the normal acceleration attainable by the rotor. However, to obtain this normal acceleration, a loss of airspeed (kinetic energy) or altitude (potential energy), or both occurs. For example, turns may be made at high transient g-levels and maintained as long as altitude permits. In this sense, transient g's are unlike the transient g's associated with fixed wing aircraft performance which may only be sustained for seconds. The maximum transient g depends on the rotor blade loading coefficient, i.e., thrust divided by blade area and dynamic pressure at the blade tip. To determine this capability, flight path deceleration (rate of loss of energy) must be computed for the given speed, altitude, g-level, and type of maneuver. Once the transient and sustained g-capability are known and the orientation from the trimmed flight condition is known for a specified g-level, speed, altitude, and type of maneuver, the flight path trajectory can then be defined.

The concepts of kinetic and potential energy are used to develop the equations to compute flight path trajectories. The rotor speed degree of freedom is not considered in the model because it would unduly complicate the representation of the pilot and would not significantly affect the accuracy of the computed flight path trajectories in high speed flight. Detailed explanation of developments of these equations can be found in Reference 1.

ENERGY MANEUVERABILITYConcepts

The concepts of energy maneuverability were originally applied to fixed wing aircraft to identify the best areas of operation during combat. Overlays of certain charts would indicate which aircraft had an advantage from energy considerations. These concepts, when applicable, were applied to the helicopter to determine the optimal areas of operation. These areas will be identified during the following discussion.

A measure of the energy state of a helicopter at any altitude-airspeed-RPM-combination can be expressed as

$$E = GW h + 1/2 mV^2 + 1/2 I\dot{\theta}^2 \quad (1)$$

The last term of the above equation is the kinetic energy of the rotor. Since most helicopters normally operate at constant RPM, the rotor energy has been assumed constant for this study. A convenient term in units of feet can be derived from equation 1 by dividing by the weight, GW, and neglecting the rotor energy term. This term, specific energy (E_s), expresses the energy state of a helicopter as a function of altitude and airspeed as follows:

$$E_s = h + \frac{V^2}{2g} \quad (2)$$

Energy management involves control of the rate of transfer between energy levels. The rate of transfer between energy levels can be determined by taking the partial derivative with respect to time of equation 2 which is expressed as follows:

$$\frac{\partial E_s}{\partial t} = \frac{\partial h}{\partial t} + \frac{V}{g} \frac{\partial V}{\partial t} \quad (3)$$

Remembering that work is accomplished in moving from one energy level to another and that power is the rate of doing work, then the left side of equation 3 must be equal to the excess power. The excess power can be determined by taking the difference in horsepower available and horsepower required at the altitude-airspeed-g flight condition. Therefore, energy rate can be expressed as

$$\begin{aligned} P_s &= \frac{\partial E_s}{\partial t} = \frac{(HP_{AVAIL} - HP_{req}) 550}{GW} \\ &= \frac{\partial h}{\partial t} + \frac{V}{g} \frac{\partial V}{\partial t} \end{aligned} \quad (4)$$



From equation 4, a value of energy rate (P_s) can be computed for any airspeed-g-altitude condition for a given amount of power available.

The aircraft's capability to change energy states is limited by the power available. Excess power may be used to increase altitude (potential energy), to accelerate the vehicle (kinetic energy), or to increase the lift above the one g value to change the aircraft's direction of flight. To change the direction of flight, a normal acceleration is required. The optimal areas of operation can be identified from the areas where change of direction (normal acceleration) is accomplished for minimum expenditure of energy. The turn radius for a specified load factor is determined from the following:

$$R = \frac{v^2}{g \sqrt{n^2 - 1}} = \frac{v^2}{g \tan^2} \quad (5)$$

Associated with minimizing turn radius would be maximizing turn rate. Turn rate is computed by

$$\dot{\phi} = \frac{g \sqrt{n^2 - 1}}{V} \quad (6)$$

The derivation of equation 5 is based on the relationship that $n = 1/\cos\phi$. A discrepancy between bank angle (ϕ) data and theory ($n = 1/\cos\phi$) is shown in Figure 1 for the AH-1G helicopter as reported in Reference 2. As a result of Figure 1, the following analysis was suggested (Reference 3) to define the relationship of normal load factor and aircraft attitudes. Coordinated flight requires only that the ball of the turn and bank indicator be centered. This requires a zero net side force in the body axis system. A zero net side force can occur in the presence of some sideslip as a result of aerodynamic side-force characteristics. If pitch attitude, angle of attack, and sideslip angle are considered, the analysis yields:

$$n_x \cos\phi = \cos\theta \cos^2\phi + \cos\theta \frac{\sin^2\phi}{1+K} + \frac{\sin\phi \tan\beta \sin\theta}{1+K} \quad (7)$$

where $K = \frac{\tan\theta \tan\alpha}{\cos\phi}$

The complete derivation of equation 7 can be found in Appendix A. A comparison of the test data and data from equation 7 is presented in Figure 2 as reported in Reference 4. A large scatter band exists, but the theory line now passes through the center of the points.



BELL HELICOPTER COMPANY

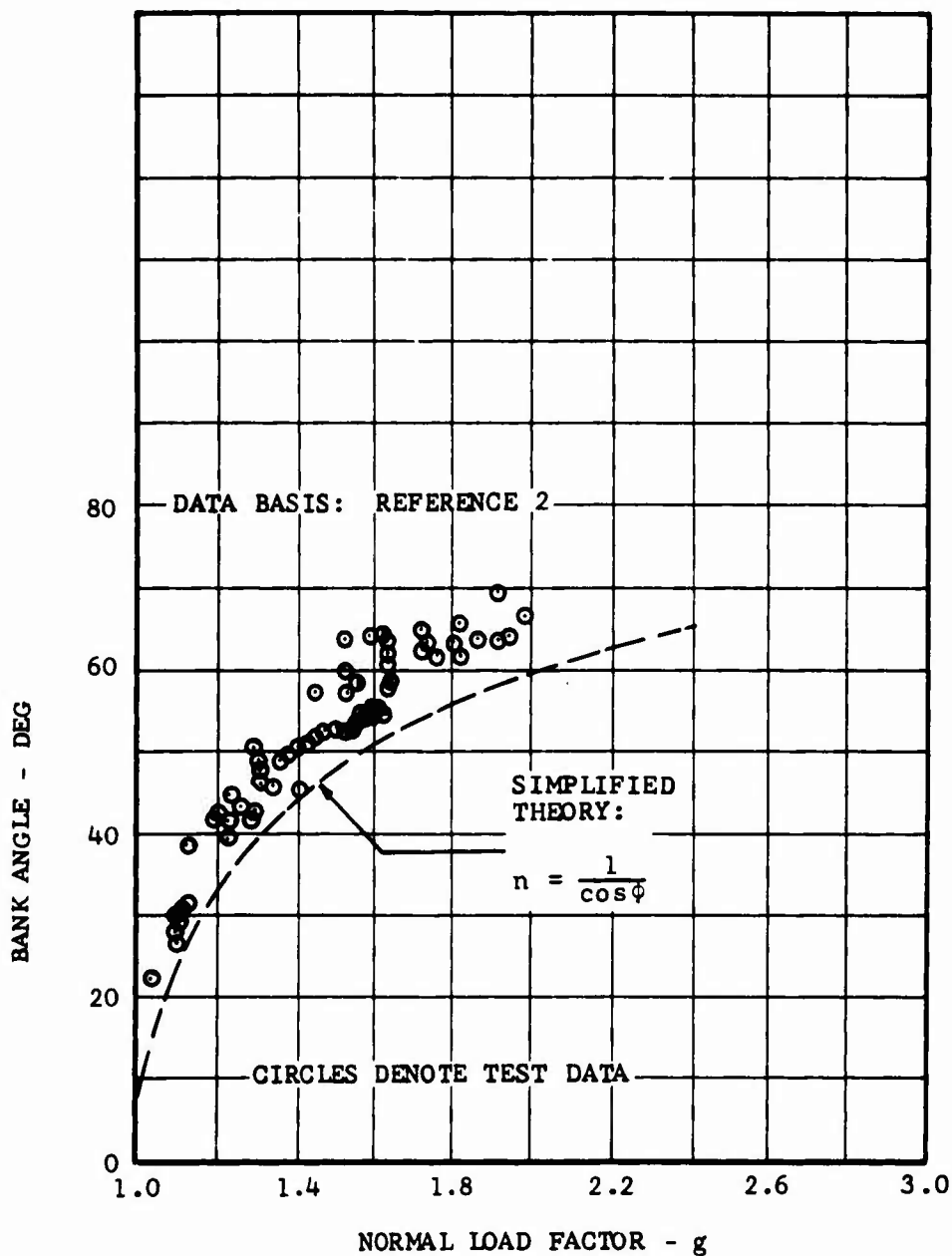


Figure 1. Bank Angle Versus Normal Load Factor for AH-1G Helicopter.

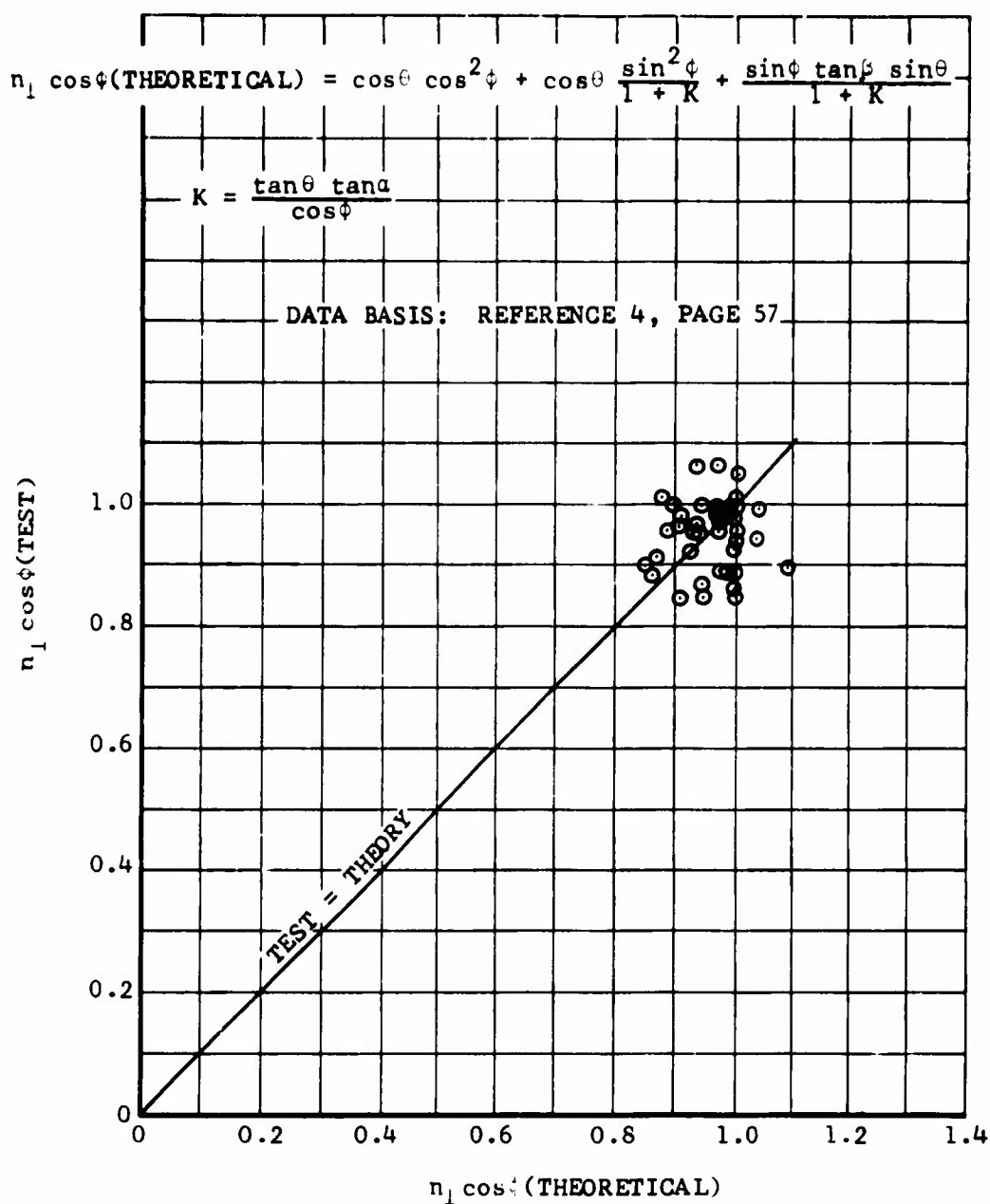


Figure 2. Comparison of Theory and Flight Test Data for Bank Angle Versus Normal Load Factor.



Energy Diagram

The energy diagram is constructed from energy rate at maximum power (P_s) versus airspeed and altitude for a specified value of normal acceleration (n). Lines of constant specific energy (E_s) and energy rate (P_s) are presented for the AH-1G helicopter in Figures 3, 4, and 5. The units of energy rate (P_s) are feet per second and indicate that the aircraft has the necessary energy to change its energy state. For example, a P_s value of 30 feet per second could result in an acceleration of 4.2 knots per second at 80 knots or a vertical rate of climb of 1800 feet per minute. Normal acceleration could be increased until the power required equalled the excess power reflected in the P_s value (equation 4). Therefore, the energy rate contours give a measure of the ability of the aircraft to change its energy state, by increasing altitude or airspeed, or increasing load factor or any combination of the above. A minimum time to climb trajectory can be determined by locating the points of tangency between energy (E_s) and energy rate (P_s) contours as detailed in Reference 5. In Figures 3 and 4 the contour defined by $P_s=0$ identifies the steady state operating boundary of the aircraft. The aircraft cannot operate outside this contour without losing energy, either in the form of altitude, airspeed, or both. On the left the boundary is the hover ceiling. On the top the boundary is the service ceiling. On the right, the boundary is the power limited airspeed.

The energy diagram can be constructed for different values of load factor. An energy diagram for the AH-1G helicopter for a load factor of 1.5 is presented in Figure 5. The negative values of energy rate (P_s) indicate that the power supplied by the engine is insufficient and that either altitude or airspeed or both must be lost in exchange for the total required power. A maneuver in the area of negative energy rates (P_s) uses the rotor's transient g capability which may be limited by blade stall, rotor instabilities, pilot comfort or vertigo at high turn rates, or vibration. The power required for transient g maneuvers is quite high and energy is lost rapidly. The rotor's capability to absorb power in a cyclic-only maneuver diminishes because it approaches the autorotative flow state at high angles of attack. Additional power may always be absorbed by increasing collective pitch but rotor loads may increase.

Maneuver Diagram

The maneuver diagram can be used to identify the region where the aircraft can maximize change of direction for the least expenditure of energy. The ability to change direction is expressed in terms of maximum turn rate and minimum turn radius at a given energy rate. Turn rate-velocity diagrams showing lines of constant energy rate (P_s), constant turn radius (R),



BELL HELICOPTER COMPANY

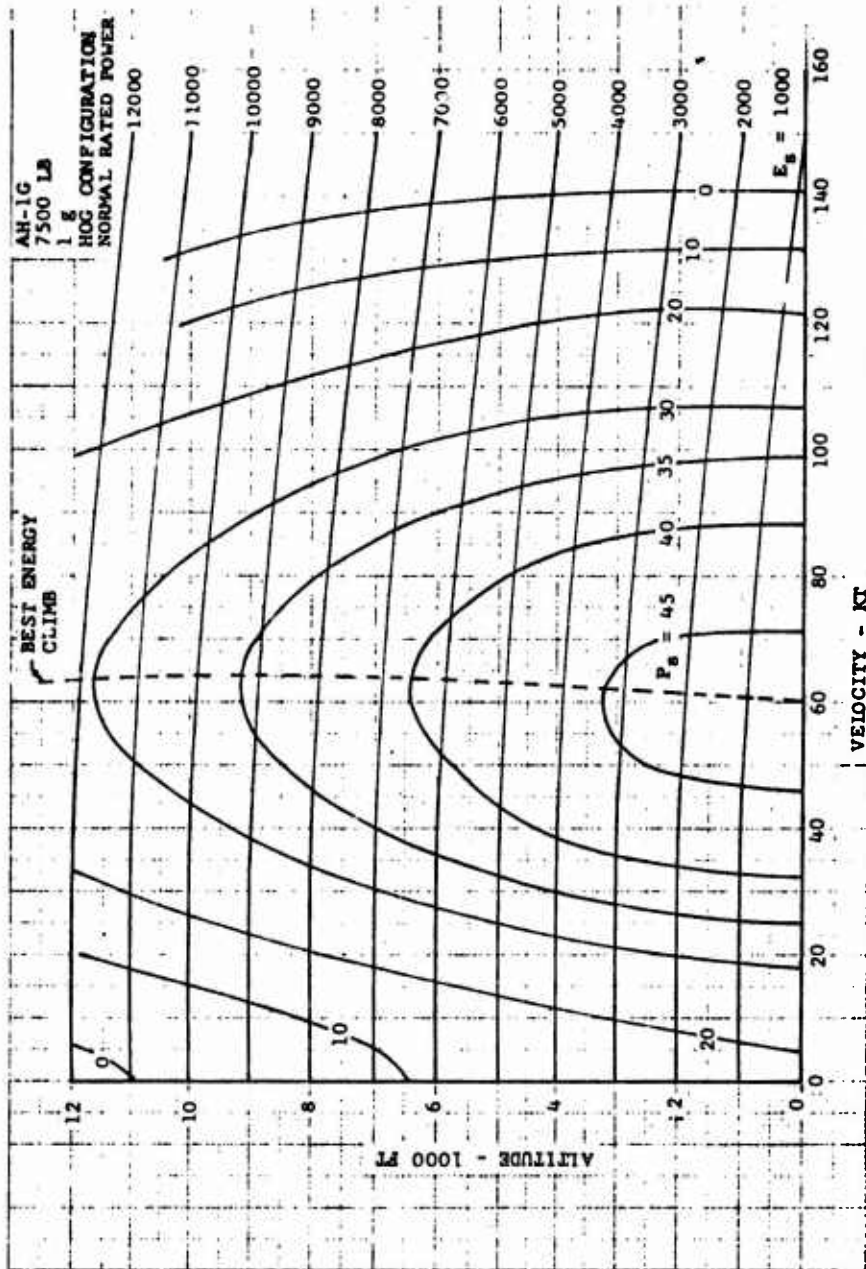


Figure 3. Energy Diagram for AH-1G Helicopter at 7500 Pounds and 1 g

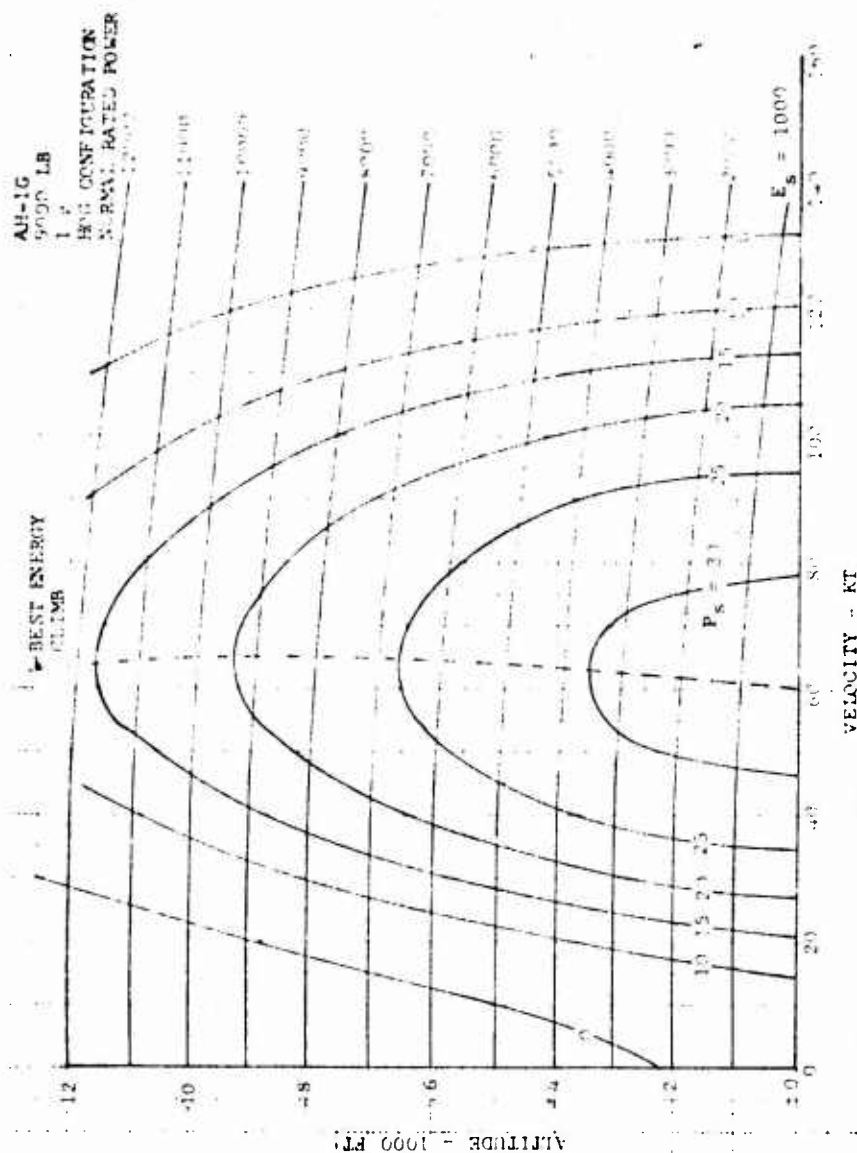


Figure 4. Energy Diagram for AH-1G Helicopter at 9000 Pounds and 1 g



BELL HELICOPTER COMPANY

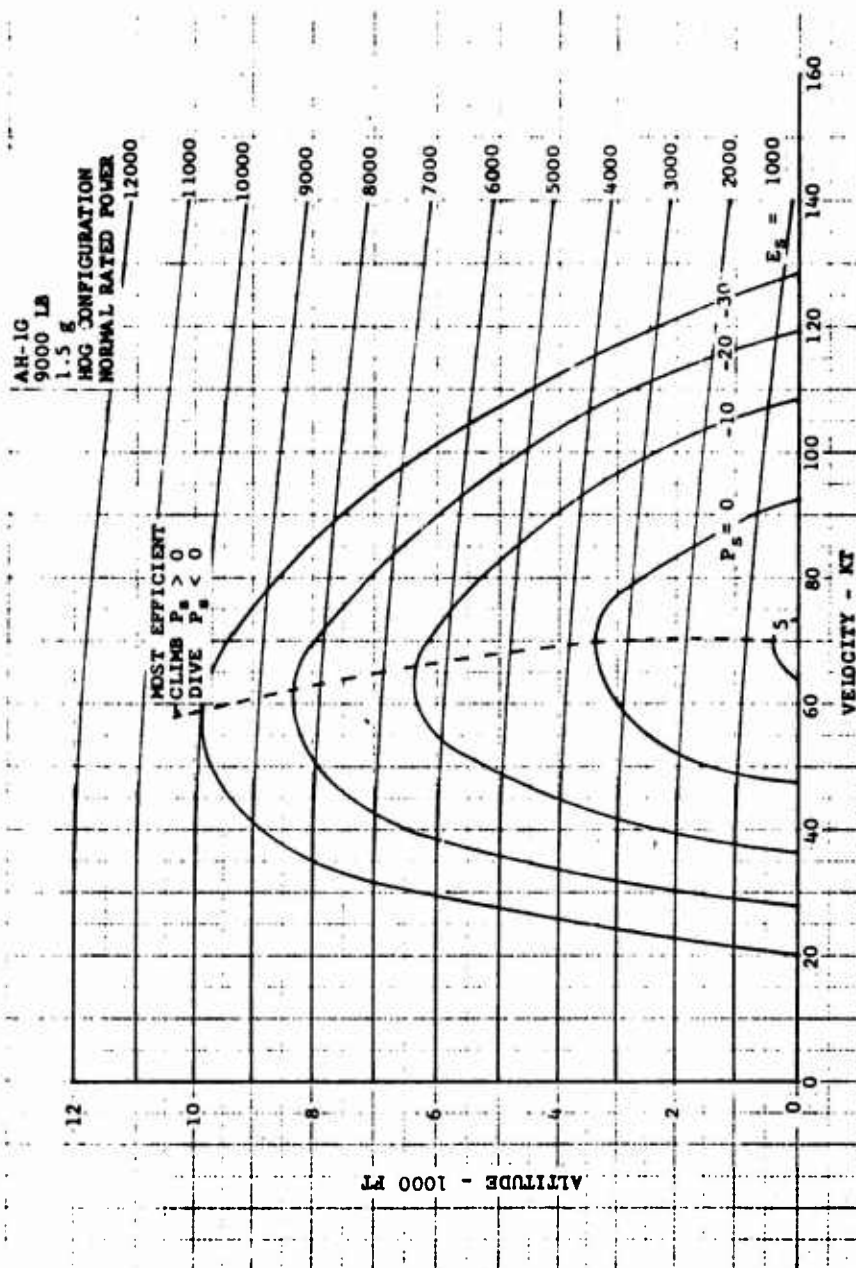


Figure 5. Energy Diagram for AH-1G Helicopter at 9000 Pounds and 1.5 g



and constant normal acceleration (n) for the AH-1G helicopter for gross weights of 7500 and 9000 pounds are presented in Figures 6 and 7. For the helicopter, turn rate is a maximum for a given energy rate (P_g) at low airspeeds. Turn rate maximums for a given energy rate are easily identified from Figures 6 and 7. Minimum turn radius occurs at the point of tangency between the constant energy rate contours and lines of constant radius. Figures 6 and 7 indicate these values occur at low airspeed. For the helicopter, operation in these regions would always require altitude (potential energy) or a positive value of excess energy rate since kinetic energy is so low. The variation of power required with airspeed for a helicopter is such that power increases as airspeed decreases for airspeeds below about 50 knots. A more important parameter than turn radius to the helicopter pilot is normal acceleration. The region where normal acceleration is maximum at a given energy rate is identified on Figures 6 and 7. The intersection of the zero energy rate line with the lines of constant normal acceleration define the steady-state g boundary. Operation outside of this line will require a corresponding loss of altitude or airspeed or both to provide the necessary energy rate required. The impact of normal acceleration and turn radius at a given energy rate can be determined from Figures 8 and 9 for the AH-1G helicopter. These figures show the airspeed at which the pilot can execute a specified turn radius and still retain an energy level.

These charts primarily reflect the sustained g capability rather than the transient g capability of the helicopter. Simply by increasing the installed power the zero energy rate line would move up in Figures 8 and 9 allowing a higher normal acceleration versus speed. Since the helicopter can operate outside the zero energy rate line by trading energy, either potential or kinetic or both, the maximum rotor thrust which can be produced is important. The maximum rotor thrust which can be produced is a function of the type of rotor system and is discussed in a later section. This maximum rotor thrust boundary is equivalent to the stall and structural boundary on a V-n diagram for a fixed wing aircraft. A copy of the computer programs used to generate the above charts can be found in Appendix A.



BELL HELICOPTER COMPANY

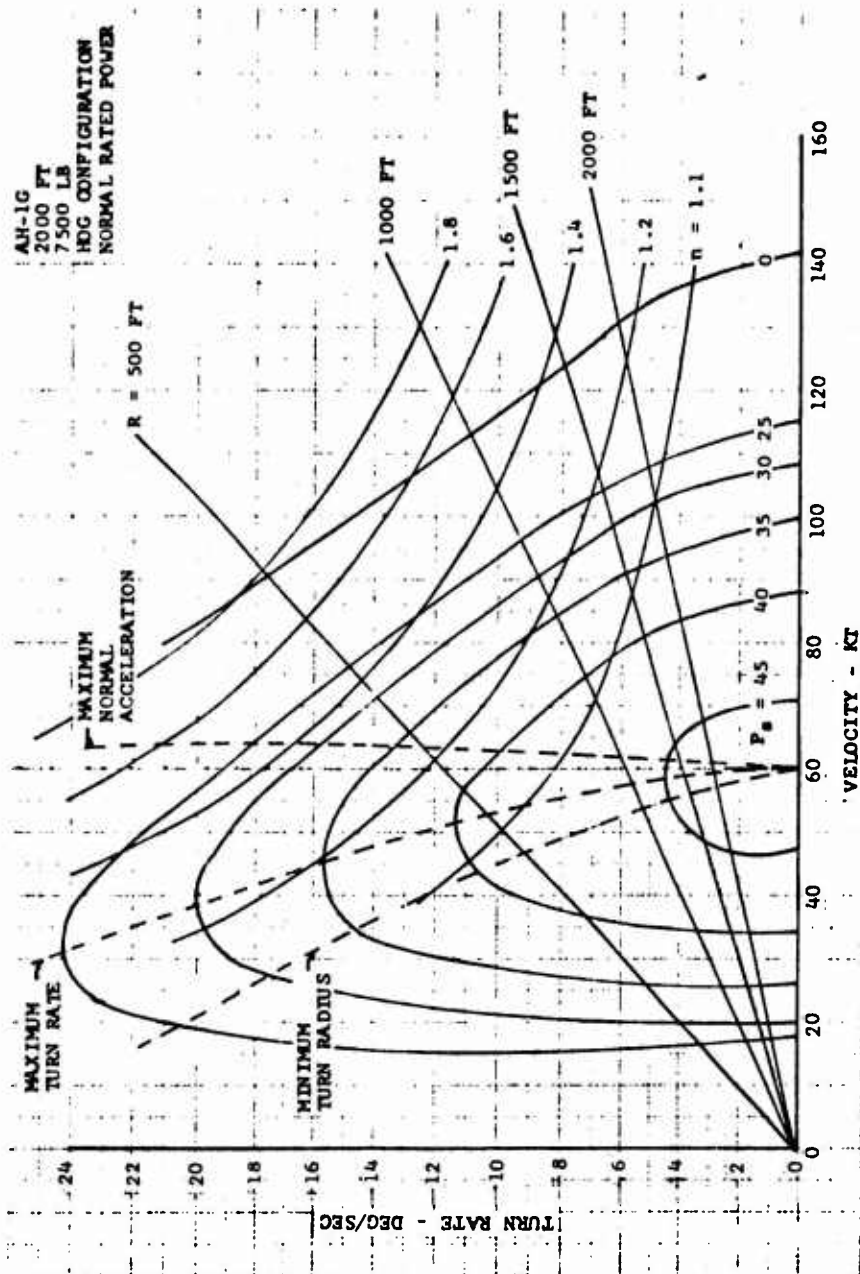


Figure 6. Maneuver Diagram for AH-1G Helicopter at 7500 Pounds and 2000 Feet



BELL HELICOPTER COMPANY

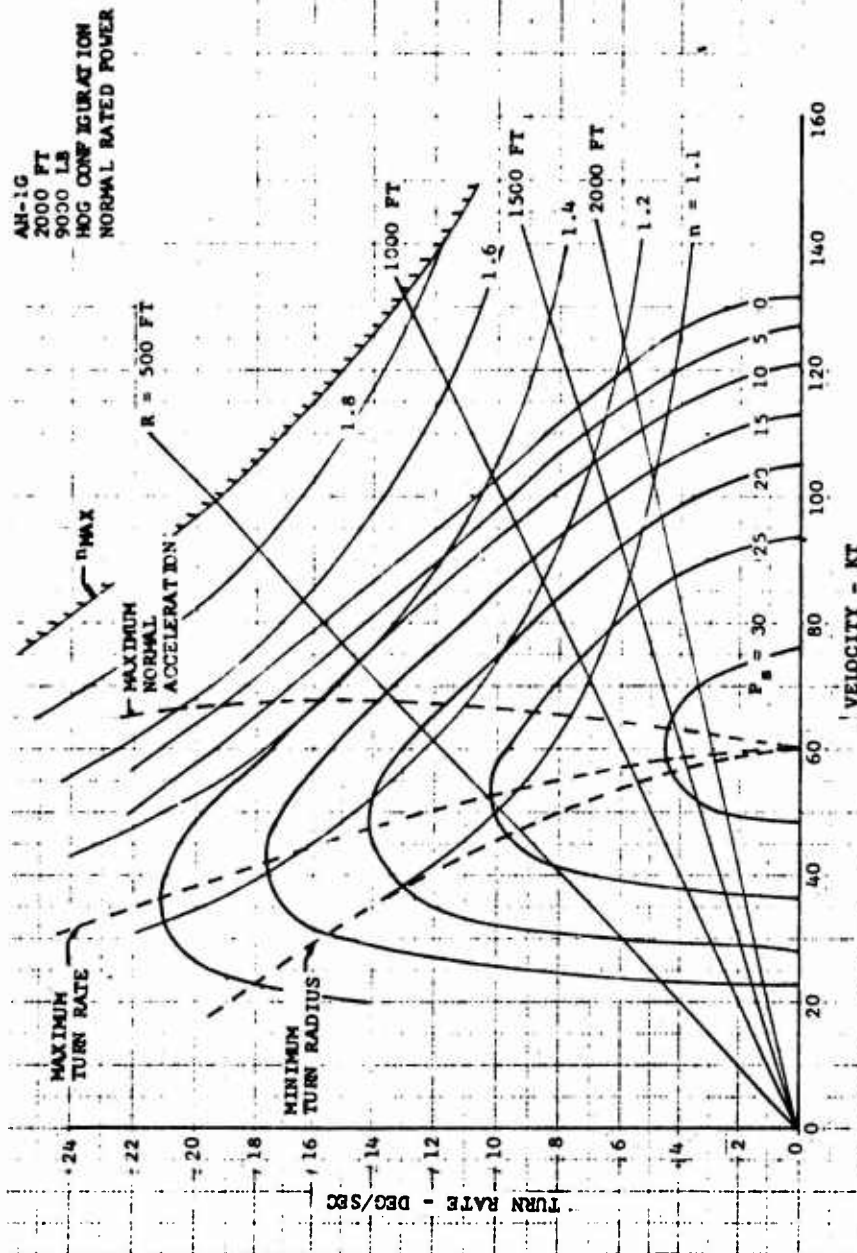


Figure 7. Maneuver Diagram for AH-1G Helicopter at 9000 Pounds and 2000 Feet

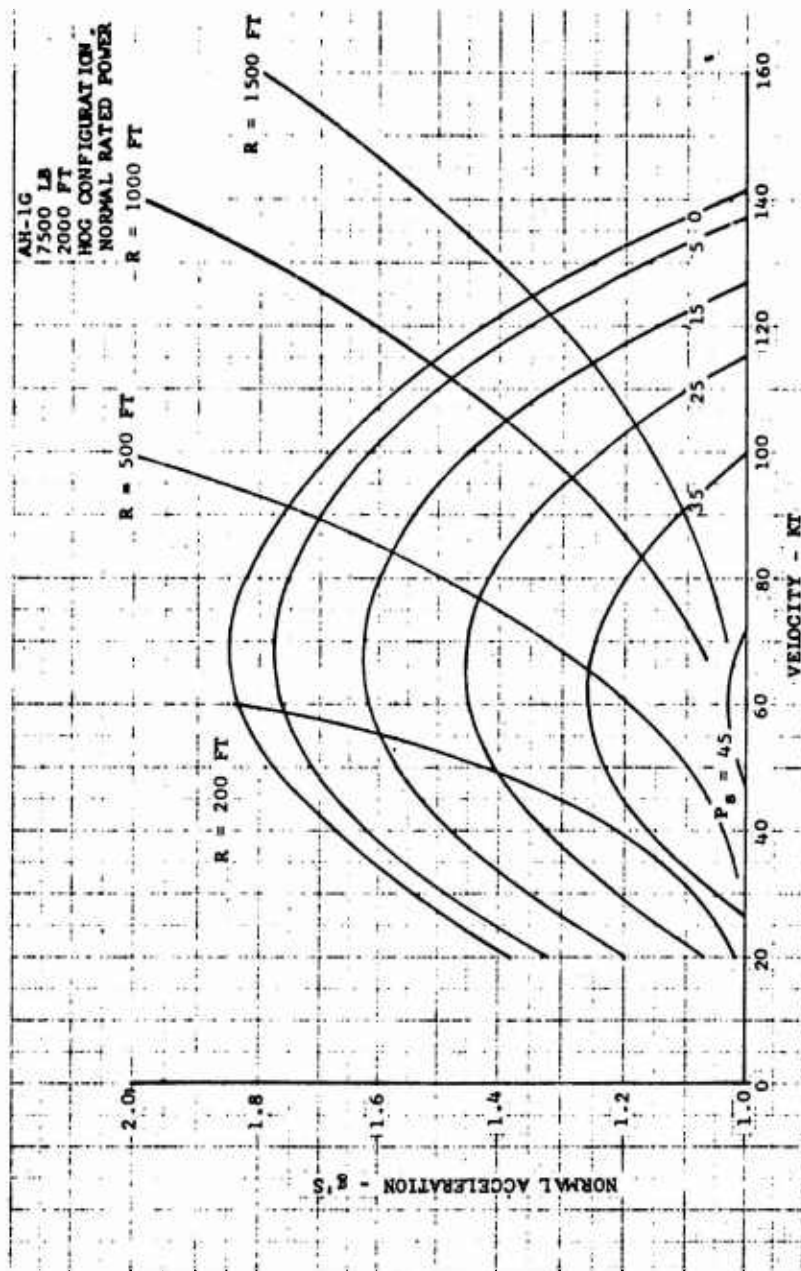


Figure 8. Normal Acceleration versus Velocity for AH-1G Helicopter at 7500 Pounds



BELL HELICOPTER COMPANY

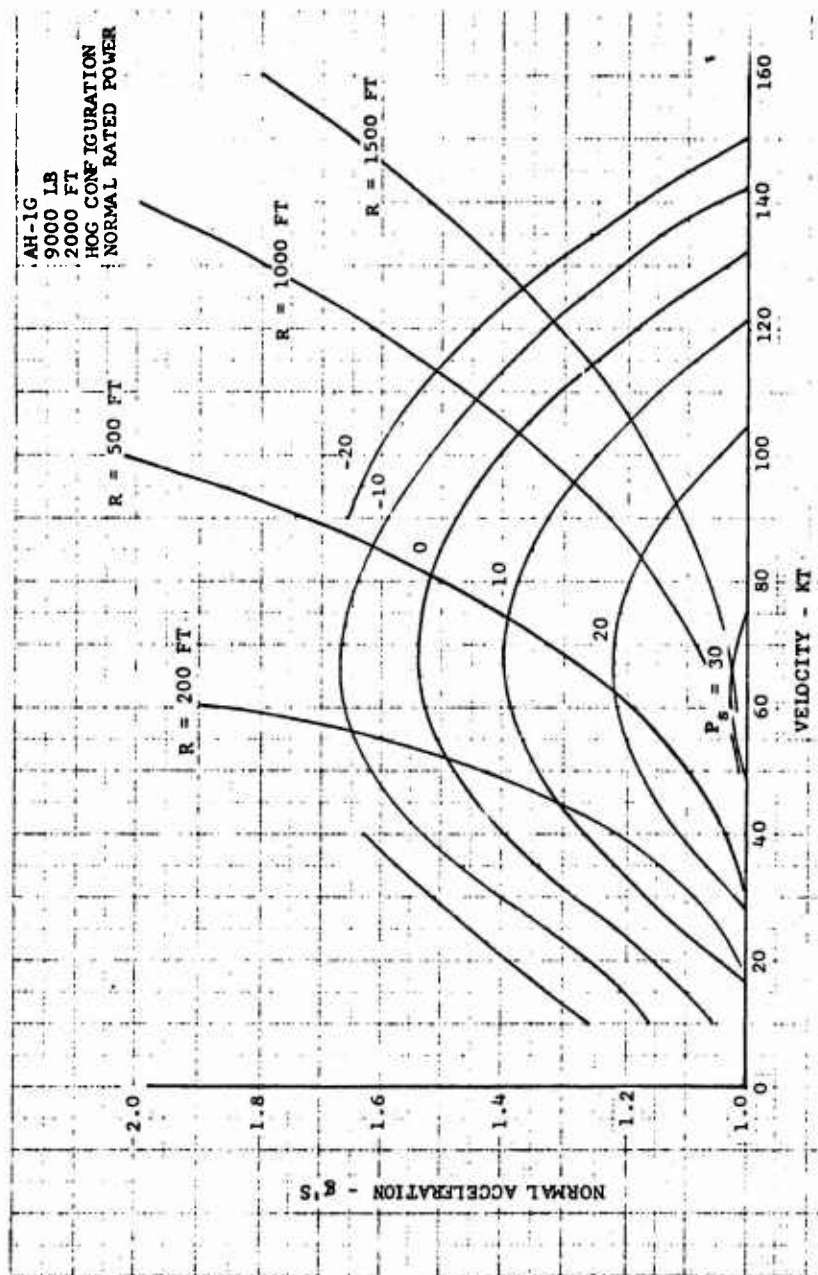


Figure 9. Normal Acceleration Versus Velocity for AH-1G Helicopter at 9000 Pounds



DERIVATION OF EQUATIONS

The necessary equations are developed below for accurately simulating the flight trajectories of single-main-rotor helicopters. Maneuverability limitations associated with different types of rotor systems are considered. A technique for simulating a particular compound helicopter is presented as a guide and the importance of the assumptions concerning the compound helicopter are emphasized.

Technical Approach

Normal acceleration is induced in fixed wing aircraft by applying longitudinal control or flap deflection to change the wing lift coefficient. The equivalent procedure for helicopters is to change main rotor blade lift coefficient. This is usually accomplished by longitudinal cyclic and collective pitch control. Normal acceleration may be induced by the use of either of these controls, independently or together. Cyclic control is usually used alone to produce normal acceleration at high speeds in maneuvers such as pullups, pushovers, and banked turns. It becomes difficult to induce g at low speeds by use of cyclic pitch alone, and so both the collective and cyclic control are used.

Two types of maneuvers were simulated as reported in Reference 1 to determine if any difference existed in power required and angle of attack caused by control technique. The power required for a symmetrical pull-up and decelerating turn were compared for the same speed and g level. The resulting power differences were small and indicated that either control technique would be satisfactory for defining the power required in accelerated flight. Description of the method of simulation of these maneuvers can be found in Reference 1.

Power Equation - Pure Helicopter

A set of closed form equations have been determined for predicting power required as a function of the flight condition, normal acceleration, and certain physical parameters of the helicopter. The development of these closed form equations is presented below.

The power required to overcome the flat-plate drag is expressed as:

$$D = 0.5f_0V^2 \quad (8)$$

$$HP_f = \frac{DV}{550} \quad (9)$$



The f in equation 8 is the equivalent ($C_D=1$) flat-plate drag area which includes the contribution of the fuselage, wing, elevator, fin, and rotor hub. D is the total drag of the helicopter. The contribution of rotor induced power is represented as follows:

$$HP_i = \frac{K_1 TV_i}{550} \quad (10)$$

This induced power is linearly dependent on the rotor induced velocity. Wing induced drag is not currently included but may be added easily if a large wing is used on the helicopter. A weighting factor (K_1) is used on this term to improve correlation with measured data in the low speed range. This factor is expressed as:

$$\begin{aligned} K_1 &= 1 - (\mu - 0.14)2.14 \\ &= 1 + .3\left(1 - \frac{\mu}{.14}\right) & \mu \leq 0.14 \\ K_1 &= 1.0 & \mu > 0.14 \end{aligned} \quad (11)$$

The total velocity parallel to the thrust vector, V_p , is expressed as:

$$V_p = \frac{DV}{T} + \frac{T}{2\rho A \sqrt{V^2 + 0.866V_p^2}} \quad (12)$$

The first term on the right hand side of equation 12 is the component of the free stream velocity, V , parallel to the thrust vector. The second term is the induced velocity and is based on momentum theory.

$$V_i = \frac{T}{2\rho A \sqrt{V^2 + 0.866V_p^2}} \quad (13)$$

The induced velocity is computed by solving equation 12 for V_p . Since V is usually much greater than V_p , a close approximation to V_i , the second term of equation 12, is given by setting $V_p = 0$. After V_p is determined, then V_i is determined from equation 13. The rotor thrust, T , used in the above equations is determined from

$$T = \sqrt{D^2 + (nGW - L_w)^2} \quad (14)$$

where L_w is the wing lift.



The wing lift is based on the following assumptions:

1. Wing has fixed incidence.
2. Wing is positioned in the downwash of the primary lifting rotor.

The wing lift equation is derived as follows:

$$L_w = qA_w a_w \alpha_w \quad (15)$$

$$\alpha_w = c_{fus} + i_w - \tan^{-1} \left(\frac{v_i}{V} \right) \quad (16)$$

Substituting equation 16 into equation 15, and assuming v_i/V to be a small angle,

$$L_w = qA_w a_w \left(c_{fus} + i_w - \frac{v_i}{V} \right) \quad (17)$$

The induced velocity of the main rotor is approximated by

$$v_i = \frac{nGW - L_w}{2rAV} \quad (18)$$

Dividing equation 18 by V and substituting into equation 17

$$L_w = qA_w a_w \left(c_{fus} + i_w - \frac{nGW - L_w}{4qA} \right) \quad (19)$$

The main rotor induced velocity factor is defined as that fraction of the main rotor induced velocity which impinges on the wing in the vertical plane. A main rotor induced velocity factor of 0.5 is assumed for this wing.

Now equation 19 becomes

$$L_w = qA_w a_w \left(c_{fus} + i_w - \frac{nGW - L_w}{8qA} \right) \quad (20)$$

Solving equation 20 for L_w

$$L_w = \frac{qA_w a_w}{\left(1 - \frac{A_w a_w}{8A} \right)} \left(c_f + i_w - \frac{nGW}{8qA} \right) \quad (21)$$



Equation 21 is based on linear theory. From a least squares curve fit technique, it was found that better correlation with C81 (Reference 6) computed values of wing lift was obtained if the wing-rotor interference term was increased by 17 percent. Therefore, wing lift is calculated by,

$$L_w = \frac{qA_w a_w}{\left(1 - \frac{A_w a_w}{8A}\right)} \left(a_f + i_w - \frac{1.17nGW}{8qA}\right) \quad (22)$$

Correlation between equation 22 and C81 values of wing lift is shown in Figure 10.

The power required to overcome wing induced drag is:

$$(HP_i)_w = \frac{L_w^2 V}{550 \pi e b^2 q} \quad (23)$$

The blade profile power is:

$$HP_p = \frac{(\epsilon_0 + \epsilon_1 \alpha + \epsilon_2 \alpha^2) bcR}{8} (1 + 4.6 \alpha^2) c \frac{(\Omega R)^3}{550} \quad (24)$$

The ϵ_0 , ϵ_1 , and ϵ_2 in equation 24 represents the constants in the drag expression for the rotor blade profile at a Mach number of $0.75\Omega R/V_s$. The ϵ_1 term is zero when a symmetrical airfoil is used.

Drag increases rapidly at high Mach number which results in an increase in power required by the rotor. This compressibility power is a function of the Mach number of the advancing blade tip, the airfoil section of the tip, and the thrust coefficient. The Mach number of the tip of the advancing blade is given by $\Omega R(1+\mu)/V_s$. If this number is below a critical value, the compressibility power is zero. The critical value is determined by evaluating M_{cr} at an α of $3.5t_c/a$ for the blade tip airfoil section. The $3.5t_c/a$ corresponds to the average angle of attack of the rotor and $t_c = 2C_T/\gamma$, the blade loading coefficient. If the velocity of the tip is greater than the critical value, then the amount above M_{cr} is determined by the equation:

$$M = \frac{\Omega R(1+\mu)}{V_s} - M_{cr} + 0.75t_c \quad (25)$$



BELL HELICOPTER COMPANY

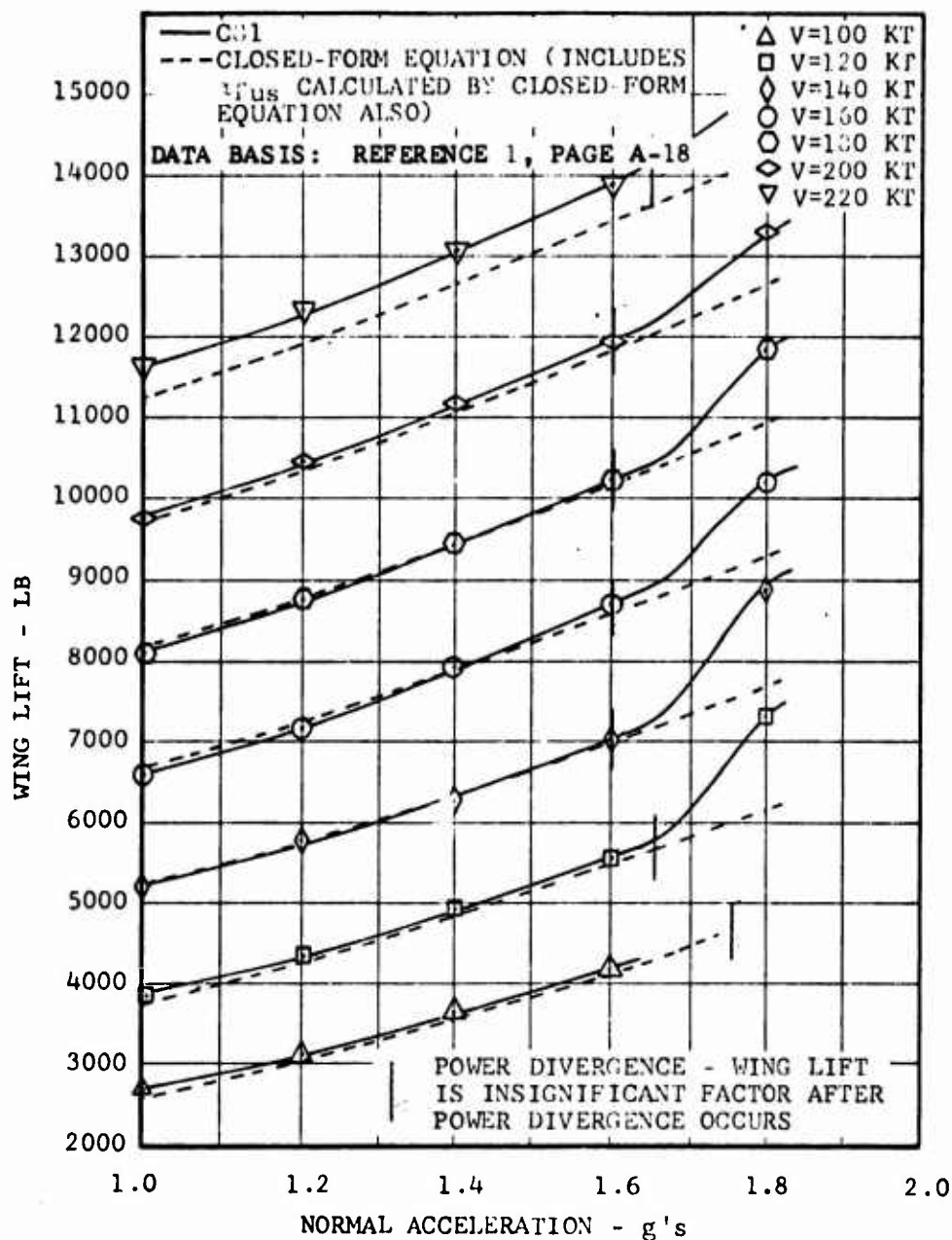


Figure 10. Wing Lift Versus Normal Acceleration at 17000 Pounds and Sea Level.



BELL HELICOPTER COMPANY

The compressibility power is then a function of the amount by which the tip Mach number exceeds M_{cr} as calculated by:

$$HP_c = \frac{0.4(SR)^3}{550} \Delta M^3 [0.0033 - \Delta M(0.022 - 0.11/\Delta M)] \quad (26)$$

Equation 26 is an empirical expression based on level flight compressibility correction for an NACA 0012 airfoil.

The thrust coefficient also is used to compute the stall power. The value of the thrust coefficient at which the power increases due to the partially stalled rotor is referred to as the divergent thrust coefficient $([t_c]_{div})$. If the thrust coefficient is less than $[t_c]_{div}$, then the stall power is a function of the amount the thrust coefficient exceeds the $[t_c]_{div}$ as expressed by:

$$HP_{STALL} = [3410(t_c - [t_c]_{div})]^{3/2} \quad (27)$$

The above expression is empirical and was determined by computing the best fit to flight test stall power data reported in Reference 4.

The last contribution to the power equation comes from consideration of vertical velocity. This term can be expressed as:

$$HP_{V_v} = \frac{V_v GW}{550\tau} \quad (28)$$

If $V_v > 0$ then $\tau = 0.85$ and if $V_v < 0$ then $\tau = 0.80$.

The sum of the above components compose the total power required to perform a specified maneuver. This power may be provided from the engine, deceleration, sink rate, or any combination of these sources. The first reported flight test data in terms of power required to perform a maneuver can be found in Reference 4 for the AH-1G helicopter. Correlation between power data calculated using the closed form equation and the flight test data is shown in Figure 11 for the AH-1G helicopter.

Power Equations - Compound Helicopter

Simulation of flight paths for compound helicopters is complicated by the addition of auxiliary propulsion. Many different main rotor collective settings and auxiliary propulsion combinations may be used to obtain a trim flight condition. Other primary differences in flight simulation between pure and compound helicopters are in pitch attitude, use of auxiliary propulsion to accelerate, and the change in normal acceleration with angle of



BELL HELICOPTER COMPANY

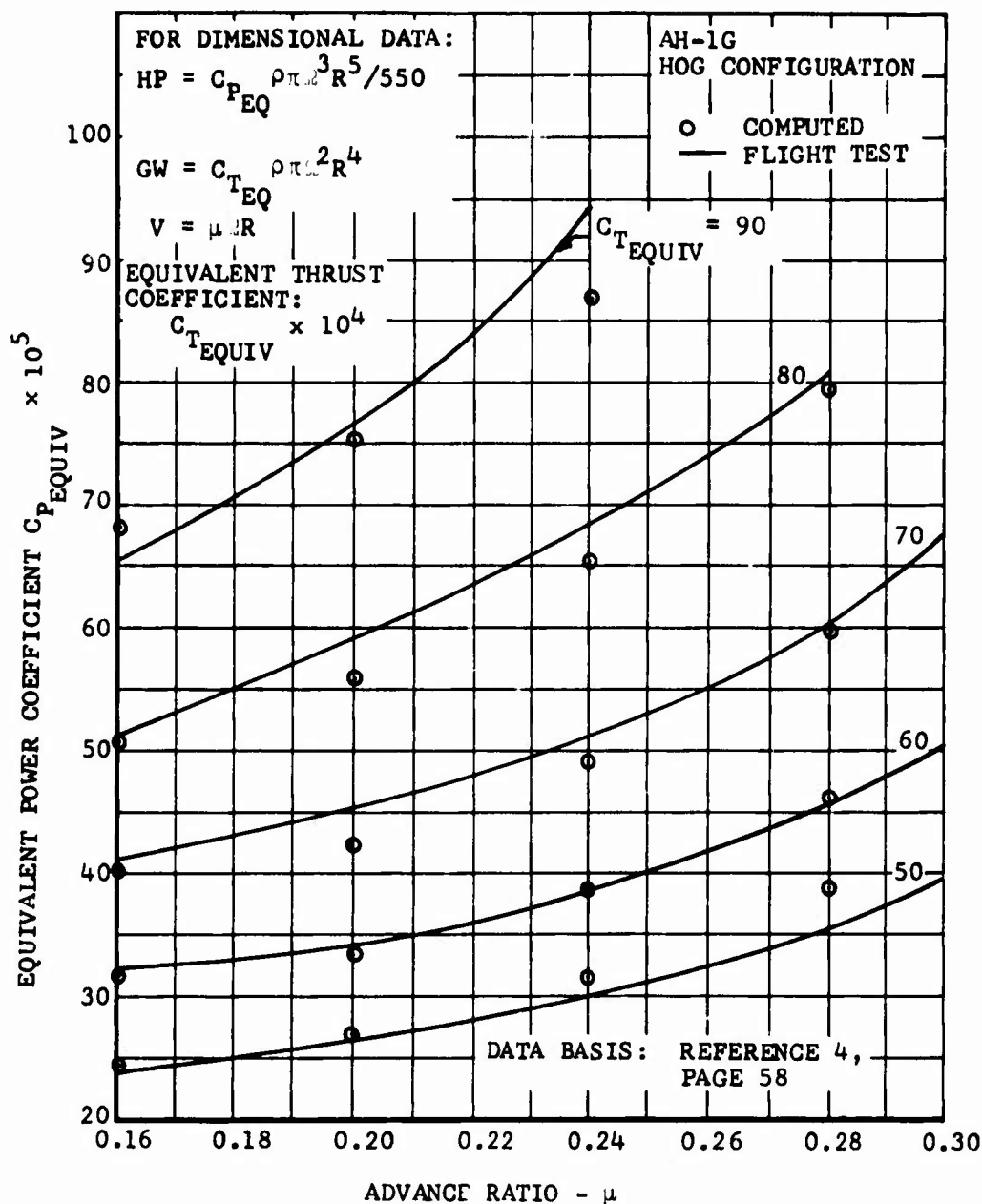


Figure 11. Minimum Equivalent Power Required in Maneuvering Flight for the AH-1G Helicopter



attack. The equations used below for a compound helicopter are valid only for certain assumptions. However, this technique is included as a guide for simulation of different compound helicopters.

Bell Helicopter Company computer program C81 (Reference 6) was used to obtain these data for a compound helicopter. The following assumptions were imposed on the simulation of the compound helicopter (Reference 1, Appendix A). For speeds less than 100 knots, no auxiliary thrust was allowed to trim the math model in level flight. At 100 knots, the collective pitch was set at 11 degrees and the math model trimmed through the use of auxiliary thrust as its speed increased. The auxiliary thrust schedule required by the math model to trim in level flight at speeds greater than 100 knots was fixed. Specifically, variations in auxiliary thrust from that value required to trim at a speed are not allowed.

In the standard helicopter, propulsive force is provided by increasing collective and tilting the rotor forward to obtain greater forward speed. For the compound helicopter, propulsive force is provided by auxiliary thrust at speeds greater than 100 knots since collective is not allowed to increase with speed. Since an auxiliary thrust control is not available in the current Air Force model, the propulsive force (auxiliary thrust) of the compound helicopter must be specified independent of any pilot control. The propulsive power term in the power equation is a function of the equivalent flat plate drag area (f). By expressing the auxiliary thrust as an equivalent flat plate drag area representing the propulsive force of the main rotor, an equivalent flat plate area was determined for a specified speed. From the above method, an equivalent flat plate drag variation with speed was determined as presented in Figure 12.

The total power required for the compound helicopter is then the sum of the individual power components as defined in equations 9, 10, 23, 24, 26, 27, and 28. The f -variation to be used in equation 9 is shown in Figure 12. The limitations of this technique should be realized and care exercised when simulating a compound helicopter which varies auxiliary propulsion in a different manner than assumed above.

The efficiency of the propeller (η_{prop}) is assumed to be constant and equal to 0.85.

The wing effectiveness in normal acceleration is considered below. The normal force is approximated by

$$nGW = T + L_w \quad (29)$$



BELL HELICOPTER COMPANY

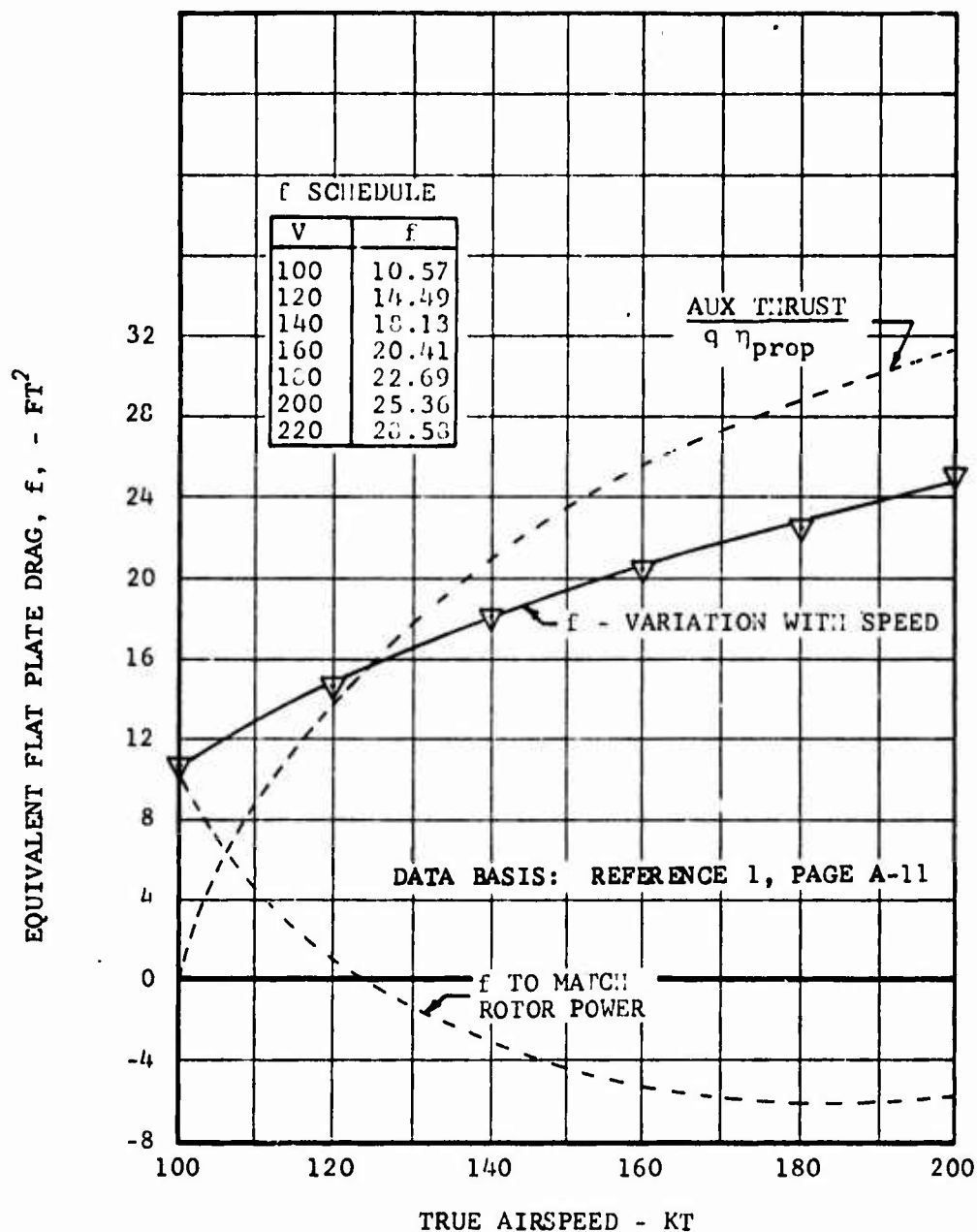


Figure 12. Equivalent Flat Plate Drag Area Versus True Airspeed.



Differentiating equation 15 with respect to fuselage angle of attack, and using equation 16:

$$\frac{dL_w}{d\alpha_f} = qA_w a_w \left\{ 1 + \frac{\partial i_w}{\partial \alpha_f} - \frac{\partial}{\partial \alpha_f} \left[\tan^{-1} \left(\frac{V_i}{V} \right) \right] \right\} \quad (30)$$

Assuming a fixed incidence wing and assuming V_i/V is a small angle,

$$\frac{\partial i_w}{\partial \alpha_f} = 0 \qquad \frac{\partial V_i}{\partial \alpha_f} = \frac{\partial V_i}{\partial T} \frac{\partial T}{\partial \alpha_f} \quad (31)$$

From equation 18 and 29

$$\frac{\partial V_i}{\partial T} = \frac{1}{2rAV} \quad (32)$$

Equation 30 now becomes

$$\frac{dL_w}{d\alpha_f} = qA_w a_w \left(1 - \frac{\partial T / \partial \alpha_f}{4Aq} \right) \quad (33)$$

Differentiating equation 29 and substituting equation 33

$$\frac{dn}{d\alpha_f} = \frac{1}{GW} \left[\frac{\partial T}{\partial \alpha_f} + qA_w a_w \left(1 - \frac{\partial T / \partial \alpha_f}{4Aq} \right) \right] \quad (34)$$

The first term of equation 34 represents the increase in thrust, and the last term represents the decrement of wing lift caused by increased rotor induced velocity.

From linear theory, the rotor thrust change with angle of attack at a constant collective pitch is

$$\frac{\partial T}{\partial \alpha_f} \approx \frac{\partial a\mu}{4} \left[C_A (C_R)^2 \right] \quad (35)$$

If collective pitch is reduced in high g maneuvers, a greater change in angle of attack will be required for the same g load than if the collective pitch is fixed. This is one way the division of lift between the wing and the rotor in maneuvering flight may be controlled.

Substituting equation 35 into 33 and using twice the dV_i/dT derivative (which assumes fully-developed rotor wake on the wing), the wing contribution becomes

$$\frac{dL_w}{d\alpha_f} = qA_w a_w \left(1 - \frac{C_A}{4\mu} \right) \quad (36)$$



The term in parentheses may be thought of as the wing's "g-effectiveness" which is zero if $\mu = \pi a/4$, and becomes increasingly positive at higher speeds. Since a is typically about 2π , if $\pi = 0.065$, the zero lift value of μ is 0.102, which corresponds to a speed of about 45 knots. At this low speed the small angle assumption (equation 17) is imprecise enough that an exact solution of equation 17 demands the use of $\tan^{-1}(V_1/V)$. The g-effectiveness of the wing would be 0.75 at 180 knots and only 0.5 at 135 knots. Thus it is apparent that a wing is effective in maneuvering flight only at high forward speeds.

Acceleration and Deceleration

Level acceleration and level deceleration are integral components of the maneuver capability of a helicopter. The prediction of deceleration is important in determining the amount of power which can be gained to perform a transient maneuver.

The time to accelerate from V_1 to V_2 is determined by the specific excess power, P_s , and the speed, V , as follows:

$$t = \int_{V_1}^{V_2} \frac{V}{\eta g P_s} dV \quad (37)$$

where η is an efficiency factor. This equation is obtained from elemental power and force, F , relations

$$F = m \frac{dV}{dt}$$

$$P = F \cdot V = mV \frac{dV}{dt}$$

Since power available has an important effect on acceleration time, care must be taken in specifying the power applied versus time when correlating with flight test data. Level acceleration data for the AH-1G helicopter can be found in Reference 7. A comparison of predicted and measured data for a level acceleration from 40 to 100 knots is shown in Figure 13. The horsepower applied versus time used was taken from a representative time history in the above report. An efficiency of 1.0 was used.

During deceleration, it is assumed that all the power required to sustain level flight is used to generate a decelerative force. In other words the power supplied by the engine to the rotor is zero and the rotor is autorotating. The time to decelerate from V_2 to V_1 is



BELL HELICOPTER COMPANY

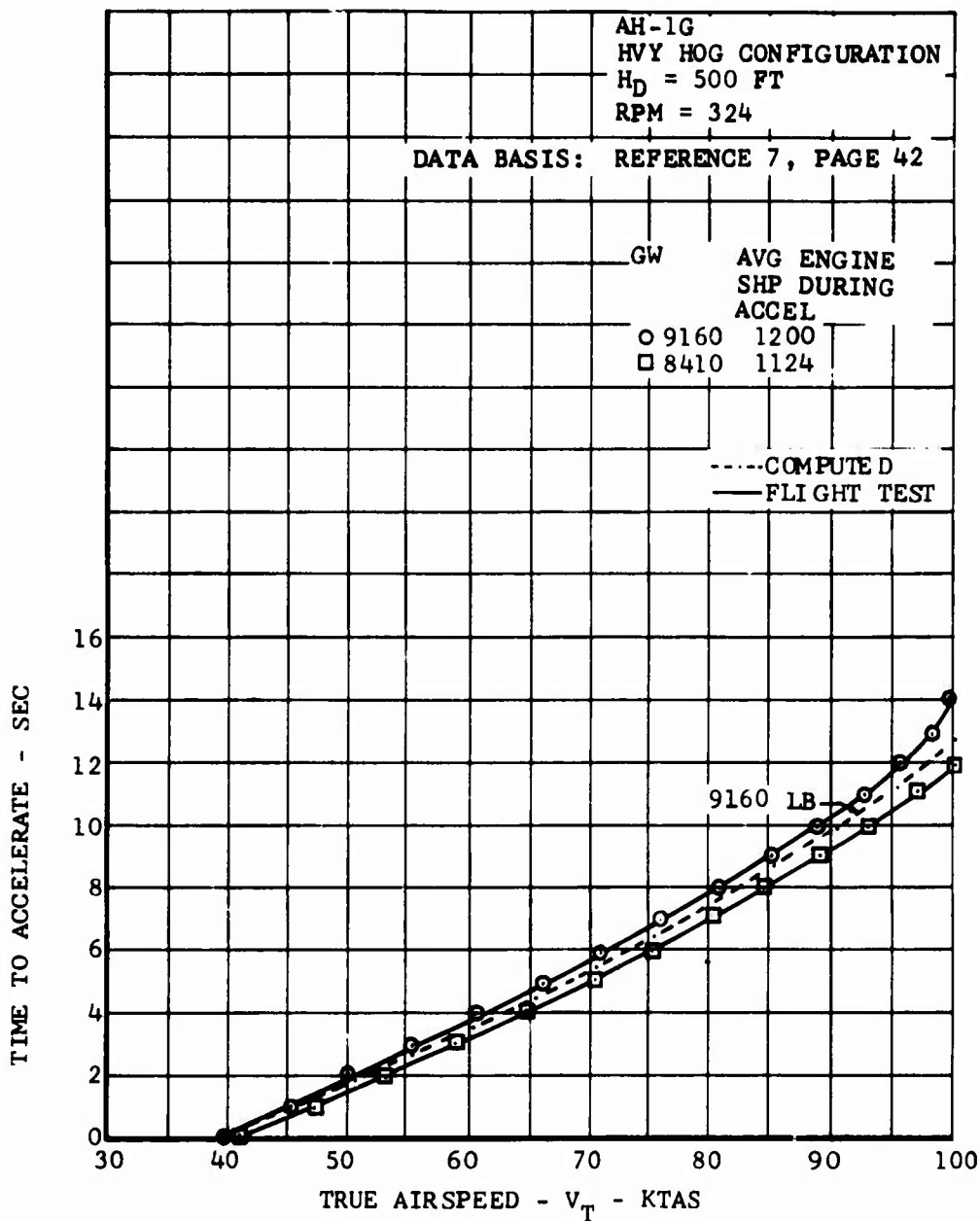


Figure 13. Acceleration Performance for AH-1G Helicopter



BELL HELICOPTER COMPANY

$$t = \int_{V_2}^{V_1} \frac{mV}{\eta^P_{req}} dV \quad (38)$$

where η is an efficiency factor. An efficiency (η) of 0.8 is used to allow the pilot a rotor overspeed margin. A comparison of predicted and measured data for a level deceleration from 113 knots to 40 knots for the AH-1G helicopter is shown in Figure 14. The measured data can be found in Reference 7. It should be noted that these data are for zero sideslip and higher deceleration can actually be obtained by sideslipping.

For simulating flight paths, the amount of excess power available determines the acceleration as follows

$$\dot{V} = \frac{\eta g P_s}{V} \quad (39)$$

If this horsepower required is greater than the horsepower available (P_s is negative) then the above equation will predict the corresponding deceleration. Proper attention should be given to the efficiency factor (η) of 1 for acceleration and 0.80 for deceleration. The limitation of equation 39 is that as V approaches zero \dot{V} becomes infinite. This is discussed further on page 76.

Alpha Equation - Pure Helicopter

The angle of attack is needed for survivability and terrain following studies. A closed form expression for the angle of attack variation with velocity and g-level has been determined by empirical techniques which use the angles of attack computed by C81 as target values. The equation is:

$$\begin{aligned} \alpha = & 8.643 \left[2.478(n-1)^2 + 10.422(n-1) \right] \frac{\sqrt{f GW}}{(c'V)^{1.6}} \\ & - 17.639V \sqrt{\frac{f_0}{GW}} - \tan^{-1} \left(\frac{0.8V_v}{V} \right) - 1.5 \\ & - \sin^{-1} \left(\frac{\dot{V}}{\eta g \left[1 + \left(\frac{V}{240} \right)^2 \right]} \right) \end{aligned} \quad (40)$$

The first term of equation 40 represents the change in α caused by normal acceleration with correction for altitude, velocity, gross weight, and drag. The second term represents the variation in angle of attack with velocity in one-g level flight. The third term accounts for the change in α for climb (positive) and descent (negative). The last term represents the change in α for a pilot-induced acceleration or deceleration. It should be

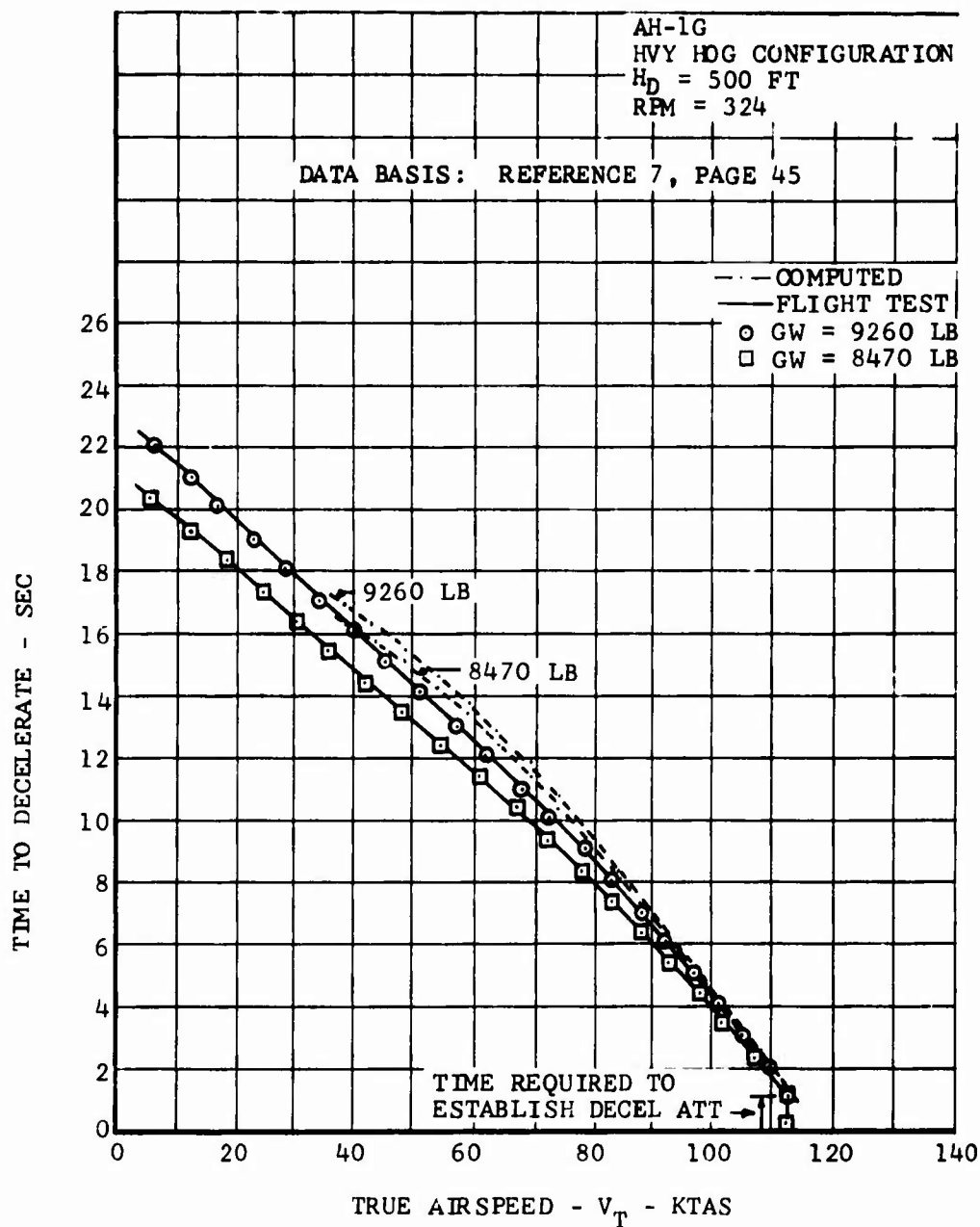


Figure 14. Deceleration Performance for AH-1G Helicopter



emphasized that this term is zero if the acceleration or deceleration is not pilot induced. A flight condition where this occurs is when the horsepower required is greater than the maximum horsepower available. This change in α results from the difference of applying the force for acceleration or deceleration at the center of gravity or at the rotor hub (pilot induced).

The constants in the angle of attack expression were determined to best fit the data computed by the C81 computer program (Reference 6) for the AH-1G helicopter. An example of the correlation between angle of attack data calculated using the equation and the C81 data is shown in Figure 15. It is recognized that the coefficients of equation 40 are for a specific helicopter, but may be used for different helicopters since most helicopters have similar attitude variations with the parameters in the equation. If angle of attack data are available from flight test for a specified helicopter, then the coefficients of equation 40 can be modified to give a better fit while retaining the basic form of the alpha equation.

Alpha Equation - Compound Helicopter

A closed form expression for the angle of attack variation with velocity and g level has been determined by empirical techniques which use the angles of attack computed by C81 (Reference 6) as target values. This equation applies only to the compound helicopter specified in Reference 1, Appendix A, but represents the basic form of the alpha equation for a pure helicopter with different coefficients. This equation is presented only as a guide for simulating a compound helicopter. The equation is

$$\alpha = 11.5671 \left[0.8667(n-1)^2 + 6.8717(n-1) \right] \frac{\sqrt{f_o GW}}{(V)^{1.6}} - 10.8159V \sqrt{\frac{\rho f_o}{GW}} + 2.5778 - \tan^{-1} \left(\frac{0.8V}{V} \right) + \Delta\alpha_f \quad (41)$$

For speeds less than 100 knots, $\Delta\alpha_f$ from pilot-induced acceleration or deceleration is as follows:

$$\Delta\alpha_{f1} = -\sin^{-1} \left(\frac{\dot{V}}{ng \left[1 + \left(\frac{V}{240} \right)^2 \right] } \right) \quad (42)$$

For speeds greater than 100 knots, $\Delta\alpha_f$ from pilot-induced acceleration or deceleration is as follows:

$$\Delta\alpha_{f2} = \frac{\Delta T_{aux}}{\left(\frac{\partial T_{aux}}{\partial \alpha_f} \right)} = \frac{m \dot{V} \eta_{prop}}{\left(\frac{\partial T_{aux}}{\partial \alpha_f} \right)} \quad (43)$$



BELL HELICOPTER COMPANY

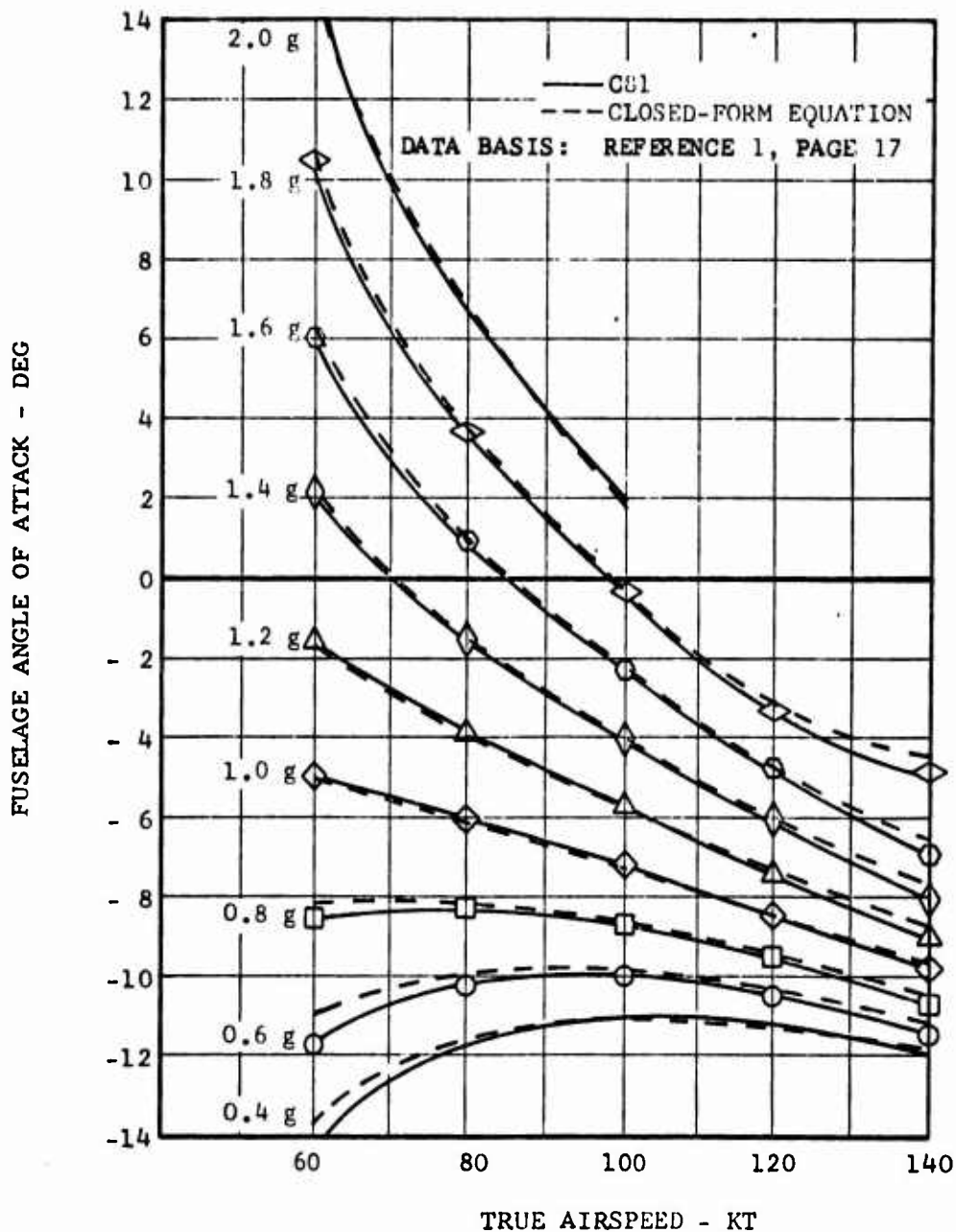


Figure 15. Fuselage Angle of Attack Versus True Airspeed for Symmetrical Pullups and Pushovers at 7500 Pounds and Sea Level.



BELL HELICOPTER COMPANY

The effect of the change of angle of attack on auxiliary thrust can be expressed as follows:

$$\frac{\partial T_{aux}}{\partial \alpha_f} = 0.0046224(n)^{1.122} v^2 + 1.52446(n)^{1.132} v + 337.4(n)^{0.426} \quad (44)$$

The above equation is based on data computed by C81 (Reference 6). A transition between $\Delta \alpha_{f1}$ and $\Delta \alpha_{f2}$ (equations 42 and 43) is provided to avoid a discontinuity between the $\Delta \alpha_{f1}$ for pure helicopter and the $\Delta \alpha_{f2}$ for compound helicopter. The equation for transition is as follows:

$$\Delta \alpha_f = [1 - 0.05 (V-135.04)] \Delta \alpha_{f1} + (0.05)(V-135.04) \Delta \alpha_{f2} \quad (45)$$

The above equation is valid between 80 and 100 knots only. The limitations of the above equation should be realized and care exercised in using the equation for simulating a compound helicopter different from the one in Reference 1, Appendix A. However, the above technique can be made to simulate different compound helicopters if a small amount of C81 data which represent the specified compound helicopter is available. The technique is still useful even though it requires some dependence on C81 or flight test data.

Maneuverability Limits

The g-capability of a fixed-wing aircraft in maneuvering flight is usually determined by consideration of structural, aerodynamic, and power limitations. The same limitations apply to a helicopter, in a slightly different manner. The structural limitation for the helicopter is primarily determined by vibration and fatigue life of rotor system components. The resulting limit is referred to as the V_{ne} speed (never-exceed velocity).

The aerodynamic limits for the helicopter are not as straightforward as those for a fixed-wing aircraft. Once stall is encountered in a fixed-wing aircraft, lift no longer increases with increasing angle of attack. Stall is not as well defined in a helicopter as in a fixed-wing aircraft. Blade stall is encountered on some parts of the rotor while other parts will not be stalled. Because stall has different effects on different rotor systems, the "stall limit" can vary widely among rotorcraft. An attempt was made to define the "stall limit" for the different rotor systems based on data available from published literature.

The data for each rotor system are reduced to a rotor blade loading coefficient (t_c) versus advance ratio (μ) curve. This coefficient is calculated by dividing rotor thrust (which is approximately equal to the load factor times the weight) by the blade area ($b c R$) and the average dynamic pressure at the blade tip $0.5 \rho (CR)^2$:



$$t_c = \frac{nGW}{0.5\rho(\sigma R)^2 (bcR)} = \frac{2C_T}{\sigma} \quad (46)$$

A brief discussion of the effect of the type of rotor system on the thrust load limit follows.

Systems that use moveable control surfaces on the main rotor blade are susceptible to partial loss of control and blade torsional instabilities when producing high thrust. A single rotor helicopter which uses this type of system is the HH-2C. Based on data from Reference 8, blade stall may be encountered if the t_c - μ curve indicated in Figure 16 is exceeded. Intentional approaches to or inducement of retreating blade stall is a prohibited maneuver as stated in the flight manual.

Fully articulated rotors exhibit large flapping and lead-lag blade motion and are susceptible to blade torsional instabilities (Reference 9) when subjected to high thrust. Several helicopters use this type of rotor system. For the CH-3C helicopter, blade stall may be encountered if the t_c - μ curve shown in Figure 17 is exceeded based on data taken from Reference 10. The flight manual states that control difficulties will arise if the stall is allowed to fully develop. For the CH-53 A/D helicopter, the t_c - μ curve shown in Figure 18 represents the flight condition where stall may be encountered based on data of Reference 11. However, the primary indication of blade stall is shown on a cruise guide indicator. These values indicate the degree of acceptable vibration that will sustain component service life. The OH-6A helicopter uses this type of system also. The t_c - μ curve is shown in Figure 19 for blade stall on the OH-6A helicopter based on data from Reference 12. The above data which were taken from respective flight manuals are assumed to be representative data of the particular type of rotor system. However, it is recognized that the data may be conservative.

The thrust load limit of hingeless rotor systems has not been very well defined because of limited flight test experience. To date, the limit that is most often encountered is a structural load limit in some component of the rotor system.

Teetering rotor systems may induce a vibratory response of the fuselage at high thrust. These systems rely on a rotor-pylon isolation system to minimize this vibration and show a high tolerance for blade stall. The maximum thrust achieved for the AH-1J helicopter expressed in terms of t_c versus μ is presented in Figure 20 (References 13 and 14). The stall alleviating effects of pitch rate (Reference 15) minimize the oscillatory thrust excitation especially for rotors with high flapping inertia. Thus, vibration has been shown by flight test to decrease with increased normal acceleration at advance ratios above 0.3 (Reference 16).



BELL HELICOPTER COMPANY

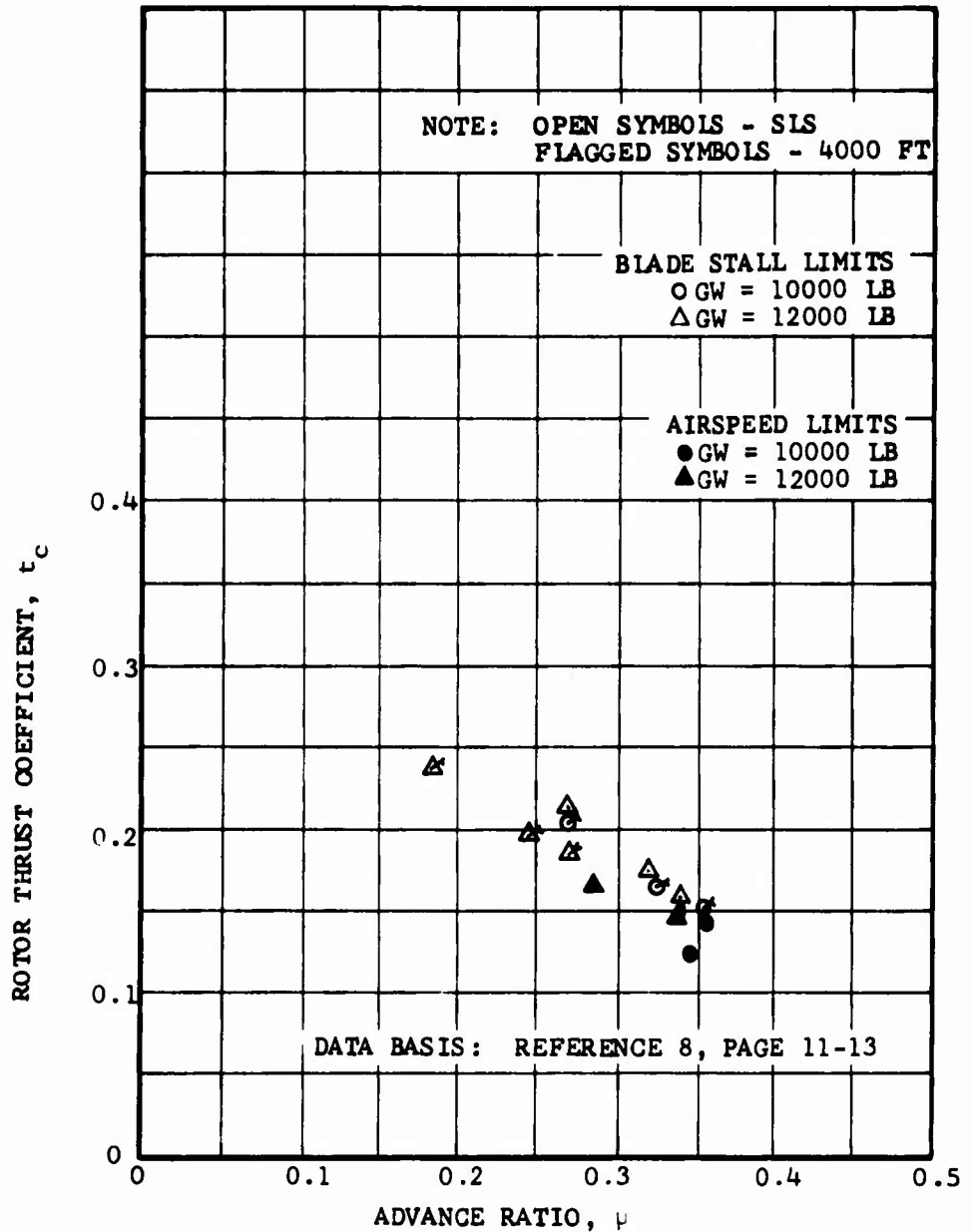


Figure 16. Rotor Thrust Limits for HH-2C Helicopter



BELL HELICOPTER COMPANY

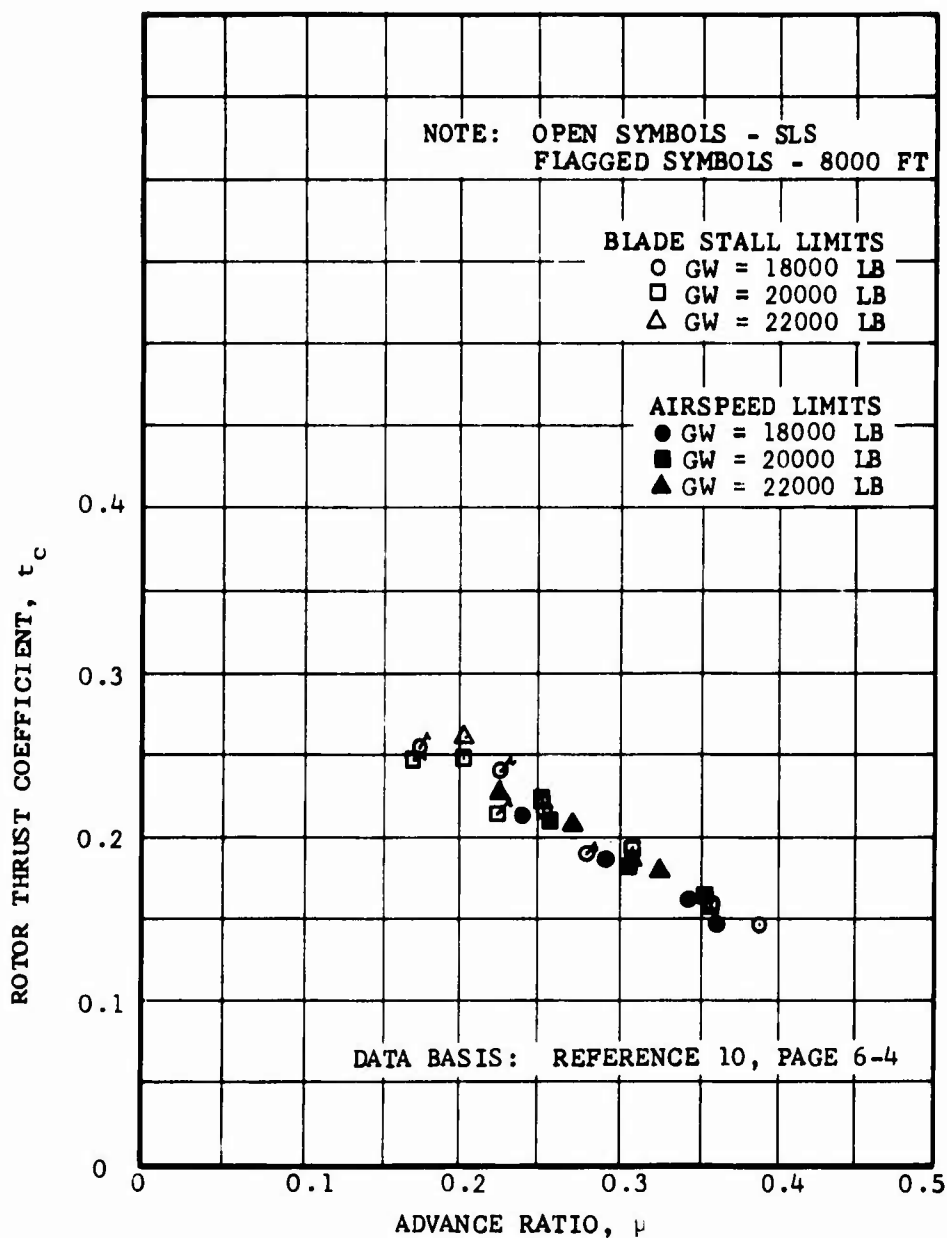


Figure 17. Rotor Thrust Limits for CH-3C Helicopter



BELL HELICOPTER COMPANY

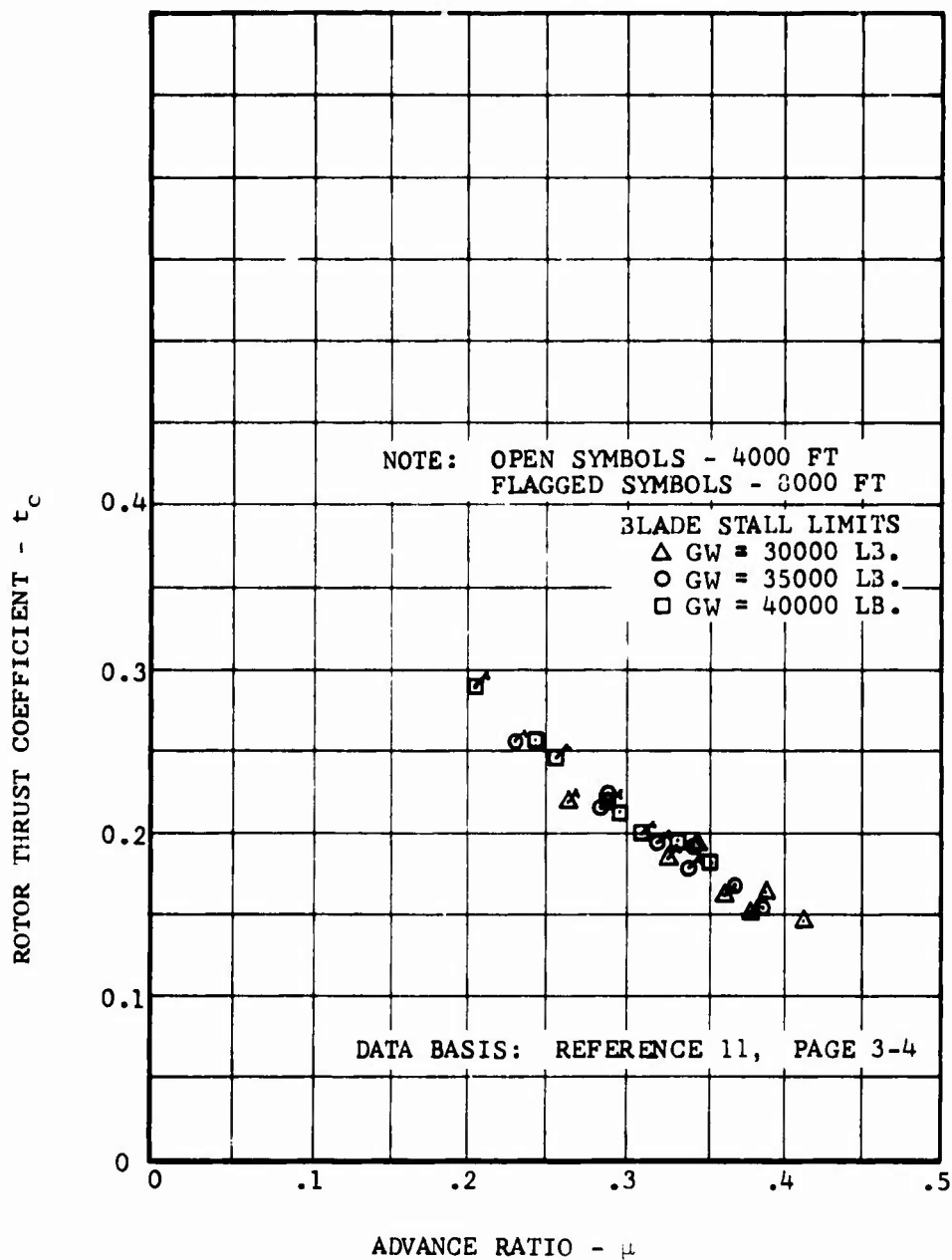


Figure 18. Rotor Thrust Limits for CH-53A Helicopter



BELL HELICOPTER COMPANY

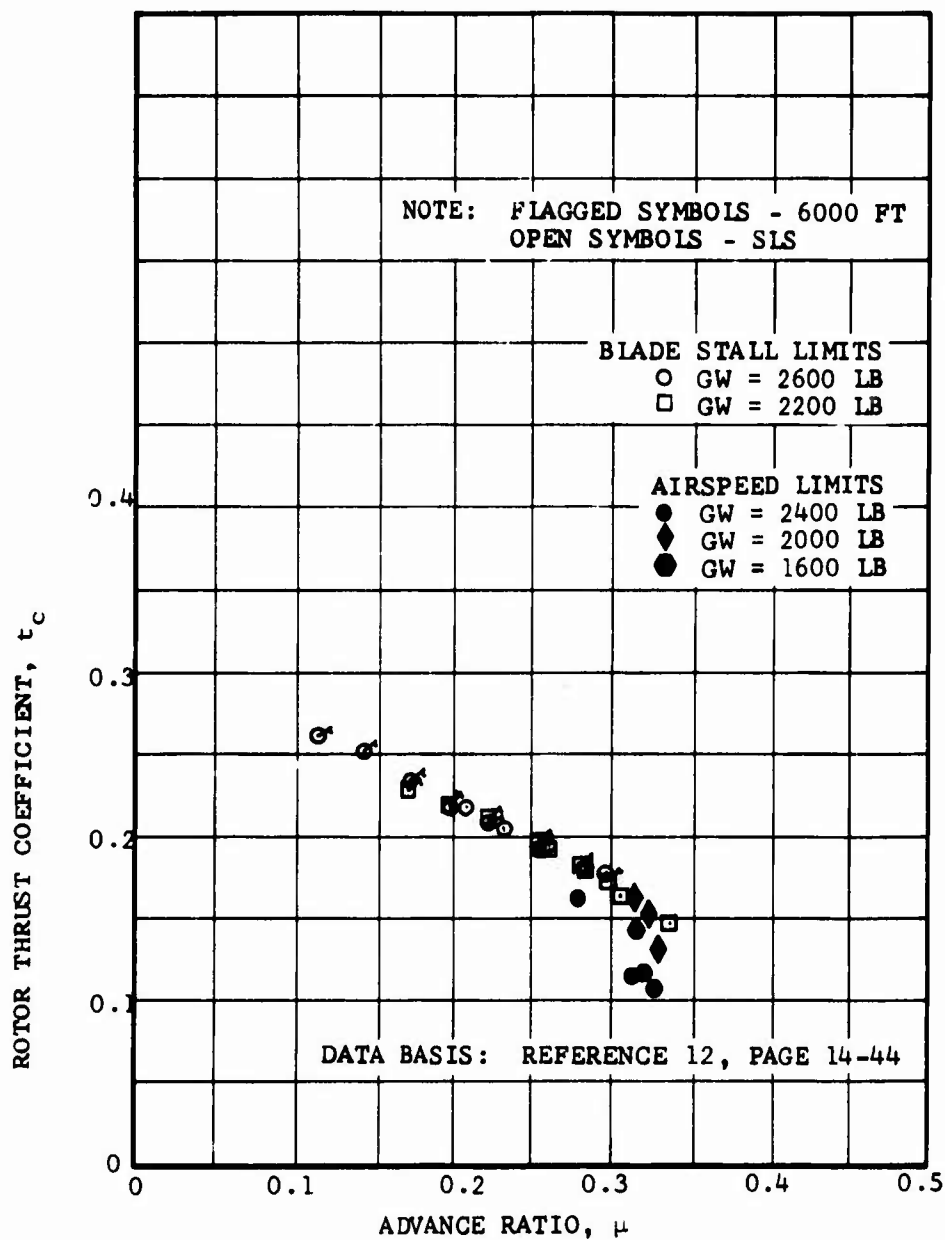


Figure 19. Rotor Thrust Limits for OH-6A Helicopter



BELL HELICOPTER COMPANY

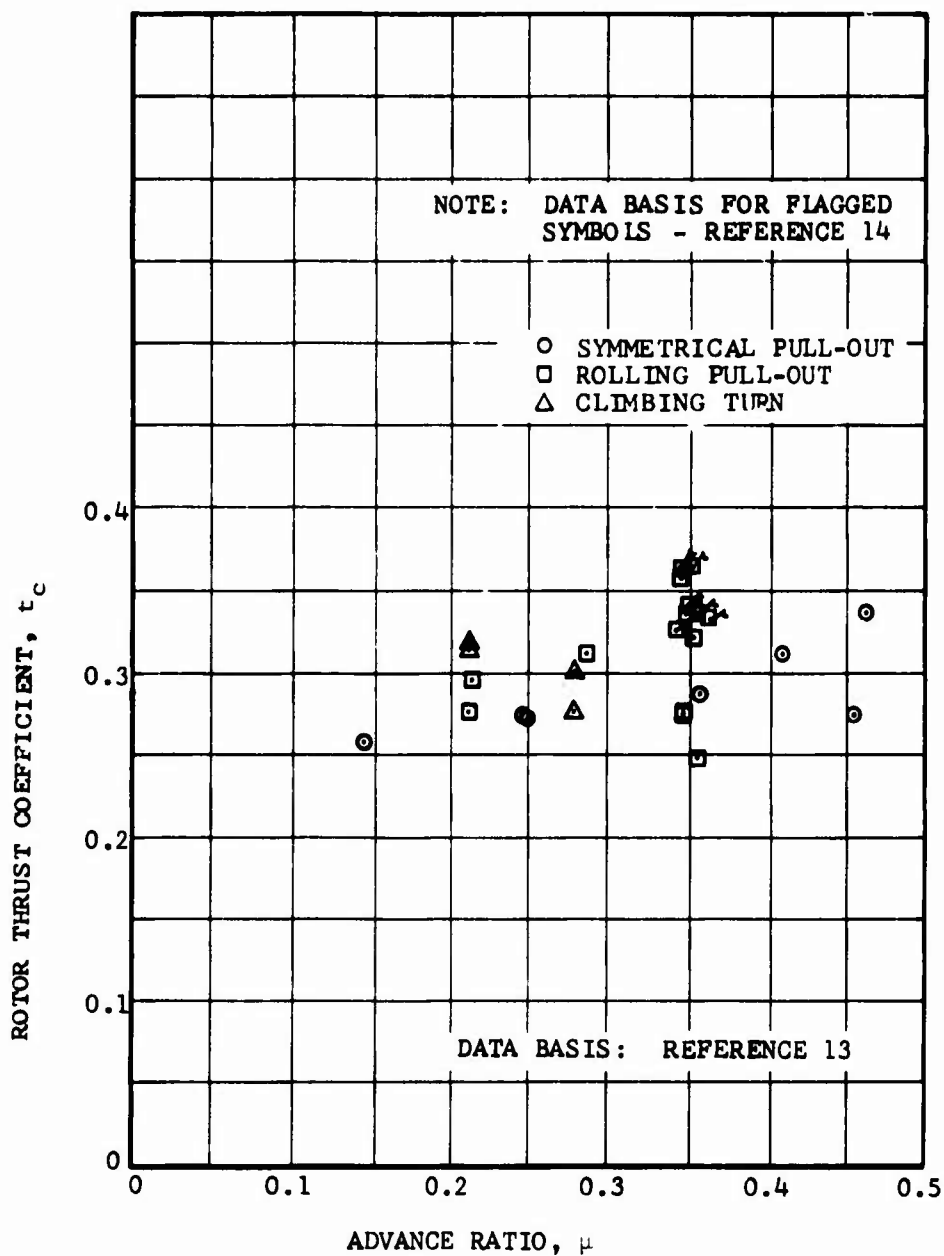


Figure 20. Rotor Thrust Capability
for AH-1G/J Helicopter



The above data on the different types of rotor systems indicate the average blade loading which should not be exceeded for the various reasons stated above. A $t_c-\mu$ curve can be used as a basis for comparison of the transient g-capability of different rotors and helicopters by taking the ratio of maximum t_c , for the speed and type of rotor, to the t_c in one-g flight at the altitude of interest.

Simplified Maximum Thrust Model

The above data indicate that the thrust limitations of different rotor systems are based on considerations of vibration, controllability, and fatigue life. In the event that flight test data are not available to identify this limit, a method is needed to give a reasonable approximation. An aerodynamically limited value of thrust coefficient (t_c) at different advance ratios (μ) can be computed if the variation of maximum lift coefficient with Mach number for the blade section is known. The mathematical model for this computation is illustrated in Figure 21. In the reverse flow region, zero rotor lift is assumed. In the retreating blade region, the blade sections are assumed to be at the maximum lift coefficient for the local Mach number. The lift in the advancing blade region is computed using the maximum lift coefficient out to the blade station at which the resulting lift moments of the advancing and retreating blades are equal and opposite. The lift is assumed to be zero outboard of that station. The effect of pitch rate on the rotor is accounted for by increasing the pitching moment which the rotor must balance. This causes a reduction of stall on the retreating blade and an increase of thrust on the advancing blade.

The results of this simplified mathematical representation are shown in Figures 22 and 23 for the AH-1J helicopter and the CH-3C helicopter. The results of this model are not satisfactory for predicting the maximum thrust for a teetering rotor system such as used by the AH-1J. For the articulated rotor, a higher thrust was predicted than was obtained. Several explanations can be offered for the lack of correlation. One such explanation is that two-dimensional C_L -Mach numbers were used. Another reason is that the articulated rotor is limited by other problems before reaching its maximum thrust capacity. Unsteady aerodynamic effects are known to increase the attainable maximum lift coefficient of an airfoil. The conditions under which this occurs, i.e., high rate of change of angle of attack, do occur on the rotor but are not considered in this simplified model. A derivation of the equations used in the simplified math model can be found in Appendix B along with a copy of the computer program.

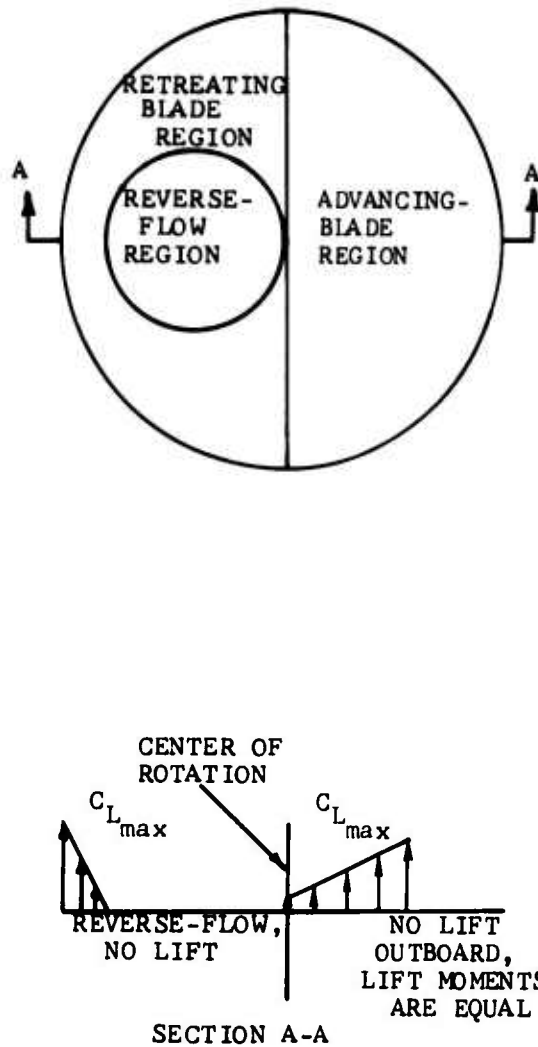


Figure 21. Analytical Model for Maximum Rotor Thrust



BELL HELICOPTER COMPANY

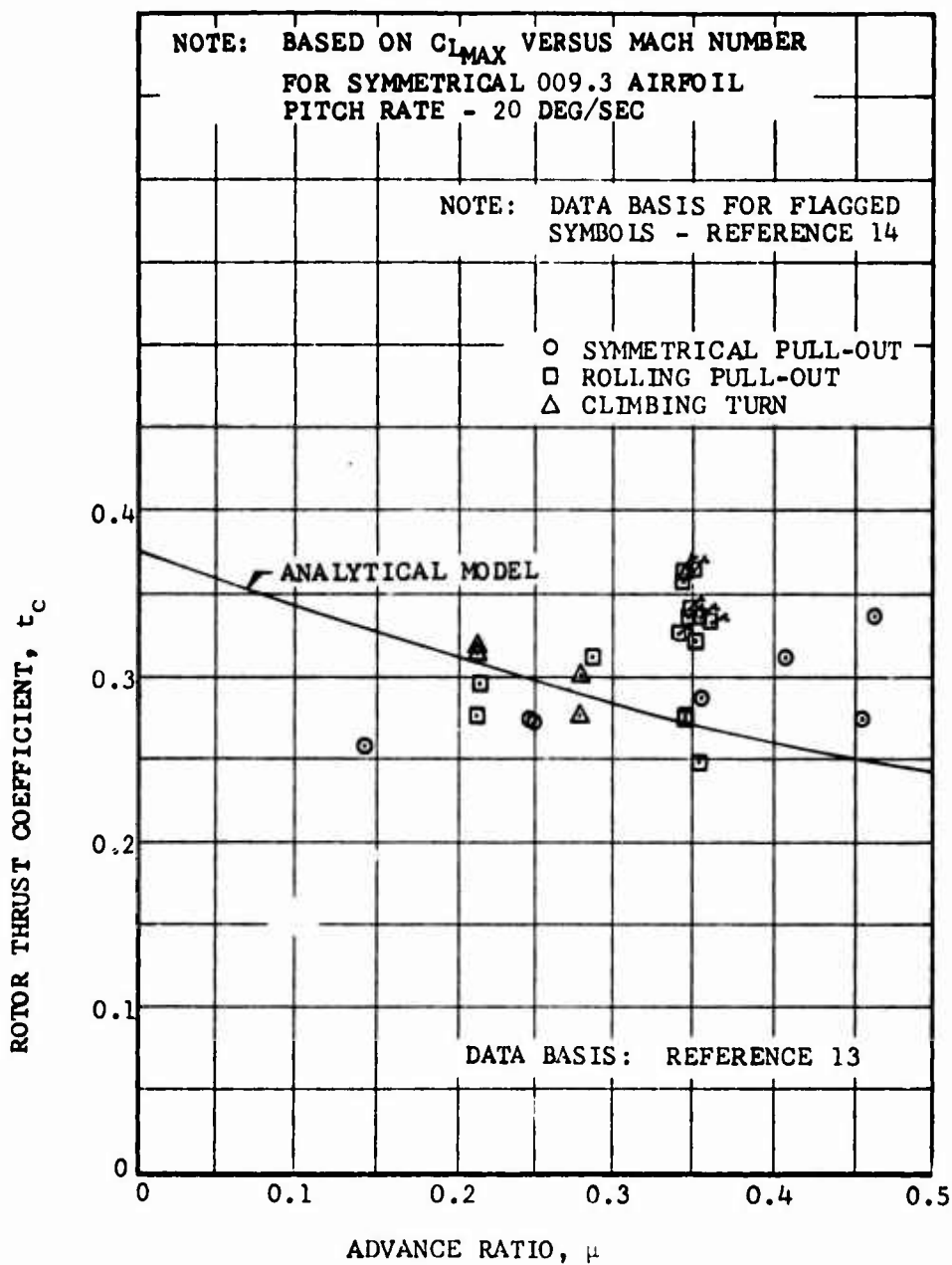


Figure 22. Maximum Thrust Predicted by Simplified Analytical Model for AH-1J Helicopter



BELL HELICOPTER COMPANY

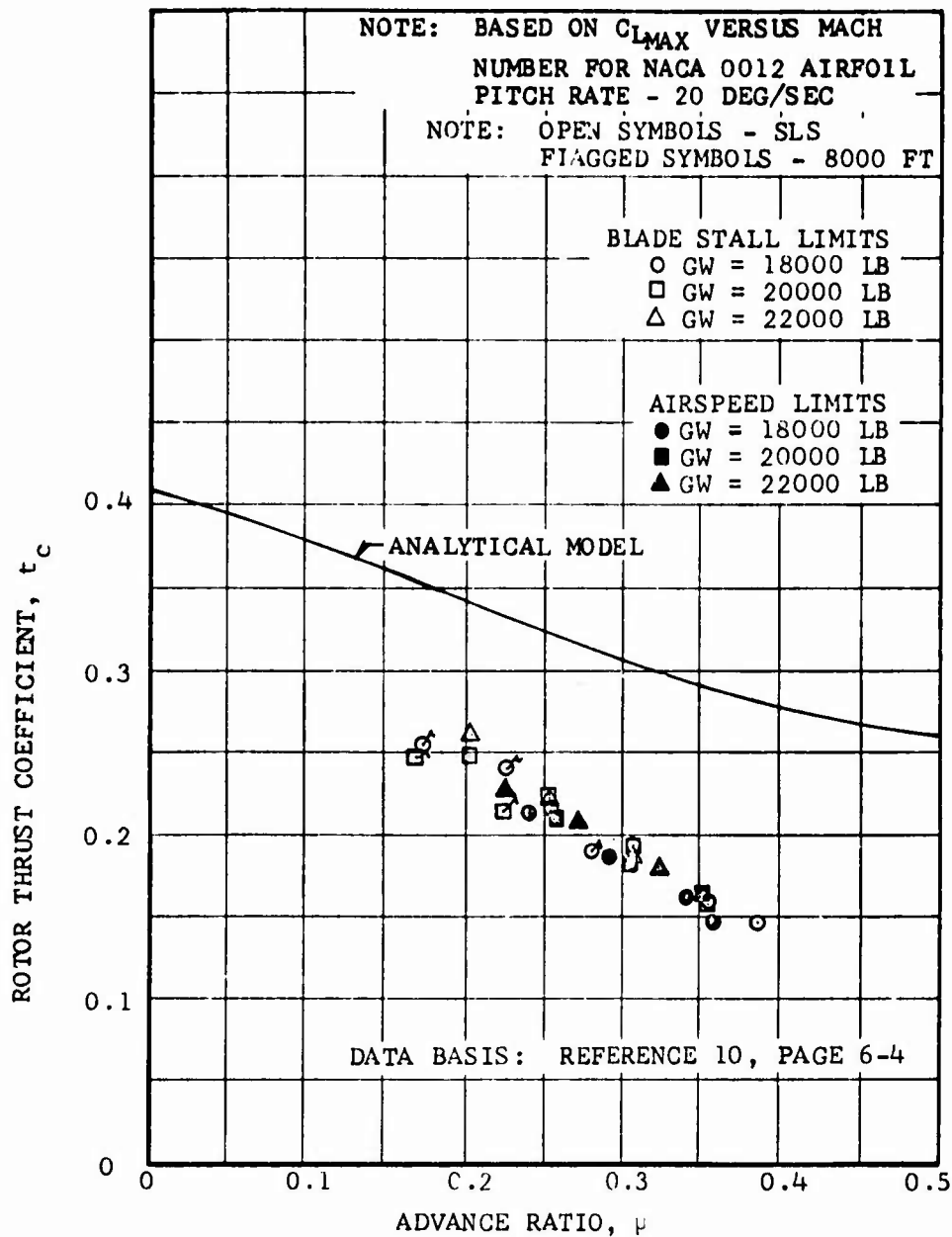


Figure 23. Maximum Thrust Predicted by Simplified Analytical Model for CH-3C Helicopter



DETERMINATION OF INPUT COEFFICIENTS

The power equations were developed specifically for predicting the total power required for the AH-1G helicopter. However, these equations are capable of predicting the total power required for different single-main-rotor helicopters within the accuracy required for flight path simulation. A set of input coefficients can be determined from the helicopter's speed-power data at different gross weights and from certain physical parameters of the helicopter. Below is a discussion and example of a method to determine the input coefficients for the power equations.

Sensitivity of Parameters

The limitations of the power equations in representing complicated rotor aerodynamics for different rotor systems should be appreciated. In some cases, the equations may not be capable of representing the flight test data. In general, the correlation between flight test data and computed data is good. The following method is only a tool to arrive at an initial starting point. Care must be exercised in choice of the input coefficient if the values from the INPUT program are not reasonable. By making small changes in the input data, correlation with flight test data can be improved.

In order to make the necessary changes in the input data, the influence of each parameter on the power curve must be understood. A discussion of each of the input parameters is given below. The AH-1G helicopter parameters are used in the graphic representations.

1. Equivalent Flat-Plate Drag (f): This parameter represents the contribution of the fuselage, wing, elevator, fin, and rotor hub to the parasite drag term. The change in horsepower with speed and f is presented in Figure 24. For example, by increasing f by 5 square feet, the horsepower curve can be increased by 142 at 140 knots to match flight test data while increasing the horsepower at 60 knots by only 10.

2. Constant Term in Rotor Blade Drag Equation: δ_0 is the constant in the drag equation $C_D = \delta_0 + \delta_2 \alpha^2$. This term accounts for the profile drag of the rotor blade at zero angle of attack. Increases in δ_0 primarily result in a constant shift of the power curve. However, the effect of speed on δ_0 is also important and is presented in Figure 25. If the calculated power differs from the flight test data by an approximately constant value, then a change in δ_0 would improve correlation.

3. Angle of Attack Term in Rotor Blade Drag Equation: δ_2 is the angle of attack coefficient in the drag equation $C_D = \delta_0 + \delta_2 \alpha^2$.



BELL HELICOPTER COMPANY

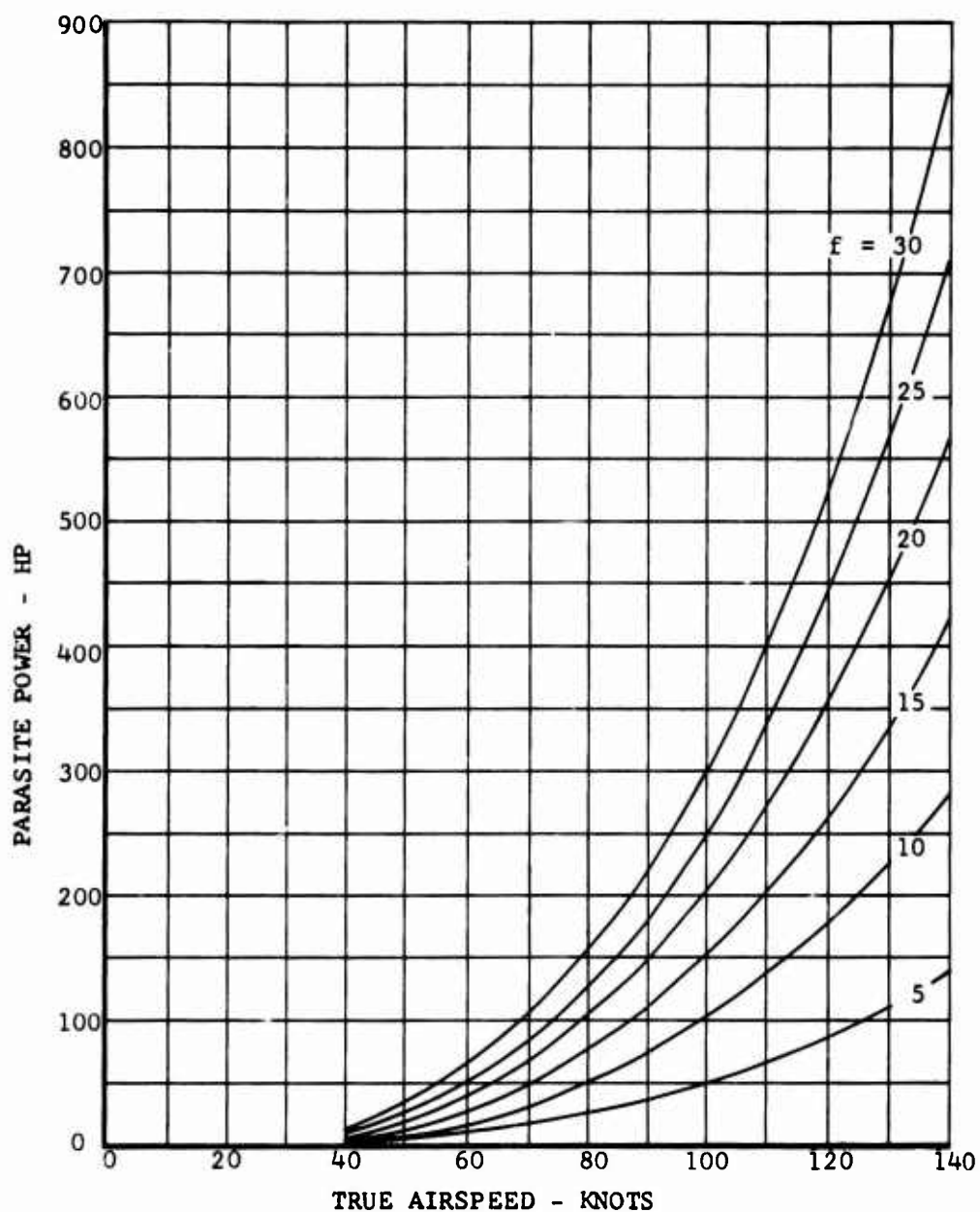


Figure 24. Variation of Parasite Power with True Airspeed and Fuselage Drag, f



BELL HELICOPTER COMPANY

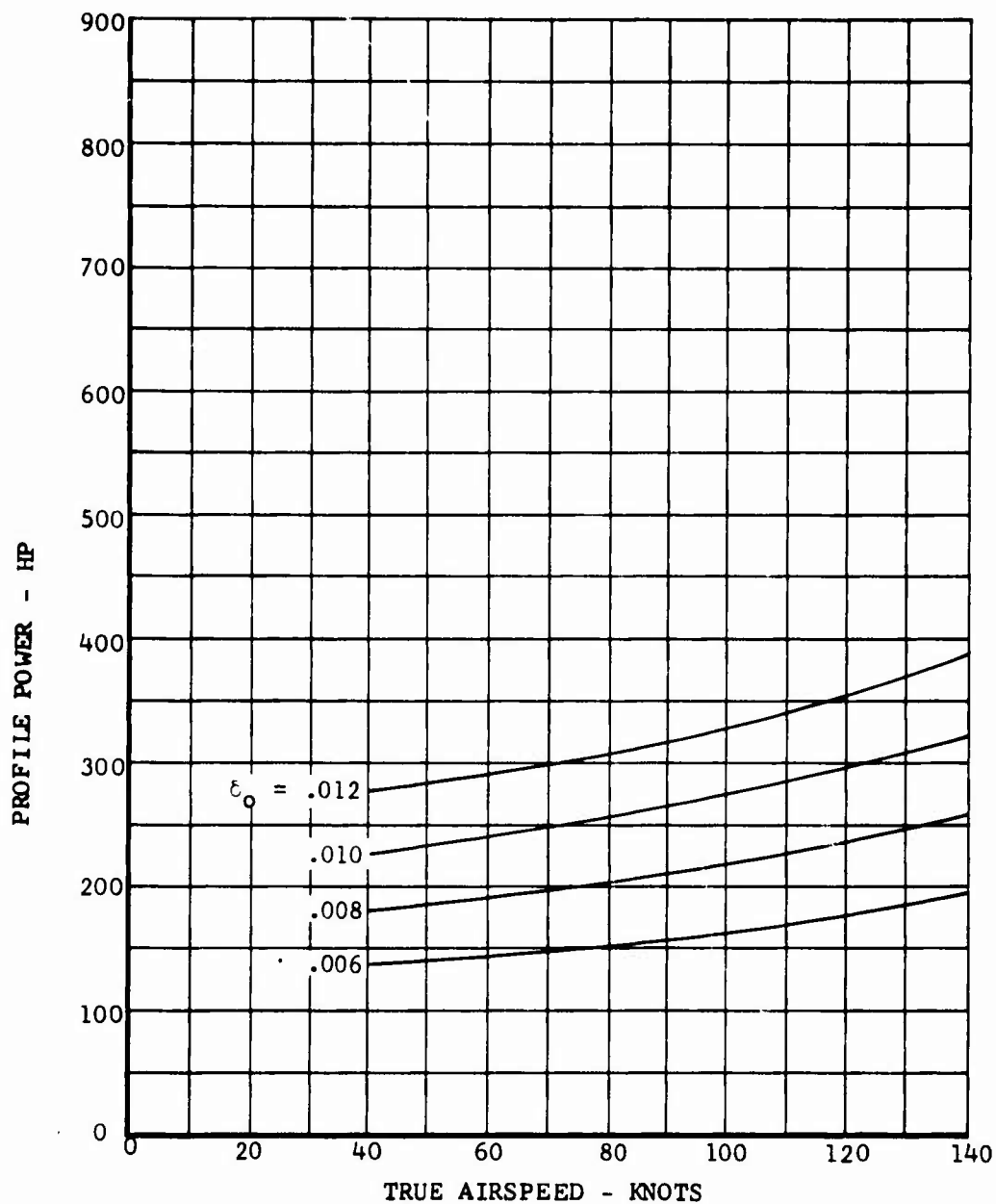


Figure 25. Variation of Profile Power with True Airspeed and Blade Profile Drag, δ_0



This term accounts for the profile drag of the rotor blade with angle of attack. The speed effect on δ_2 is presented in Figure 26. The difference in power between different gross weights in hover comes from the contribution of δ_2 and changes in induced power. If the calculated power between two different gross weights differs from flight test data, then a change in δ_2 would improve correlation.

4. Rotor Induced Velocity: The variation of induced velocity with airspeed is presented in Figure 27. A weighting factor is used to increase the rotor induced velocity at low airspeeds to improve correlation with measured data. Usually this factor is equal to one above a speed of 60 knots. This factor varies with airspeed and is valid for several single rotor helicopters.

5. Compressibility Critical Mach Number: Decreases in critical Mach number result in increased power required at high speeds as shown in Figure 28. Choice of the two-dimensional critical Mach number for a given blade section may be a good initial value, but the final value may differ as a result of not knowing the lift coefficient at which the blade is operating and not knowing the rotor's aerodynamic environment. If the calculated power does not increase as rapidly as the flight test data and the tip Mach number is high, then decreasing the critical Mach number will result in improved correlation.

6. Stall: The prediction of stall actually requires a very sophisticated analysis which calculates the angle of attack at each radial and azimuth station. The method for predicting stall in these power equations is empirical and is a function of a divergent value of t_c versus μ . The amount of stall for a given flight condition depends on the amount by which the critical value of t_c is exceeded. Therefore, the critical question becomes the determination of this divergent t_c versus μ curve for each helicopter. From the flight test data, stall is usually seen as a rapid rise in power required at high speed. If the tip Mach number is not high and the flight test data increases suddenly at high speeds, then lowering the divergent t_c versus μ curve would improve correlation. The increase of stall horsepower is a function of the amount t_c exceeds the divergent value of t_c as presented in Figure 29. The divergent t_c versus μ curve for the AH-1G helicopter is

$$t_{c \text{ div}} = .1 + \frac{.2}{\sqrt{1 + 50\mu^2}} \quad (47)$$

Very recent data have indicated that blade flapping inertia significantly affects the divergent t_c versus μ curve. This effect should be investigated further.



BELL HELICOPTER COMPANY

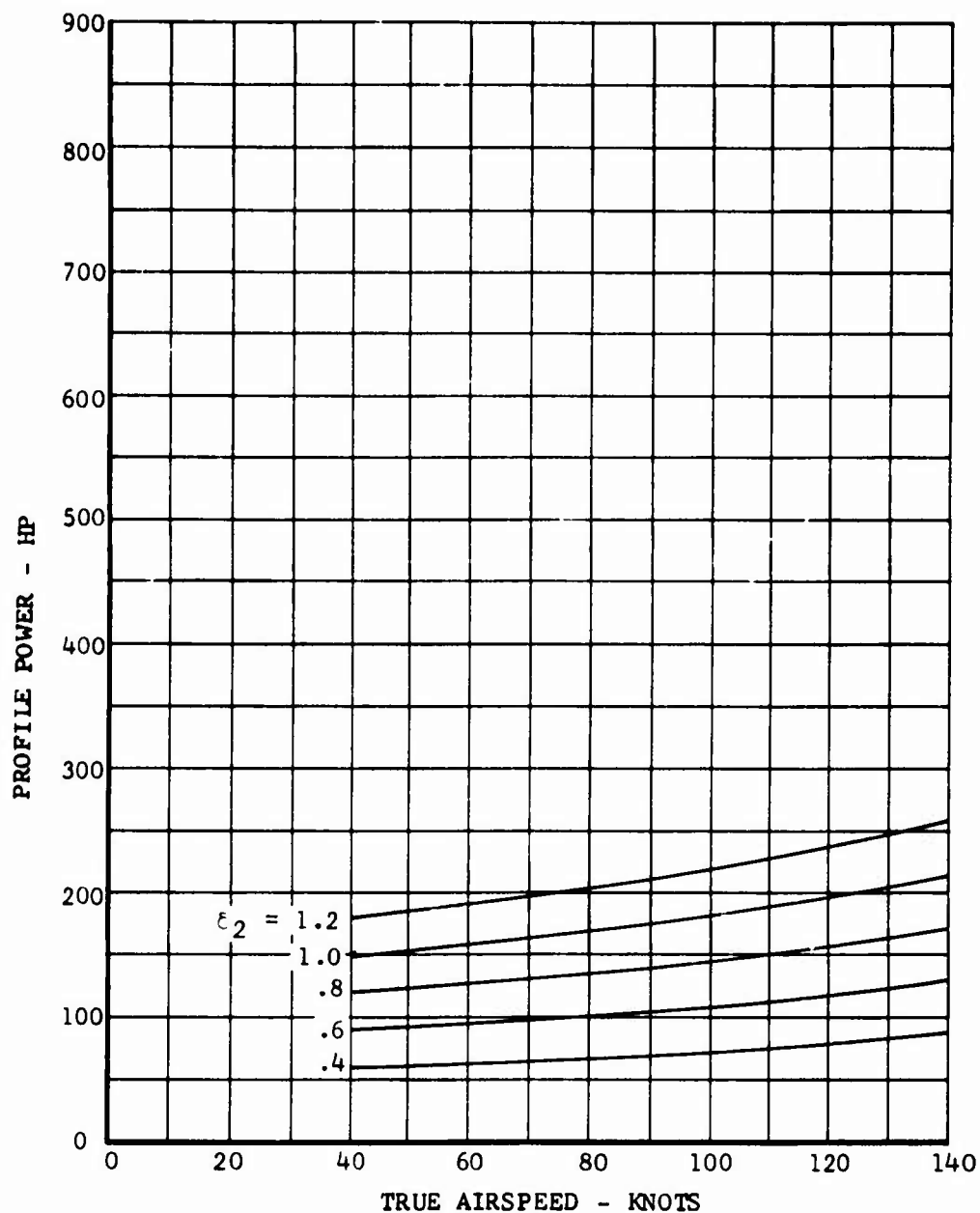


Figure 26. Variation of Profile Power with True Airspeed and Blade Profile Drag, δ_2



BELL HELICOPTER COMPANY

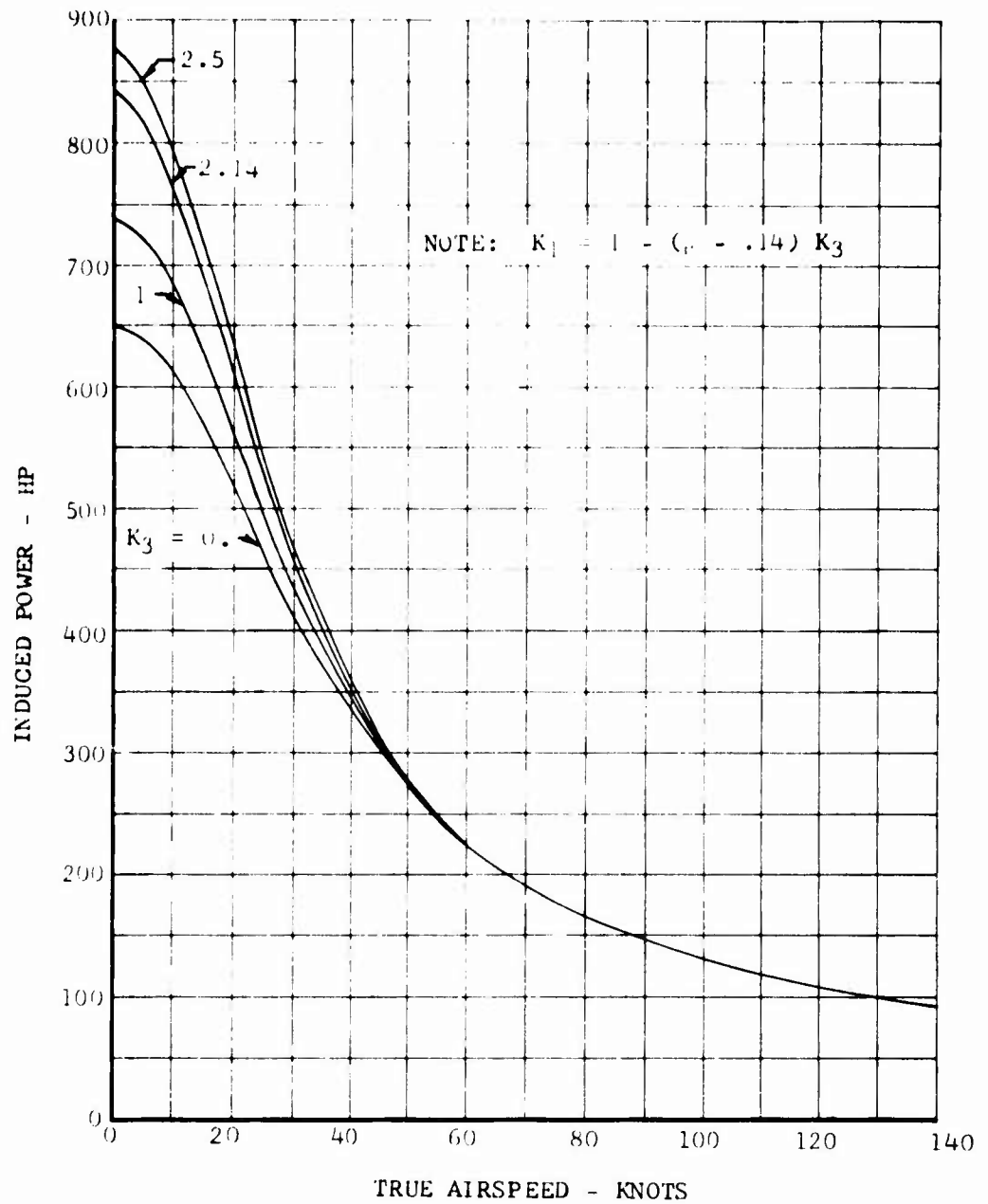


Figure 27. Variation of Induced Power with True Airspeed and Weighting Factor, K_1



BELL HELICOPTER COMPANY

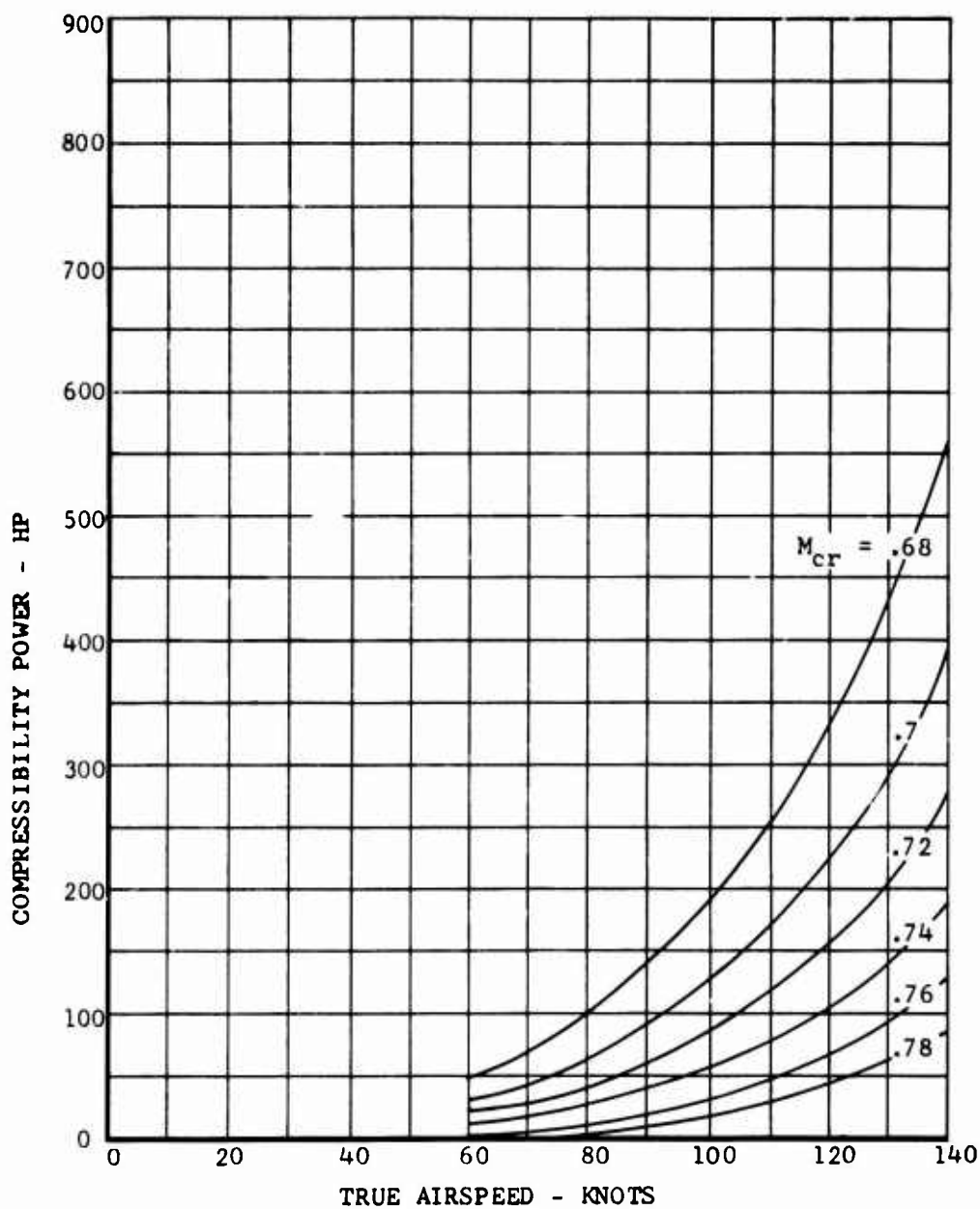


Figure 28. Variation of Compressibility Power with True Airspeed and Critical Mach Number



BELL HELICOPTER COMPANY

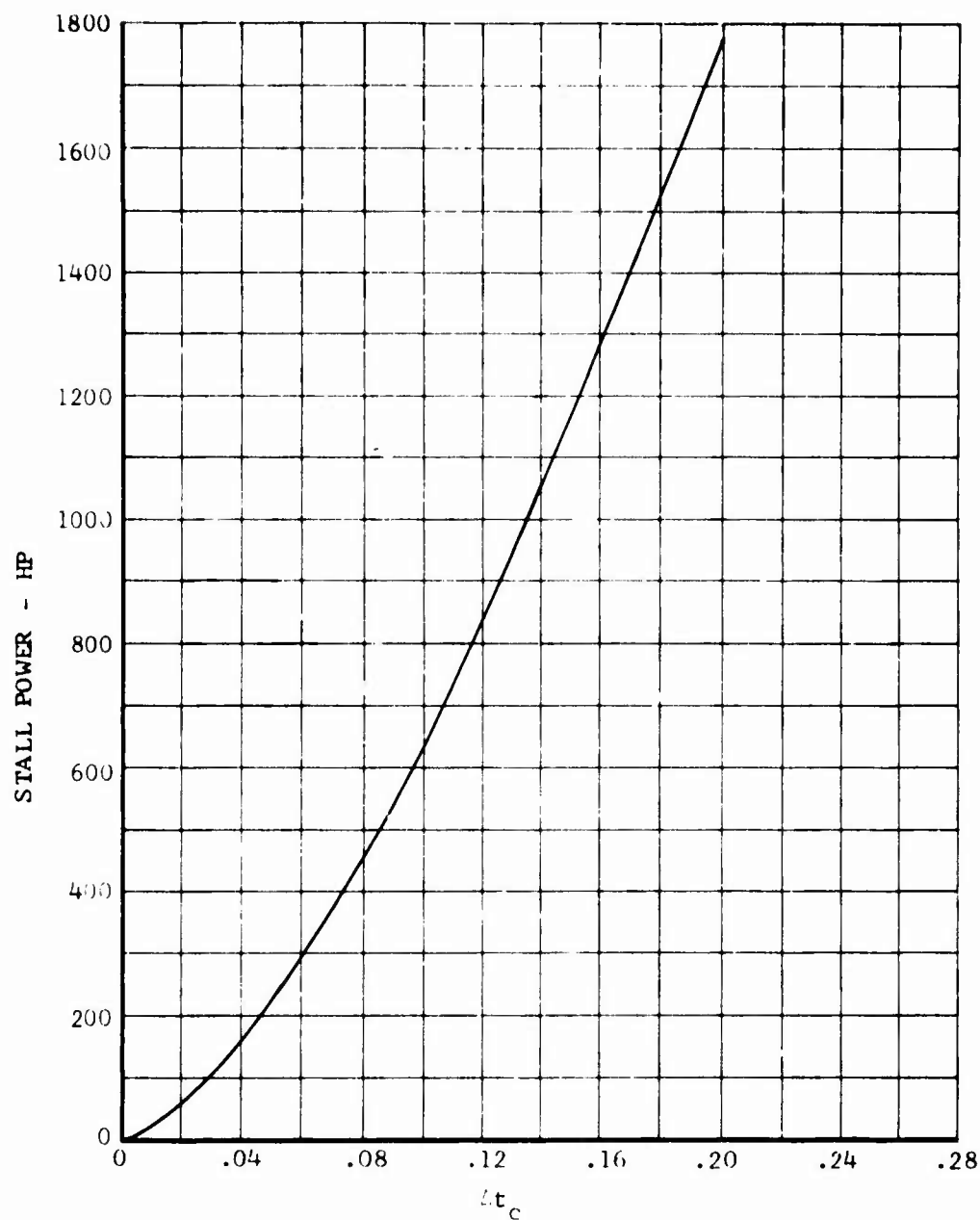


Figure 29. Stall Power Versus Δt_c



Methodology

The INPUT program approximates the coefficients to the power required equations based on the given power required versus airspeed data. The correlation between predicted and actual values of power is given in terms of percent error. The calculated coefficient may be refined further by the user to improve correlation. It is the intent of this program to only approximate these values while the final coefficients are determined by the user.

A flow diagram of the logic used for this program is presented in Figure 30. A copy of this program is in Appendix C. The required data for the program are: (1) Power required versus airspeed for two different gross weights at the same altitude, density, and rotor rpm; (2) hover power required out of ground effect for the same conditions in (1); and (3) physical parameters of the helicopter: rotor radius, rotor chord, number of blades, rotor tip speed, and estimated value of equivalent flat plate drag area.

Power data at three speeds and two weights are required for the actual computation of the input coefficients. These are hover, minimum power, and maximum speed desired. At each of these speeds a residual power is computed. This power results from the subtraction of each component of the power equation as they are determined from the total power. The remaining power represents the contributions of the components not yet determined. First, the induced power is calculated and subtracted from the total power for both gross weights. Now the difference in power at hover between the two gross weights is due to the δ_2 power term. Knowing this difference, δ_2 is computed. The contribution of δ_2 to power is now subtracted from the residual power term. Next the values of stall power are calculated and subtracted from the residual power term. At V_{MAX} , the difference in power (ΔHP) between the two gross weights will reflect the amount of compressibility power through the ΔM calculation which is a function of t_c , ($\Delta M = M_{TIP} - M_{Cr} + .75 t_c$). Now a slope of $\Delta HP / (\Delta M_2 - \Delta M_1)$ is computed where 1 and 2 refer to the gross weights. Then values of M_{Cr} are swept until the value of $(HP_{c2} - HP_{c1}) / (\Delta M_2 - \Delta M_1)$ is equal to the computed value of $\Delta HP / (\Delta M_2 - \Delta M_1)$. Knowing the value of M_{Cr} , the compressibility power is calculated and subtracted from the residual power term.

The value of δ_0 is determined from consideration of the residual power at V_{MIN} power speed for the lighter gross weight.

The power required by the input value of drag area is subtracted from the residual power at the speed for minimum power for the lighter gross weight. At V_{MAX} , the power required by δ_0 is

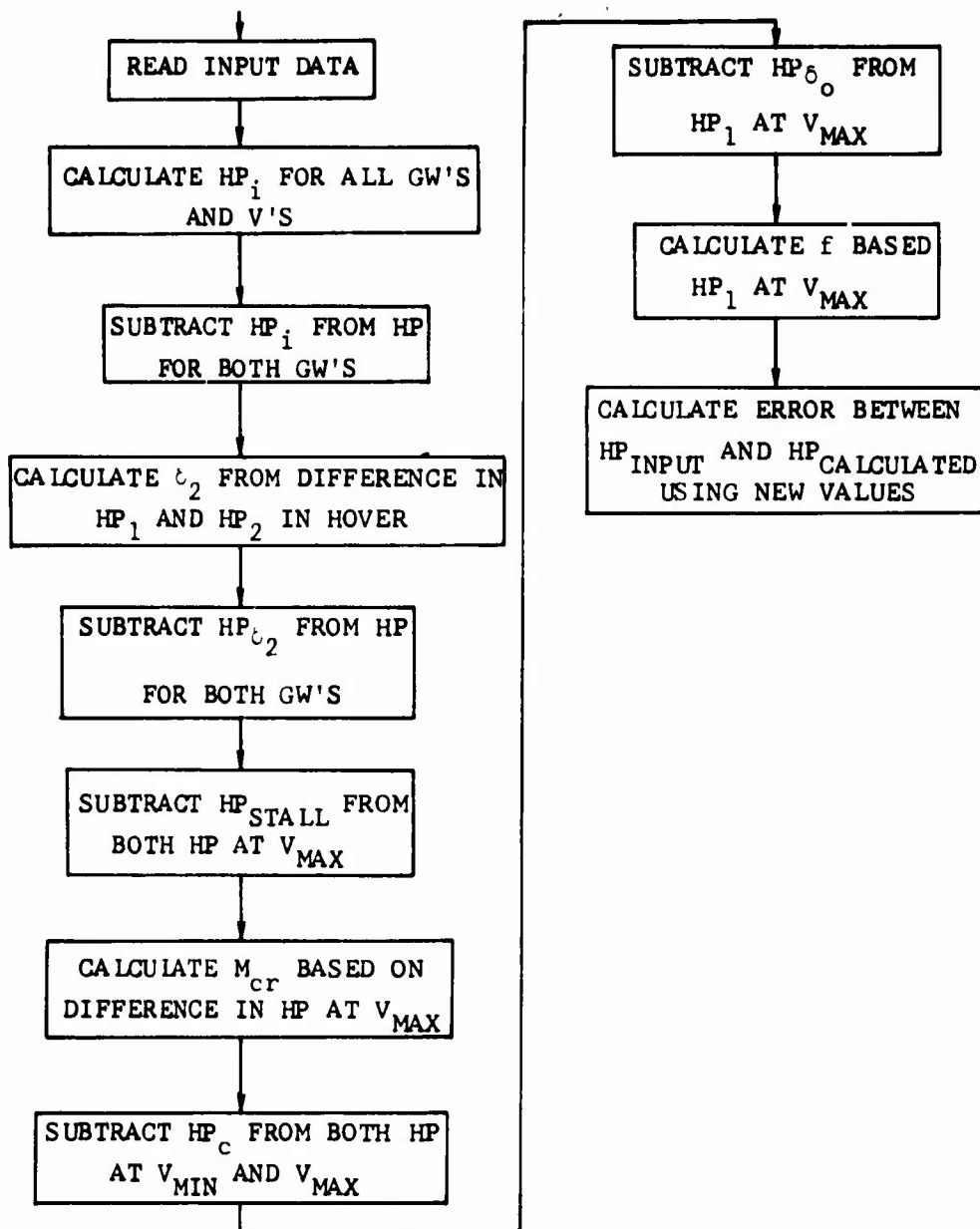


Figure 30. Flow Diagram for Input Coefficient Program



subtracted from the residual power term leaving the power required for f . The equivalent drag is calculated from this power. Finally the total power required is calculated based on the computed coefficients and compared to the input value of horsepower.

Items of importance to note when using the above method are discussed below. The value of the weighting factor used for the induced velocity strongly affects the value of δ_2 . If the values of δ_2 are unreasonable, then the weighting factor K_3 is probably incorrect. Some typical values of K_3 are given in Figure 31 for different helicopters. The method by which these values are chosen follows.

First, the power is computed for hover using standard values of input coefficients such as the ones for the AH-1G helicopter. Then the value of K_3 is increased until correlation is improved. However, reasonable values of δ_0 , δ_2 , and M_{cr} must be used. This factor is used to increase the induced velocity to improve power correlation in the low speed range and account for download on the fuselage in hover.

Also some modification is required in the angle of attack expression for the different helicopters. This change yields improved correlation while maintaining reasonable values of δ_0 and δ_2 . The average angle of attack of the rotor is approximated by $\left(\frac{7C_T}{ca}\right)$. However, for the CH-3C and CH-53 helicopters, better results were achieved by using $\left(\frac{9C_T}{ca}\right)$. In the input coefficient program, the angle of attack is approximated by $\left(\frac{K_6 C_T}{ca}\right)$. Values of K_6 for the various helicopters are presented in Figure 31.

The only parameter not directly determined by the INPUT program is the amount of stall power. The user must input the divergent t_c versus μ curve. The value of f is influenced by the amount of stall power. For example, if a small amount of stall power is calculated at V_{MAX} , the program will calculate a large value of f to match the power at that point. This f results in too much power in the immediate speed range and the percent error will be large. By increasing the amount of stall power, the new f will decrease and result in improved correlation.

To aid the user in determining the proper divergent t_c versus μ curve, data from Reference 18 are presented in terms of a t_c versus μ curve in Figure 32. This data approximates the t_c value at which stall is encountered. This region is bounded by the lower line for light stall ($\alpha = 12$ degrees) and the upper line ($\alpha = 16$ degrees) for heavy stall. The divergent t_c versus μ curve from Equation 47 is also shown.



HELICOPTER	K_3^*	K_6^{**}
AH-1G	2.14	7
UH-1H	2.30	7
CH-3C	2.50	9
CH-53	2.50	9
OH-6A	2.14	7
OH-58A	2.14	7

$$* \quad K_1 = 1 - (\mu - .14) K_3$$

$$** \quad \left(\frac{K_6 C_T}{c_a} \right)$$

Figure 31. Typical Values of K_3 and K_6 for Various Helicopters



BELL HELICOPTER COMPANY

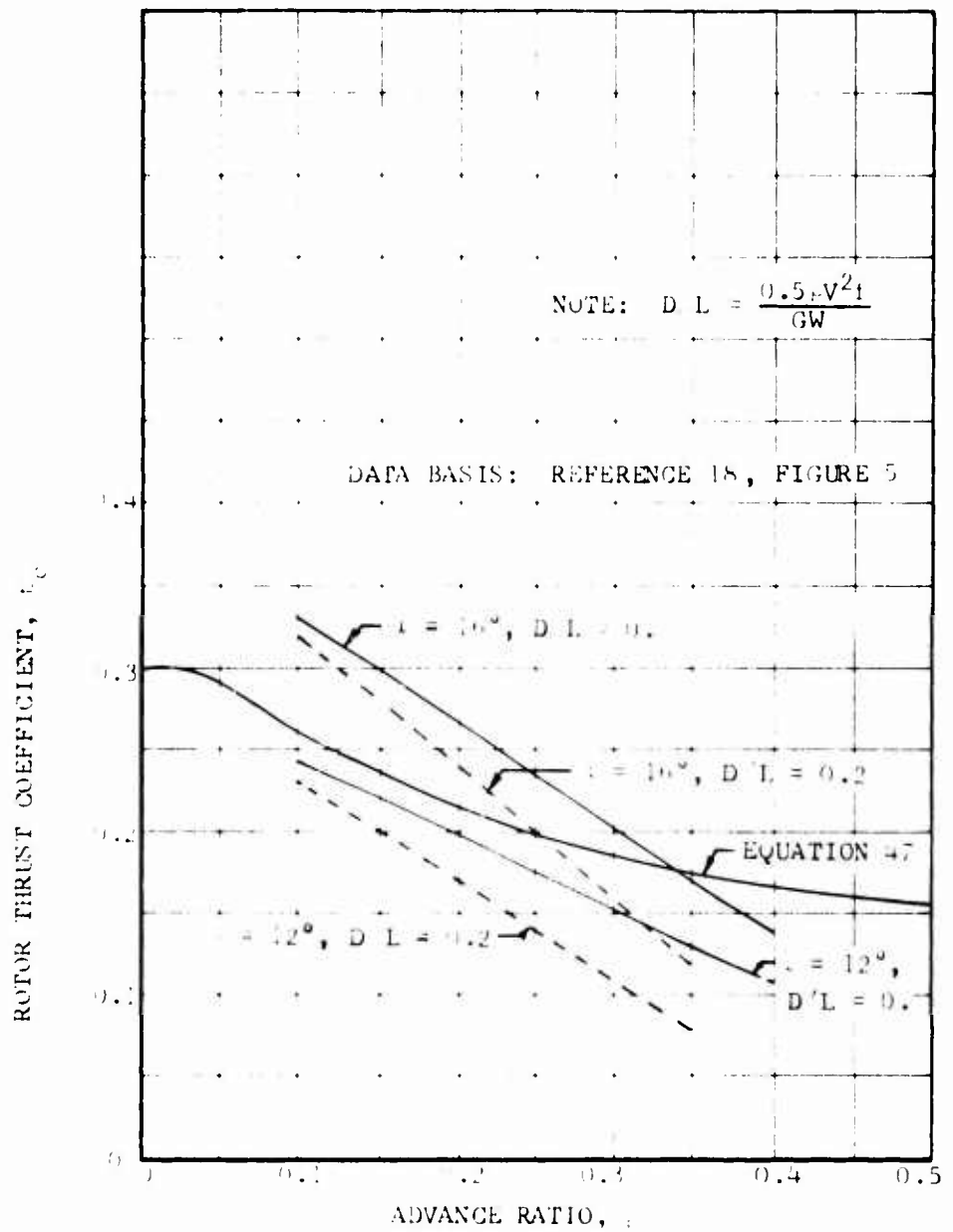


Figure 32. Divergent Rotor Thrust Coefficient versus Advance Ratio



Results

Several current operational helicopters were considered in the evaluation of the equations. The necessary physical parameters for these helicopters are given in Table I. A set of input coefficients for these helicopters is presented in Table II.

A comparison between predicted data and flight test data for the various helicopters is presented in Figures 33 through 38. The predicted data used the coefficients presented in Table II. This comparison was made using representative level flight performance for the different helicopters. Based on the flight test data used, the equations yield satisfactory results for use in simulating flight paths of these helicopters.

Example Problem

The AH-1G helicopter is used to demonstrate the above methodology. A sample input/output of the input coefficient program (Appendix C) is presented in Figure 39. Power required versus airspeed is usually presented as shown in Figure 36 or Figure 38. If the data do not extend to include hover, then hovering out-of-ground-effect power data are needed as is the case in Figure 36. The data of Figure 36 can be reduced to dimensional terms using the following equations:

$$C_T = \frac{GW}{\rho A (\Omega R)^2} \quad (48)$$

$$C_P = \frac{HP 550}{\rho A (\Omega R)^3} \quad (49)$$

$$\mu = \frac{V}{\Omega R} \quad (50)$$

From Figure 38, the power required data for the AH-1G helicopter for two different gross weights can be obtained. It should be noted that the power data at different gross weights must be at the same flight conditions, i.e., rotor rpm, density, and Mach number.

The order in which the power required data are input is important. A one-to-one correspondence must exist between the power required and velocity. In addition, the first point must always be the hover point, while the second point is the power required at the velocity for minimum power required. The input value of m determines which input velocity (v_c) is V_{MAX} . In the example, $m = 7$ means $V_{MAX} = 150$ knots, $m = 6$ would mean $V_{MAX} = 140$ knots, etc. Intermediate velocities are used to give insight into the degree of correlation obtained.



BELL HELICOPTER COMPANY

Helicopter	Type of Rotor System	Rotor Radius Ft	Blade Chord in	Number of Blades	Rotor Solidity	Tip Speed Ft/Sec	Blade Airfoil	Gross Weight Lb
AH-1G	Teetering	22	27	2	.0651	746	9 1/3" Symmetrical	7000
OH-58A	Teetering	17.65	13	2	.03897	654	11.3" Modified Droop Snoot	9500
OH-6A	Articulated	13.165	6.75	4	.0544	648	NACA 0015	2200
CH-3C	Articulated	31	18.25	5	.07808	659	NACA 0012	3000
YUH-1H	Teetering	24	21	2	.0464	814	NACA 0012	2900
CH-53A	Articulated	36.1	26	6	.1146	699	NACA 0012	15000
								22900
								7000
								9500
								23000
								40000

Table I. Dimensional Data for Various Helicopters

Helicopter	Configuration	f	ϵ_0	ϵ_1	δ_2	M_{cr}
AH-1G	Hog	19.5	.0075	0	1	.75
OH-6A	Clean	6	.0075	0	.59	.75
UH-1H	Clean	20	.0075	0	.59	.77
OH-58A	Clean	9.7	.0075	0	.59	.75
CH-3C	Clean	35	.0075	0	.59	.75
CH-53A	Clean	60	.0085	0	.59	.75

Table II. Input Coefficients for Various Helicopters



BELL HELICOPTER COMPANY

OH-58A
CLEAN CONFIGURATION
RPM - 354

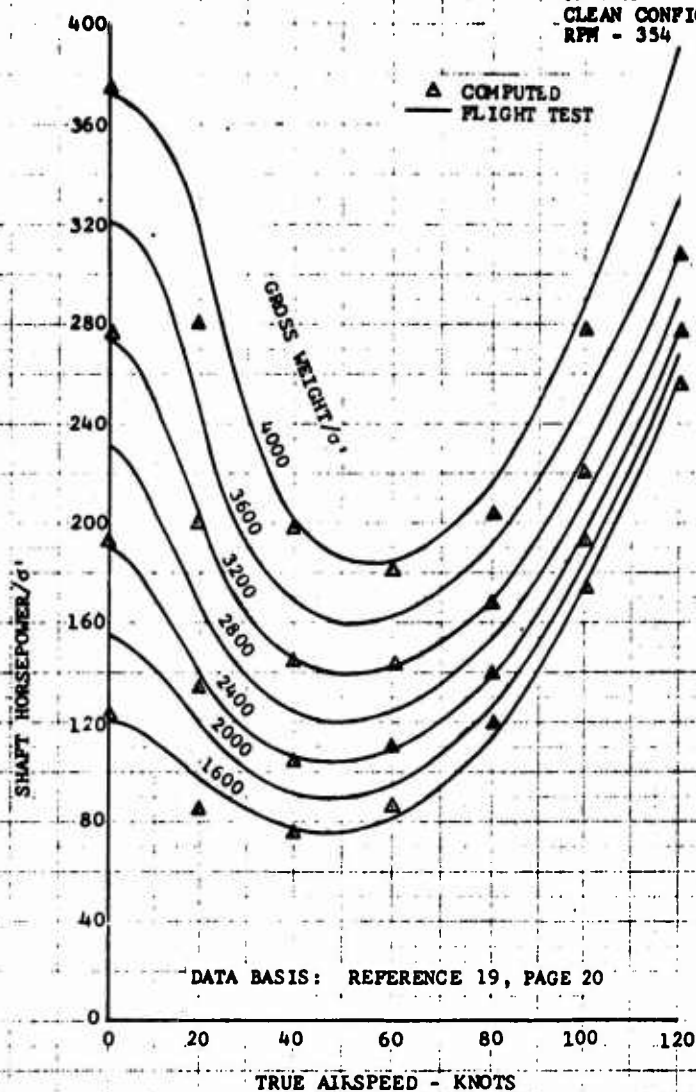


Figure 33. Level Flight Performance for OH-58A Helicopter



BELL HELICOPTER COMPANY

YUH-1H
CLEAN CONFIGURATION
GW = 8487 LB
H = 3,140 FT
AMBIENT TEMP = 25°C
RPM = 324
C_T = .003454

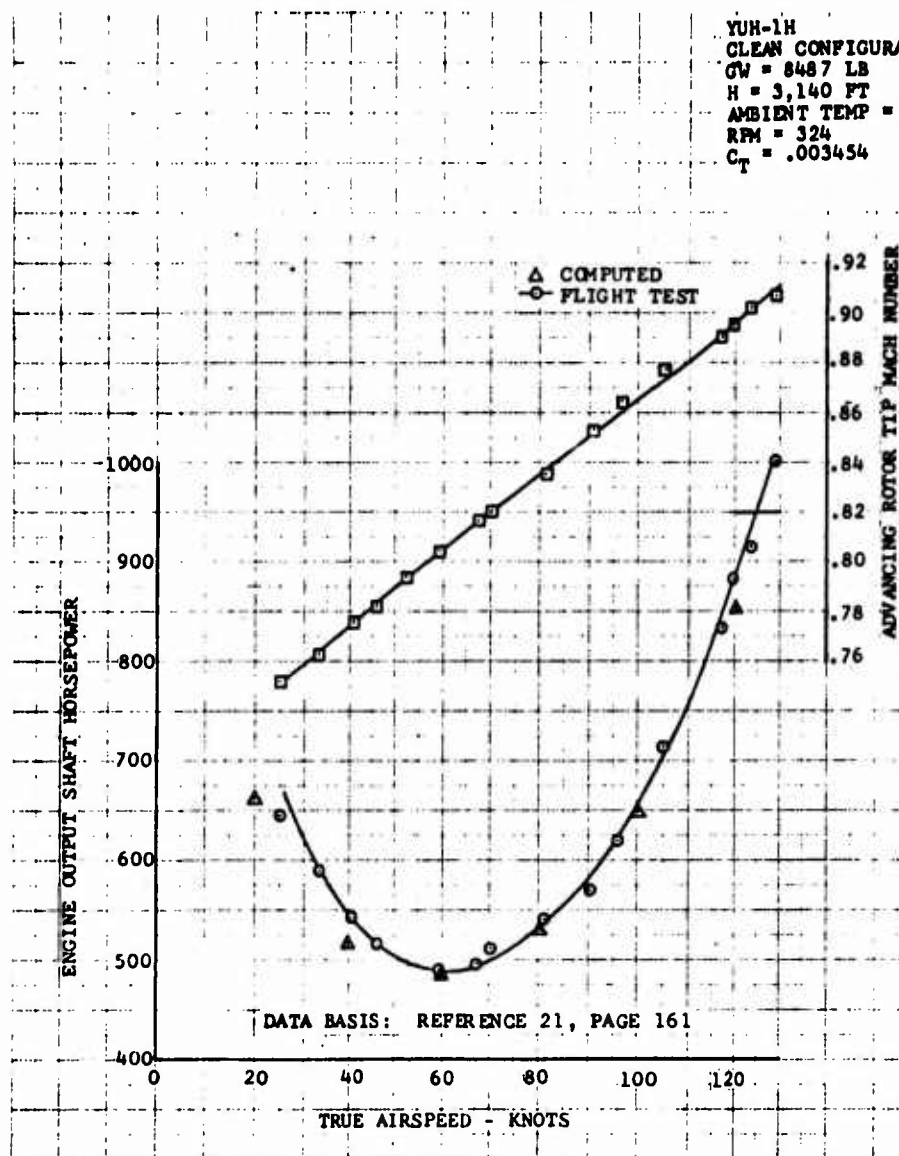


Figure 35. Level Flight Performance for YUH-1H Helicopter



BELL HELICOPTER COMPANY

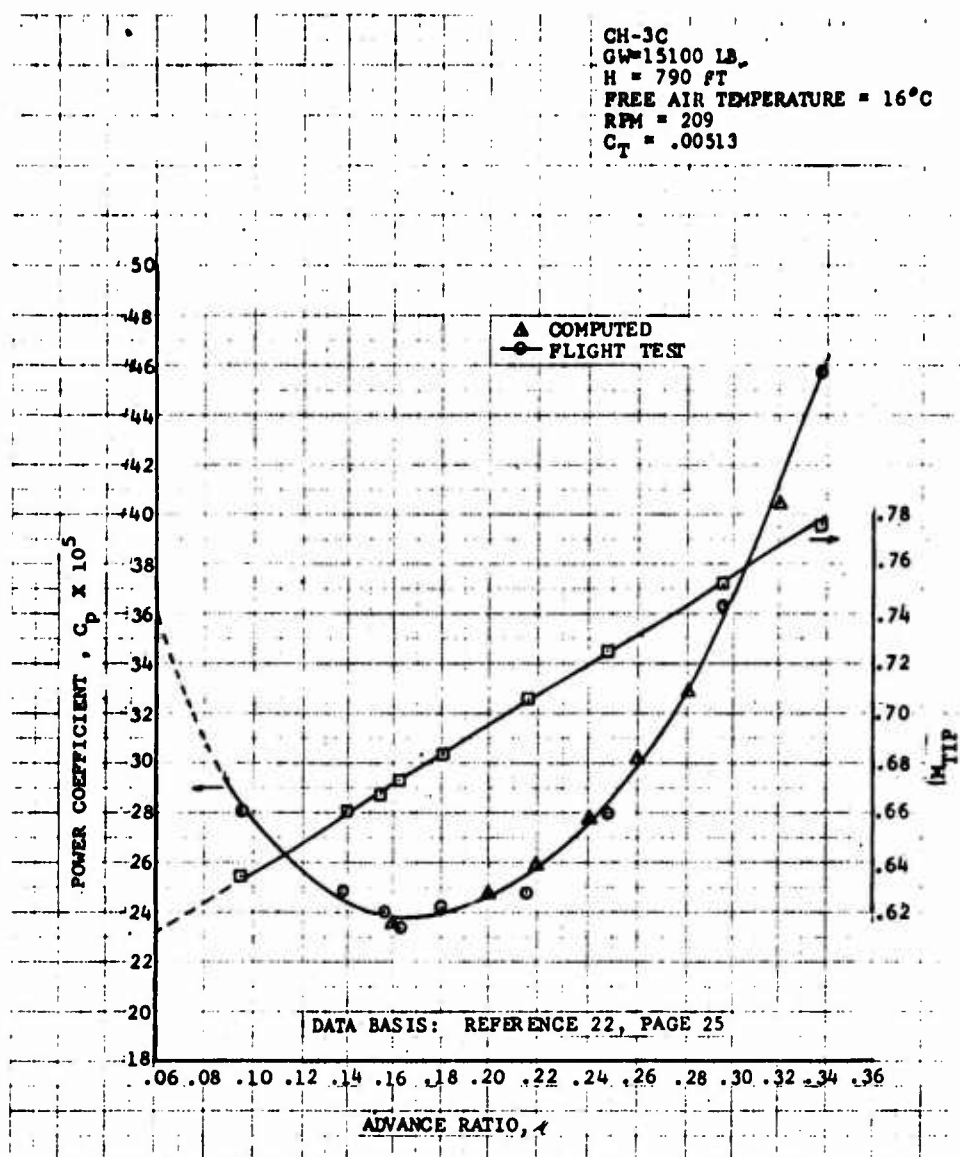


Figure 36. Level Flight Performance for CH-3C Helicopter



BELL HELICOPTER COMPANY

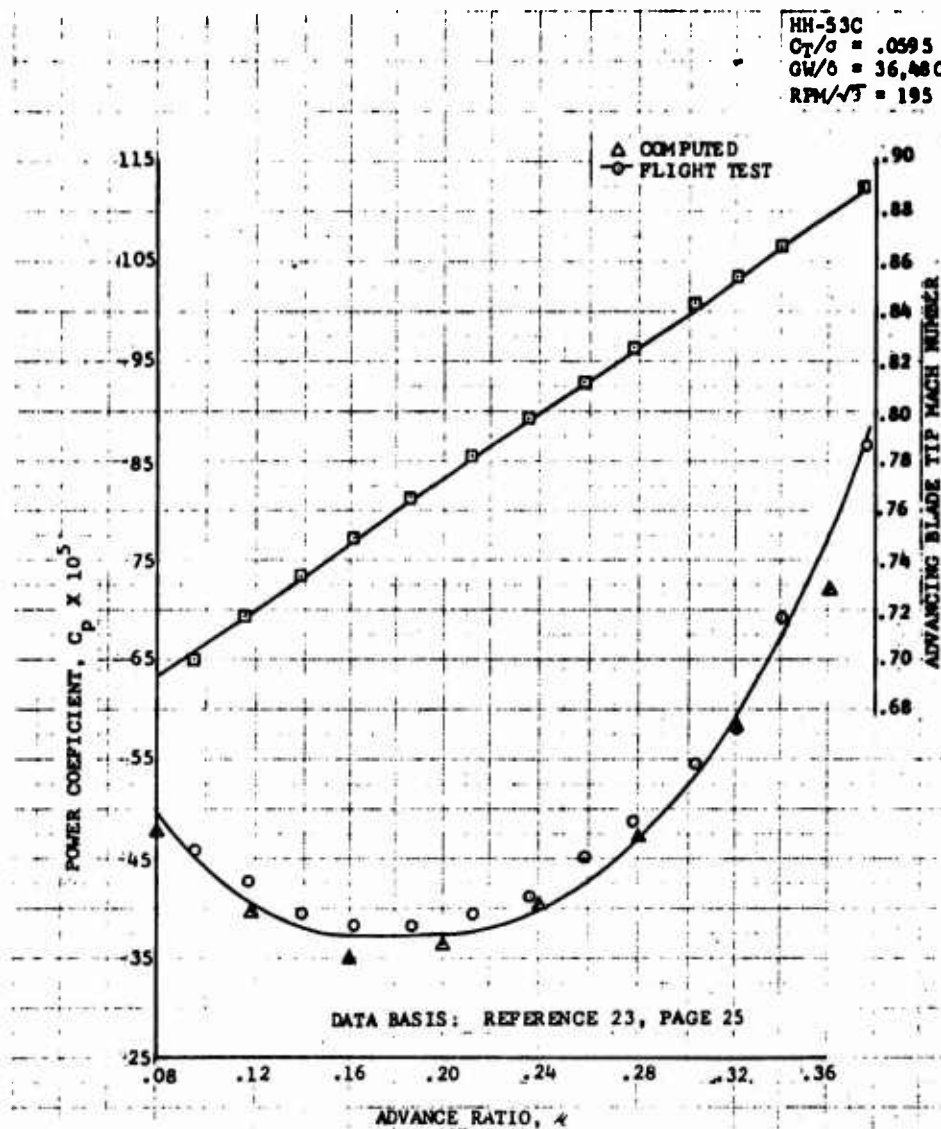


Figure 37. Level Flight Performance for HH-53C Helicopter



BELL HELICOPTER COMPANY

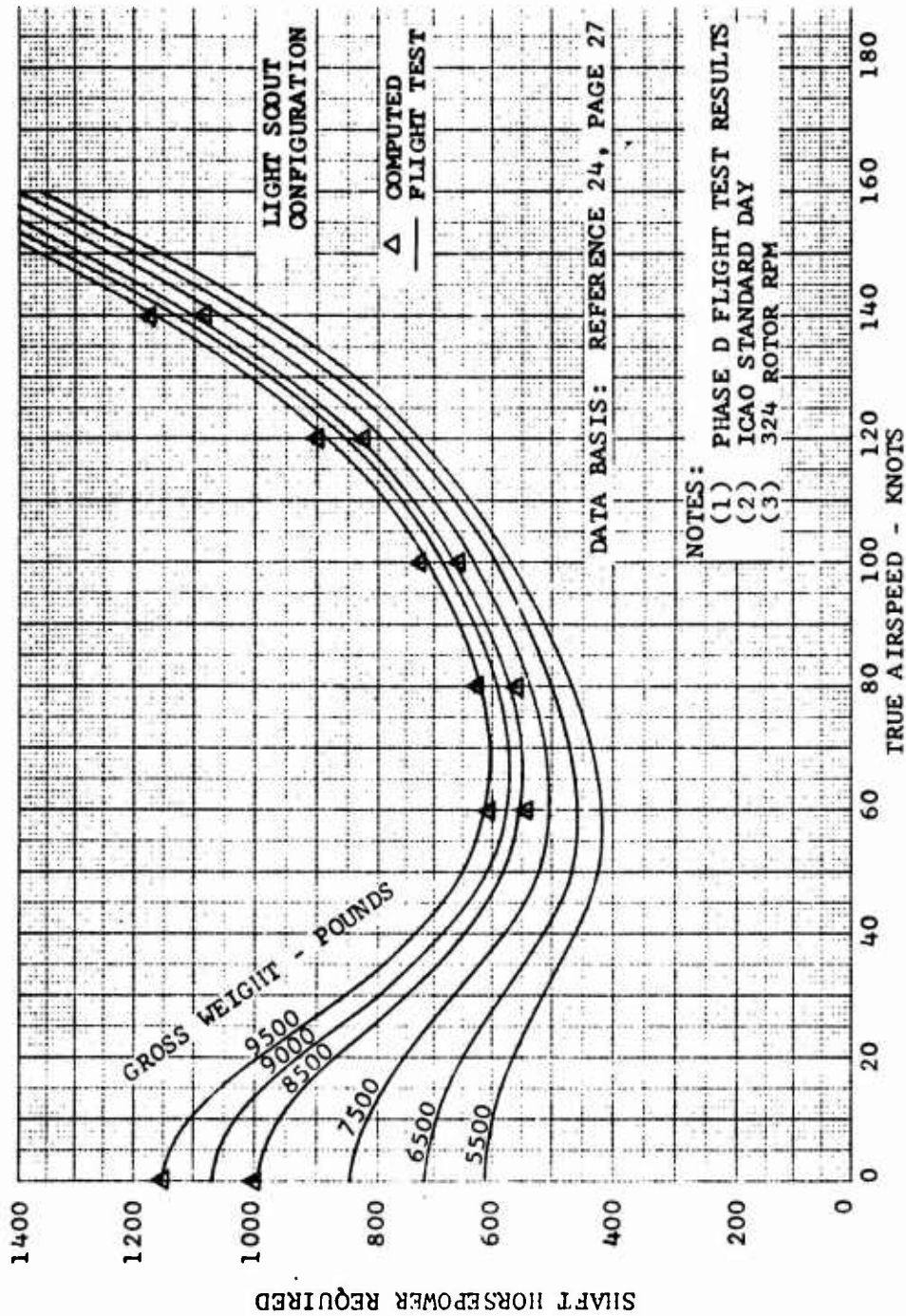


Figure 38. Level Flight Performance for AH-1G Helicopter.



```

x001
.1
1
001(1)
1000 555 570 665 830 1100 1280
0,2(1)
1150 010 020 710 835 1100 1300
vc(1)
0 50 80 100 120 140 150

```

$$\begin{array}{r} 22 \\ \times 1.25 \\ \hline 110 \\ 440 \\ 000 \\ \hline 27.50 \end{array}$$

4
 oat
15
 641
6500
 642
 9500

SW	V	HP	HPC	ERROR	PERC
SW= 3500.	V= 0.	HP= 1600.00	HPC= 999.95	error= .07	perc= .01
SW= 3500.	V= 60.00	HP= 555.00	HPC= 534.81	error= 20.99	perc= 3.78
SW= 4500.	V= 80.00	HP= 570.00	HPC= 566.89	error= 3.11	perc= .55
SW= 8500.	V= 100.00	HP= 605.00	HPC= 676.25	error= -9.25	perc= -1.53
SW= 9500.	V= 120.00	HP= 650.00	HPC= 645.93	error= -19.99	perc= -3.02
SW= 9500.	V= 140.00	HP= 1100.00	HPC= 1076.15	error= 1.85	perc= .17
SW= 9500.	V= 150.00	HP= 1200.00	HPC= 1209.56	error= 20.44	perc= 1.60
SW= 9500.	V= 3.	HP= 1100.00	HPC= 1157.95	error= .57	perc= .01
SW= 9500.	V= 60.00	HP= 610.00	HPC= 609.58	error= .70	perc= .11
SW= 9500.	V= 80.00	HP= 620.00	HPC= 632.92	error= -12.92	perc= -2.08
SW= 9500.	V= 100.00	HP= 710.00	HPC= 740.09	error= -50.89	perc= -4.24
SW= 9500.	V= 120.00	HP= 835.00	HPC= 914.62	error= -29.02	perc= -3.23
SW= 9500.	V= 140.00	HP= 1160.00	HPC= 1173.52	error= -13.52	perc= -1.15
SW= 9500.	V= 150.00	HP= 1300.00	HPC= 1340.34	error= 19.66	perc= 1.45

Figure 39. Example of Input and Output from Input Coefficient Program



BELL HELICOPTER COMPANY

The physical dimensions required (Table I) are rotor radius (feet), rotor chord (feet), number of blades, rotor tip speed (feet per second), K_3 and K_6 . Also required are altitude (feet) and temperature (degree Centigrade) for the given data. The lower gross weight and the upper gross weight are the final data required.

The input data are compared with the computed data using the values of f , c_0 , c_1 , and M_{cr} determined in the program. The actual error and percent error are printed for each speed power polar at both gross weights. The values of f , c_0 , c_2 , and M_{cr} determined in the program and used to compute horsepower required are printed as can be seen in Figure 39.

The sensitivity of each of the parameters as related to magnitude can be seen in Figures 24 through 28. Some variation from the computed values may be used with little change in the power required. This is the reason for the differences in the values of Table II for the AH-1G and the value calculated by the INPUT coefficient program. Also it should be understood that a set of coefficients do not define a unique solution, i.e., there could be several sets of coefficients which could result in approximately the same degree of correlation.

APPLICATIONSTerrain Following

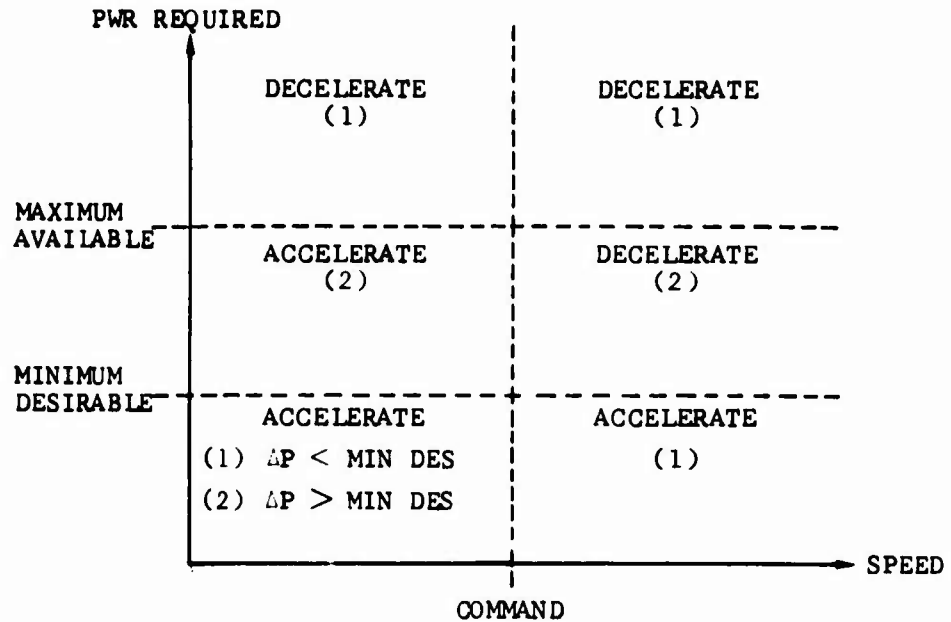
The equations developed above can be integrated into a terrain following model to generate an accurate flight profile. An example of such a terrain following model can be found in Reference 25. In this model, the aircraft's terrain following ability can be investigated as a function of (1) the aircraft's characteristics, (2) terrain following subsystem, (3) load factor limits, (4) command clearance altitude, (5) command speed, (6) terrain type, and other operational parameters. The pilot logic was developed from an energy viewpoint along with some logical decisions about how the pilot flies the helicopter. The pilot logic is shown in Figure 40. The helicopter will always be in one of the six areas of speed and power illustrated in Figure 40. Equation 1 (Figure 40) was derived from $F = m\dot{V}$ and $P = F \cdot V$ relationships. It is used to determine the linear acceleration (or deceleration). The difference between the required and set power determine ΔP . Equation 2 (Figure 40) shows the use of the weighting function. This function attempts to recognize that pilots do not correct in the same way for both large and small deviations from the command speed. The weighting function is compared to unity before use in equation 2, and the smaller value is used. An example of the flight profile generated from this terrain following model is shown in Figure 41.

Decelerating Turns

The question of penetration distance and time to execute a 180-degree turn at constant altitude are frequently used in comparison of different helicopters. The following methodology was developed for prediction of distance and time for a decelerating turn.

The pilot can choose to decelerate at constant altitude in order to supply additional power for a high-g turn. The time history of the flight path must be constructed of a series of circular arcs since speed, radius, and g-level are varying throughout the turn. The procedure is described below.

- (1) Determine the variation with speed of the maximum transient thrust capability of the rotor (see Maneuverability Limits). Divide this by the weight to get the V-n curve. This maximum thrust capability may be limited by rotor instabilities like flutter or weaving, or by loads, vibration, or stall -- depending on the specific rotor system.
- (2) Determine the power required at the maximum rotor thrust using the power equations.



$$(1) \quad \dot{V} = \frac{\Delta P}{mV}$$

$$(2) \quad \dot{V} = \frac{\Delta P}{mV} \left(\frac{V - V_{\text{com}}}{V_{\text{tol}}} \right)^2$$

Figure 40. Pilot Logic for Terrain Following Model.



BELL HELICOPTER COMPANY

Computed Performance

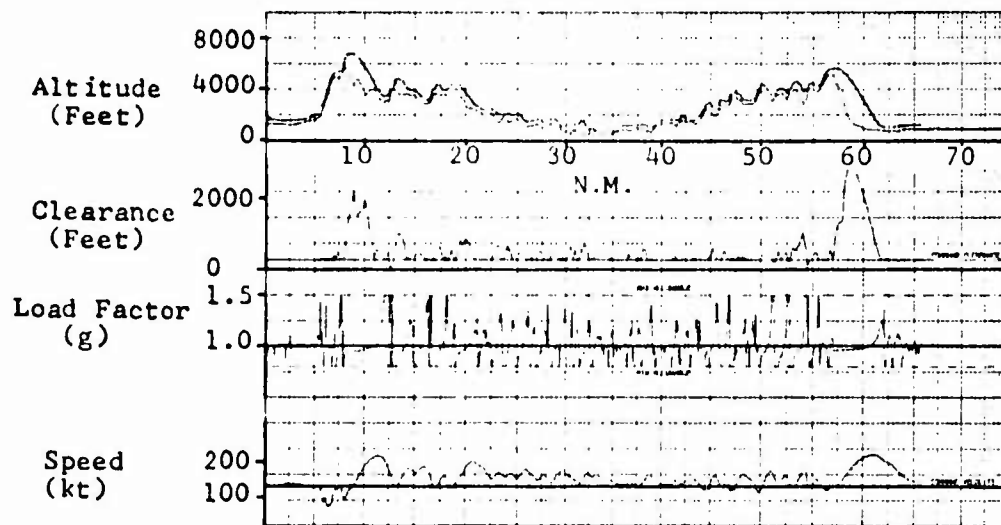


Figure 41. Terrain Following Flight Profile



BELL HELICOPTER COMPANY

- (3) Determine how deceleration varies with speed using equation 39.
- (4) Select the time interval to be used. One second is usually sufficient.
- (5) Determine the average deceleration for the first time interval. Then compute the average speed and determine the radius of turn from

$$R = V^2 / (g \sqrt{n^2 - 1})$$

- (6) The amount of arc traversed in the first time interval is given by $d\theta/dt = V/R$ for a t of one second. If computed instead of graphically constructed, the penetration distance is calculated as follows:

$$\text{penetration distance} = V_t \cos(\theta \text{ heading change}) / t$$

- (7) For the next time point the entry speed is the exit speed of the first time interval. Return to (5) and continue until the desired heading change is achieved.

An example of a 180-degree decelerating turn is shown in Figure 42. A comparison of predicted data using the above procedure and measured data from Reference 7 for the AH-1G helicopter is presented in Figure 42. Entry airspeed for the above example was 150 knots.

Low Speed Maneuvering

The helicopter has a capability of accelerating in any direction from hovering flight. This can be used to increase the survivability at very low speeds since changing the direction and magnitude of flight path acceleration complicates the ground gunner's problem. Using the methodology from preceding sections and observing physical laws, a method (Reference 26) for determining the capability of the helicopter to accelerate both vertically and horizontally at the same time is presented. In high speed flight at moderate altitudes, maximum g-capability can be used since the power required can be supplied by loss of energy (altitude or airspeed). However, rotor maximum g-capability cannot be used effectively in low speed flight since kinetic, potential and rotor energy levels are low and nearly constant. Therefore, low speed maneuvers are done at constant power. Horizontal acceleration is most efficiently done by tilting the rotor thrust vector so that the horizontal component acts to accelerate the helicopter as illustrated in Figure 43. The main rotor thrust must be increased to maintain altitude. This requires an excess of power above that required to hover and is the means by which excess power is converted to accelerative force.



BELL HELICOPTER COMPANY

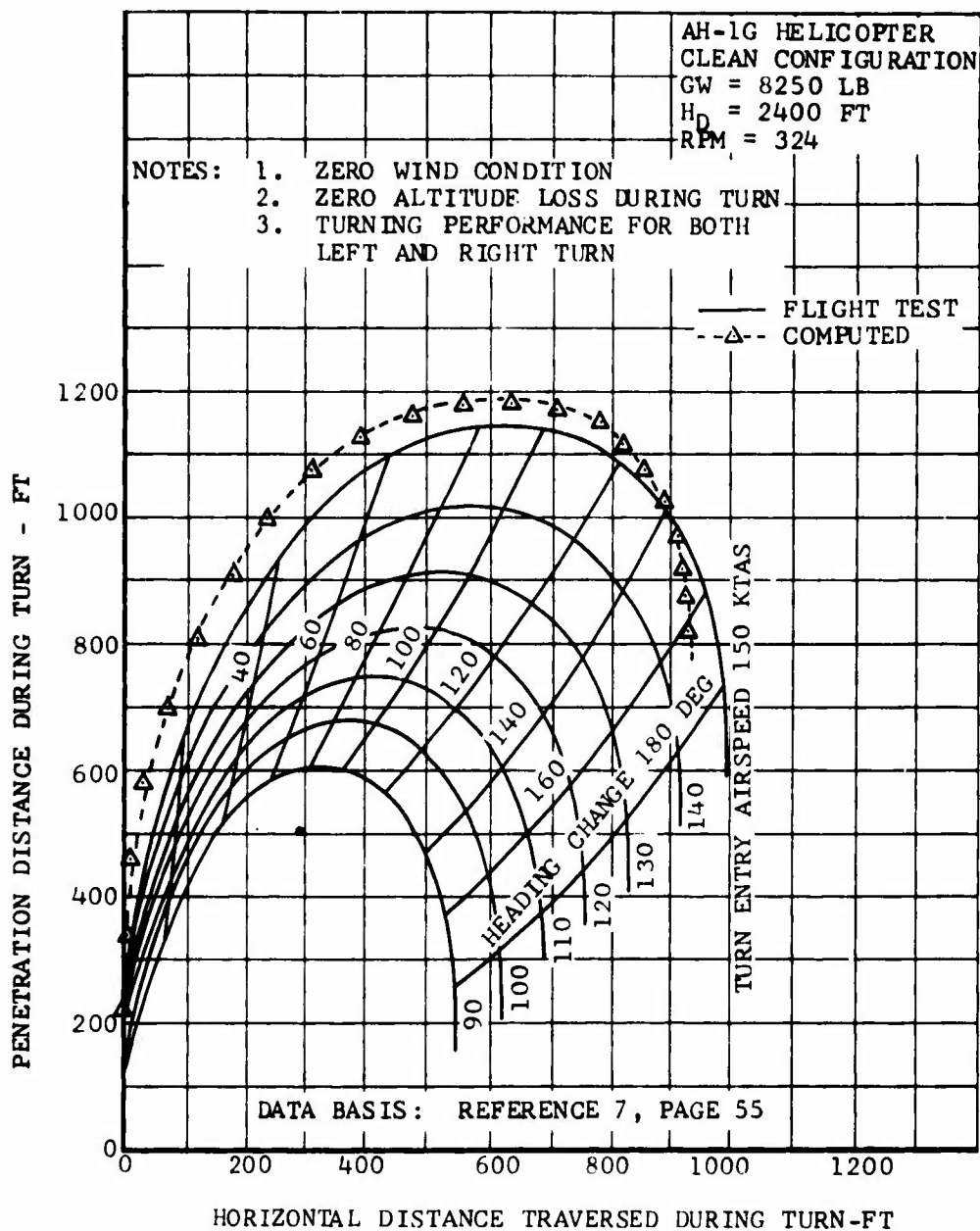


Figure 42 - 180 Degree Turning Performance for the AH-1G Helicopter



BELL HELICOPTER COMPANY

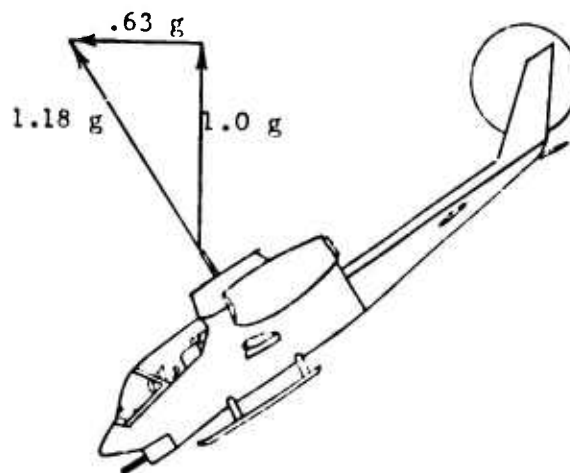
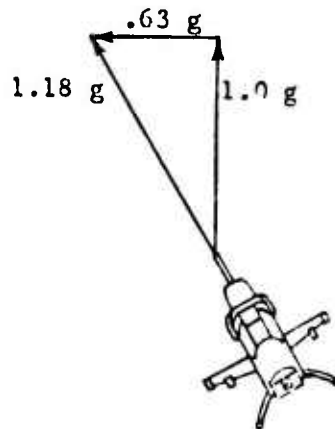


Figure 43. Thrust Vectoring for Linear Acceleration.



The power required by a typical high-performance helicopter in forward flight is illustrated in Figure 44. The effects of normal acceleration on power are indicated by the lines of constant g . The pilot may elect to use the normal acceleration capability to accelerate vertically (increase rate of climb or arrest rate of descent) or to accelerate parallel to the ground while maintaining a 1- g vertical component of the thrust vector. The power-limited g -capability may be determined from the data of Figure 44 by noting the g -capability at each speed at a constant power level. Turning flight requires acceleration normal to the flight path and the power required that is associated with producing increased thrust. Level flight acceleration requires power (equation 39). Thus, the maximum acceleration, \dot{V} , is determined by the excess power available and the velocity. It should be noted that the predicted \dot{V} tends to infinity as V tends to 0 which is a limitation of the \dot{V} equation. A graphical presentation of the \dot{V} equation is given in Figure 45 for a helicopter of 12,500 pounds gross weight.

The preceding discussion has assumed that there is no gain or loss of altitude (potential energy). The power required to climb is given by equation 28. To account for climb and descent effects, the power computed by equation 28 is added to (descent) or subtracted from (climb) the maximum power available. A horizontal line is drawn across Figure 44 at the new power available and the corresponding acceleration capabilities are determined as before. For example, a 10 ft/sec rate of climb would require 267.4 horsepower for the example helicopter. The maximum power available then would be $1830 - 267.4 = 1562.6$ horsepower. The normal acceleration in hover would then decrease from 1.18 to about 1.05 in a 600 ft/min vertical climb.

The power-limited linear (flight path) acceleration at a specified value of normal acceleration can be determined from the data of Figures 44 and 45. For example, if the helicopter is banked 45° , sustaining 1.414 g in level flight, the power required at 60 knots is 1110 horsepower from Figure 44. This gives an excess of 720 horsepower which may be used to increase flight path velocity. Entering Figure 45 with 720 horsepower at 60 knots gives about 0.31 g (5.9 kt/sec) linear acceleration. This normal and linear acceleration is approximately correct except that the vector sum of 1.414 and 0.31 is 1.447. Since the power required data of Figure 44 refers to the total thrust produced, the vector sum of the normal and linear acceleration must be used to obtain the power required. This involves reentering Figure 44 at the higher normal acceleration (1.447) and obtaining the power required. Figure 45 then shows a linear acceleration attainable of 0.29. This iterative process continues until accelerations are determined which are compatible with power and vector summation constraints. Figure 46 is a combination of Figures 44 and 45 which indicates the approximate combined acceleration capability if the vector sum is not included.



BELL HELICOPTER COMPANY

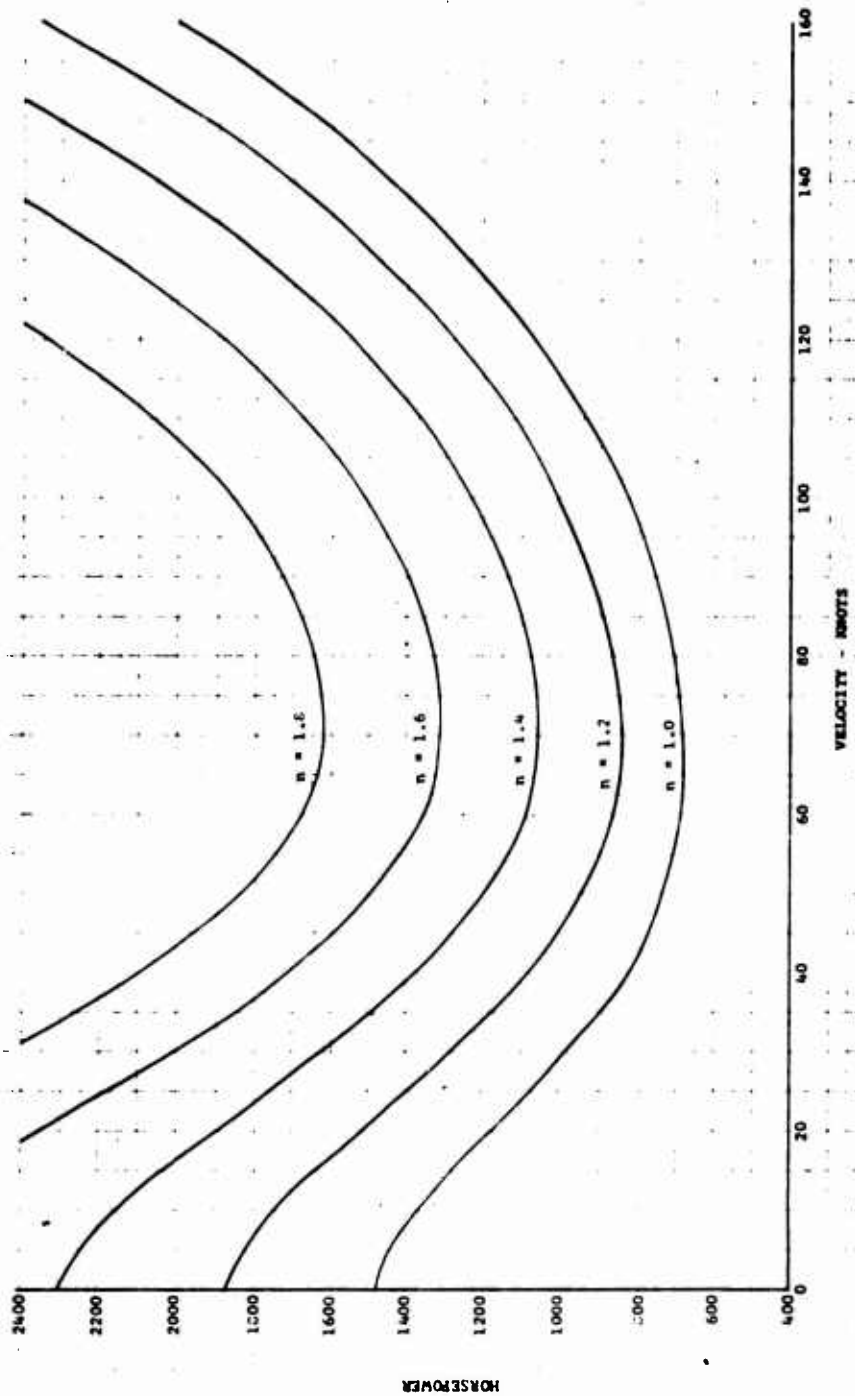


Figure 44. Power Required in Accelerated Flight.

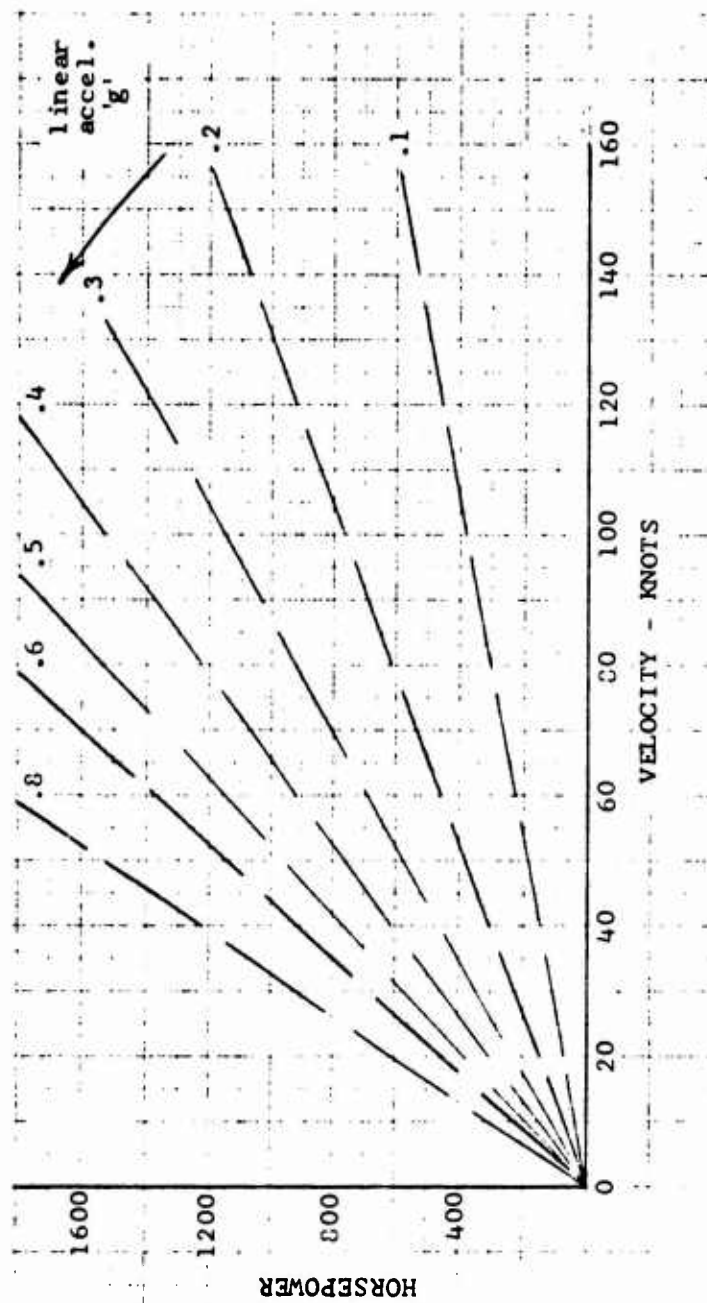


Figure 45. Linear Acceleration Produced by Excess Power.



BELL HELICOPTER COMPANY

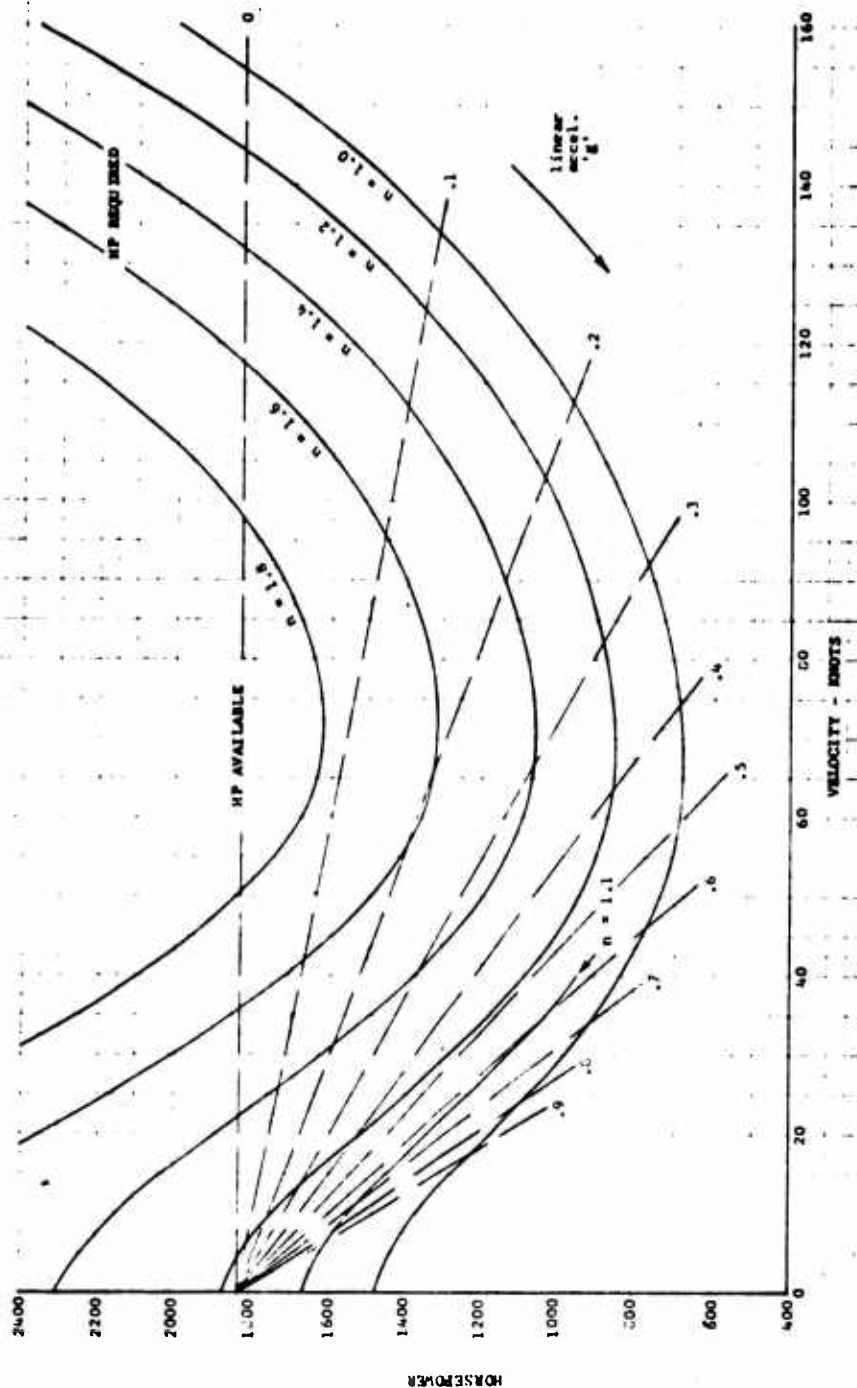


Figure 46. Approximate Combined Normal and Linear Acceleration Capability.



To determine accurately the combined acceleration capability, the data of Figure 46 are replotted in Figure 47 at speeds of interest. The curves starting at the 1.0, 1.2, 1.4 and 1.6 g values of n are constructed from the geometric relationships of a right triangle as indicated. The values of $n_{||}$ and n_{\perp} at the points where the parabolas intersect the speed lines obtained from Figure 46 satisfy both power and geometric constraints. For example, from Figure 46 the indicated linear acceleration capability in level flight ($n=1.0$) at 30 knots is $0.74g$. This is point A on Figure 47. The rest of the 30-knot line of Figure 47 is determined by reading corresponding values of n and $n_{||}$ (linear acceleration) from Figure 46 along the vertical 30-knot line. Where the 30-knot line intersects the geometric curves previously described, both power and geometric constraints are satisfied. Point B on Figure 47 indicates a level flight acceleration of $0.56g$ at 30 knots. The normal and linear acceleration capability for the example helicopter is given in Figure 48.

In hovering flight the above method fails since the linear acceleration equation is infinite. The maneuvering limits near hover are determined by the horizontal and vertical acceleration which results from directing a thrust vector of constant length, $1.18g$ for the example case. The magnitude of this thrust is determined by power available as indicated in Figure 44. The result is a circular arc with a radius equal to the g capability with $V = 0$. The above combined acceleration capability is graphically portrayed in Figure 49 for low speed flight. Figure 50 is a similar presentation which shows data from hover to maximum speed. The kinetic energy available at high speeds enables considerably higher g -levels to be sustained for short periods to make rapid changes in the flight path. The power required for these maneuvers is provided by loss of speed (kinetic energy) during the maneuver. Altitude (potential energy) can be lost to gain power for maneuvering at g -levels outside the envelope indicated in Figure 50.

At this time, no flight test data are available to validate this theory.

Survivability

Survivability studies require some type of flight path determination. The impact of the accuracy of these trajectories varies depending on the survivability model itself. This simplified method for determination of flight trajectories offers accurate representation of the flight path trajectories for minimum computer run time and computer storage space.



BELL HELICOPTER COMPANY

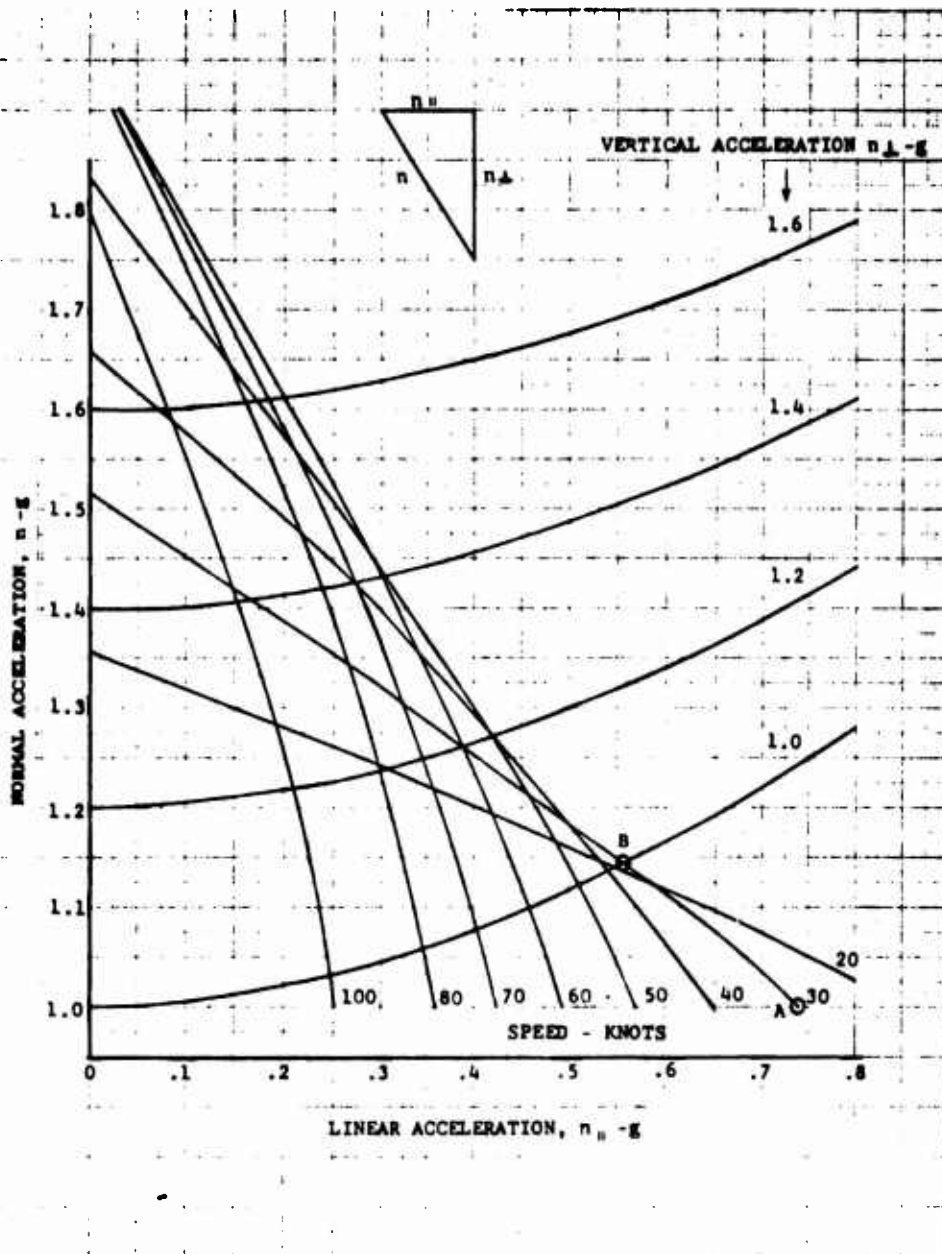


Figure 47. Technique for Matching Power and Geometric Constraints



BELL HELICOPTER COMPANY

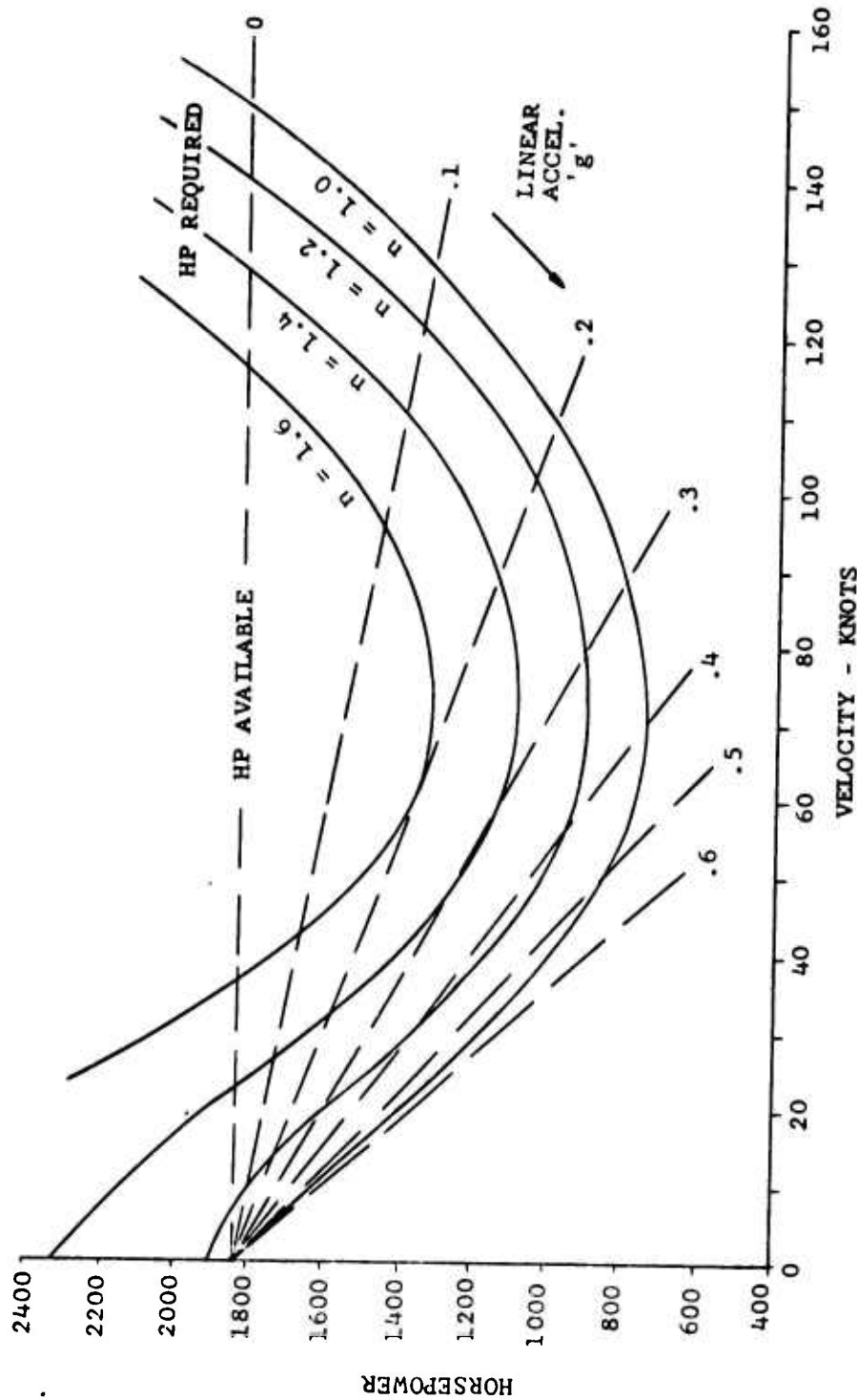


Figure 48. Normal and Linear Acceleration Capability.



BELL HELICOPTER COMPANY

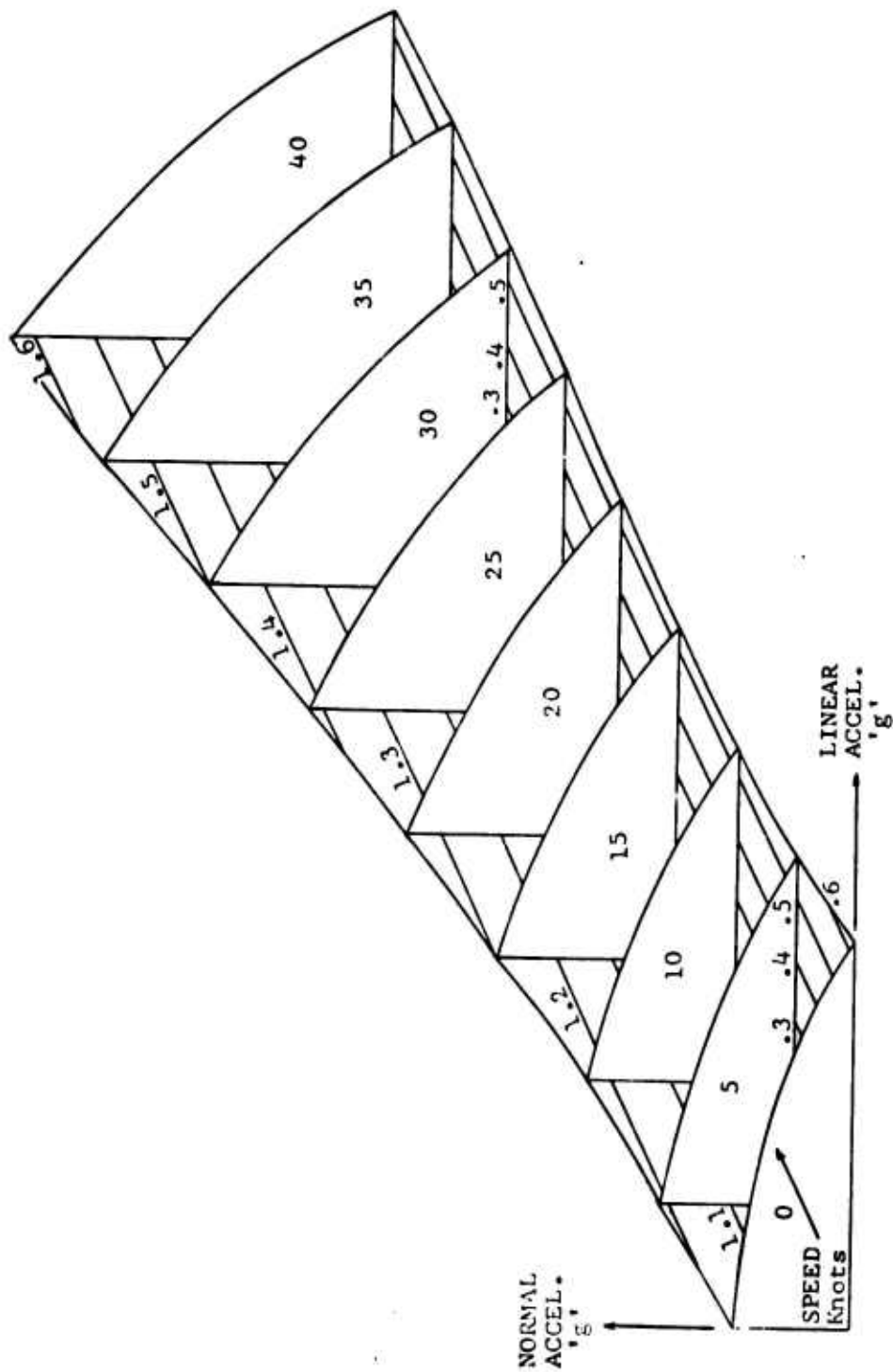


Figure 49. Effect of Speed on Normal and Linear Acceleration at Constant Power.

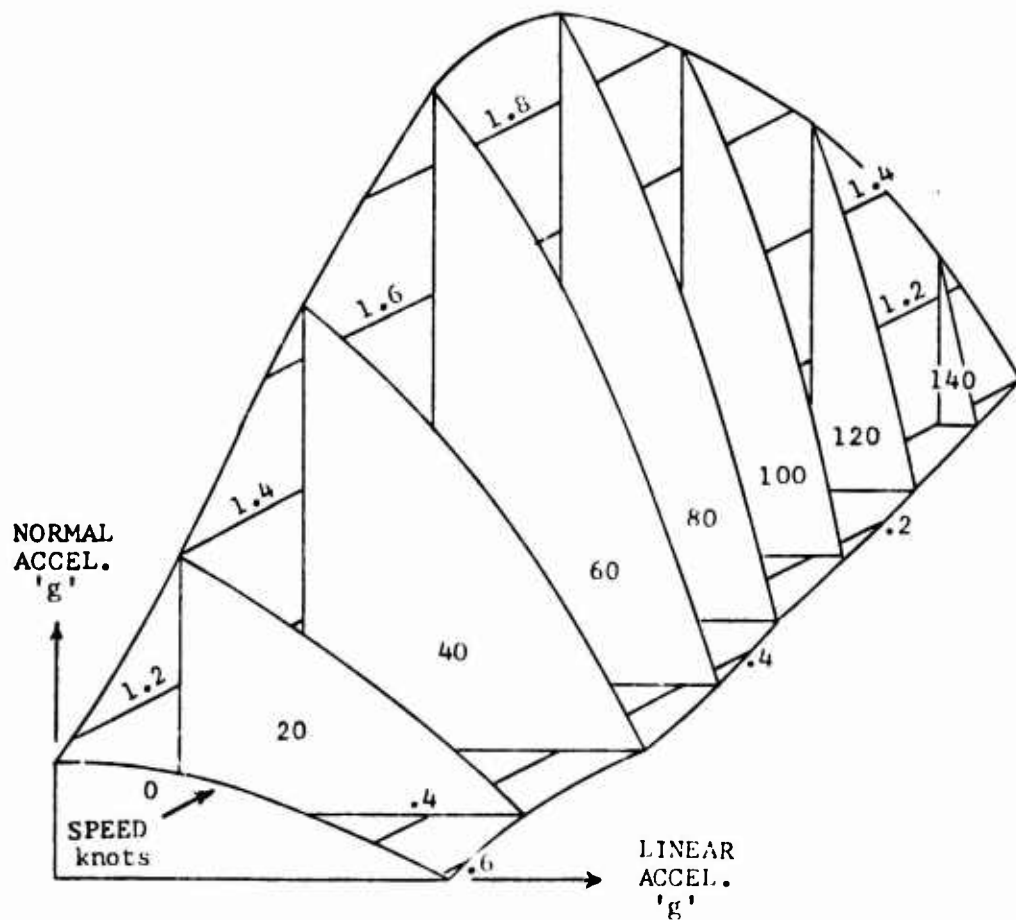


Figure 50. Constant Energy Acceleration Capability from Hover to Maximum Speed.



Flight Test

The evaluation of the maneuver capability of a helicopter in flight test often results in data which reflect pilot technique more than the actual capability of the helicopter. From Reference 4, return-to-target maneuvers were performed by three different pilots using the AH-1G helicopter. A standard deviation of 1.01 seconds was calculated for level turns. From a statistical viewpoint, this is a very large scatter band. The large variations observed in the test results degrade precise quantitative comparisons of maneuvering performance. If one is faced with comparing the maneuver capability of two different helicopters, the influence of pilot technique may reduce or augment the helicopter's performance. For this reason, a method is needed for the evaluator to compare maneuver capability of different helicopters independent of pilot technique. The analytical methods to predict acceleration, deceleration, and turning performance are presented in the preceding sections. These parameters, combined with conventional performance parameters, define the total performance capability of the helicopter. Almost all maneuvers are combinations of one or more of the above basic maneuvers, and energy methods may be used to combine these basic maneuvers. The total performance capability of different helicopters may be quickly compared by the overlay of the energy diagram such as Figures 3 and 4. In addition, since power required at different altitudes is calculated by the power equations for the energy diagram, the fuel flow can be determined depending on the engine. Then a chart of specific range and endurance may be constructed as a function of altitude and airspeed as shown in Reference 27. To properly consider differences in gross weights and loading conditions with different helicopters, it would appear reasonable to compare total performance at a gross weight where both configurations can exert the same maximum "g" load. For example, consider a comparison of the charts at a "g" load of 1.5. The energy diagram for the AH-1G helicopter at a "g" load of 1.5 is given in Figure 5. This would assure the evaluator of a given level of maneuverability while comparing other aspects of performance. Since the techniques used to develop g-capability are primarily based on energy and momentum considerations, the efforts of different configurations on performance parameters are minimized.



RECOMMENDATIONS

1. Additional work should be initiated for continued development of the low speed maneuvering theory.
2. The existing theory should be validated with flight test data and the rotor degree of freedom added to the equations for low speed.
3. Methods of improving the helicopter's capability in the low-speed regime should be investigated.
4. Investigate further the effects of blade flapping inertia on the maximum t_c versus μ relationship.

REFERENCES

1. Wood, T. L., A Technique for Computing the Maneuvering Flight Trajectories of Helicopters, Bell Helicopter Company Report 299-099-472, Revision A, 6 March 1970.
2. Lewis II, R. B., "HueyCobra Maneuvering Investigations", Technical Paper, American Helicopter Society, No. 472, June 1970.
3. Livingston, C. L., "Computation of Turning Flight by C81", BHC IOM 87:CLL:lw jt-586, 7 July 1970.
4. Lewis II, R. B., et al, Engineering Flight Test, AH-1G Helicopter (HueyCobra), Maneuvering Limitations, Final Report, USAASTA, Project No. 69-11, March 1971.
5. Boyd, J. R., Christie, T. P., and Gibson, J. R., Energy Maneuverability, APGC-TR-66-4, Volume 1, Force Proving Ground, Eglin Air Force Base, Florida, 1966, SECRET.
6. Blankenship, B. L., and Bird, B. J., Project AGAJ63 Rotorcraft Flight Simulation, Volume II of II, Bell Helicopter Company Report 599-068-904, 25 September 1969.
7. Finnestead, R. L., et al, Engineering Flight Test, AH-1G Helicopter (HueyCobra), Part II, Performance Addendum, Final Report, USAASTA, Project No. 66-06, March 1971.
8. Natops Flight Manual, Navy Models HH-2C HH-2D Helicopters, NAVAIR 01-260HHC-1, 1 September 1970.
9. Hamm, N. D., and Young, M. I., "Torsional Oscillation of Helicopter Blades Due to Stall", Journal of Aircraft, Vol. 3, No. 3, 1966, pp. 218 ff.
10. Flight Manual, USAF Series CH-3C Helicopter, T.O. 1H-3(c)C-1, 17 June 1964.
11. Natops Flight Manual, Navy Model CH-53A Helicopters, NAVAIR 01-230HMA-1, 15 March 1966.
12. Technical Manual, Operator's Manual Helicopter, Observation OH-6A (Hughes), TM 55-1520-214-10, December 1967.
13. Montes, P.G., Structural Demonstration of the Model AH-1J Helicopter, Bell Helicopter Company Report 209-099-229, 20 August 1969.
14. Melton, J., "Military Pilot Demonstration of Rocket Attack Maneuvers with the Model AH-1J Helicopter", BHC IOM 81:JRM:im-2341, 9 August 1971.



15. Brown, E. L., and Schmidt, P. S., "The Effect of Helicopter Pitching Velocity on Rotor Lift Capability", Journal of the American Helicopter Society, Vol. 8, No. 4, October 1963.
16. Melton, J., "Model 309 Maneuver Points", BHC IOM 81:JRM:im-2380, 18 October 1971.
17. Etkin, Bernard, Dynamics of Flight, Stability and Control, John Wiley and Sons, Inc., New York, 1967.
18. Gustafson, F. B., and Myers, Jr., G. C., "Stalling of Helicopter Blades", NACA TN No. 1083, June 1946.
19. VanHorn, S., OH-58A Aerodynamic Substantiating Data Report for Standard Aircraft Characteristics Charts and Flight Manual Based on Final Army Flight Test Results (USAASTA Project 68-30), Bell Helicopter Company Report 206-099-264, 30 June 1971.
20. Nagata, J. and Shapley, Jr., J., Engineering Flight Test of the OH-6A Helicopter (Cayuse), Phase D, Final Report, USAASTA Project No. 65-37, April 1969.
21. Dominick, F. and Nelson, E., Engineering Flight Test YUH-1H Helicopter, Phase D (Limited), Final Report, USAASTA Project No. 66-04, November 1970.
22. Barbini, W., and Heft, E., Determination of the Effects of Rotor Blade Compressibility on the Level Flight Performance of the CH-3C Helicopter, FTC-TR-67-10, Air Force Flight Test Center, Aug. 1967.
23. Barbini, W., Balfe, P., and Lovrien, Jr., G., Category II Performance and Flying Qualities Test of the HH-53C Helicopter, FTC-SD-70-8, Air Force Flight Test Center, May 1970.
24. Smith, R., AH-1G Aerodynamic Substantiating Data Report for Standard Aircraft Characteristics Charts and Flight Manual Based on Army Phase D Flight Test Results, Bell Helicopter Company Report 209-099-274, June 1971.
25. UTTAS Avionics System Study: Appendix F - Combat Attrition (U), Bell Helicopter Company Report 299-099-807, February 1971, CONFIDENTIAL.
26. Livingston, C. L., "Maneuvering the Helicopter Near Hover", Unpublished Paper, 30 June 1971.
27. Livingston, C. L., Maneuverability Prediction, Technical Paper, Southwest Region of American Helicopter Society, December 1966.



BELL HELICOPTER COMPANY

APPENDIX A

DERIVATION OF BANK ANGLE, LOAD FACTOR RELATIONSHIP

Equation (7) was derived from equations on page 116 of Reference 17 as follows:

Assume the aircraft is turning about a vertical axis. Thus, Euler $\dot{\phi}$ and $\dot{\psi}$ are zero and the body angular rates become

$$\begin{aligned} p &= -\dot{\theta} \sin\theta \\ q &= \dot{\theta} \cos\theta \sin\phi \\ r &= \dot{\theta} \cos\theta \cos\phi \end{aligned} \quad (A-1)$$

where

$$\begin{aligned} p &= \text{roll velocity} & \theta &= \text{pitch attitude} \\ q &= \text{pitch velocity} & \phi &= \text{roll attitude} \\ r &= \text{yaw velocity} & \psi &= \text{yaw attitude} \end{aligned}$$

These angular rates are then substituted into the generalized equations of force equilibrium:

$$\begin{aligned} X - mg \sin\theta &= m(\dot{u} + qw - ru) \\ Y + mg \cos\theta \sin\phi &= m(\dot{v} + ru - pw) \\ Z + mg \cos\theta \cos\phi &= m(\dot{w} + pv - qu) \end{aligned} \quad (A-2)$$

where

$$\begin{aligned} X &= \text{force on vehicle in X direction} \\ Y &= \text{force on vehicle in Y direction} \\ Z &= \text{force on vehicle in Z direction} \\ m &= \text{aircraft mass} \\ u &= \text{velocity in X direction} \\ v &= \text{velocity in Y direction} \\ w &= \text{velocity in Z direction} \end{aligned}$$

Assume, for coordinated flight, that $Y = 0$. Also assume no change in linear velocities so that \dot{u} , \dot{v} , \dot{w} are zero. Thus,

$$g \cos\theta \sin\phi = ru - pw = u(\cos\theta \cos\phi + \sin\theta \tan\alpha) \quad (A-3)$$

if we define

$$\tan\alpha = \frac{w}{u}$$

and

$$\tan\beta = \frac{v}{u}$$

Now solving equation A-3 for $\frac{u \dot{\psi}}{g}$

$$\frac{u \dot{\psi}}{g} = \frac{\tan \phi}{1 + K} \quad (A-4)$$

when

$$K = \frac{\tan \phi \tan \alpha}{\cos \phi}$$

Use equation A-1 in the Z force equation and substitute equation A-4 for $u \dot{\psi}/g$. Equate Z/mg to $-n$:

$$n = \frac{-u \dot{\psi} \sin \phi \tan \alpha}{g} - \frac{u \dot{\psi} \cos \phi \sin \phi}{g} - \cos \phi \cos \alpha \quad (A-5)$$

Then,

$$n \cos \phi = \cos \phi \cos^2 \alpha + \cos \phi \frac{\sin^2 \phi}{1 + K} + \frac{\sin \phi \tan \phi \sin \alpha}{1 + K} \quad (A-6)$$

Consider the following:

1. If $\alpha = \phi = \psi = 0$, then the usual equation is obtained.

$$n \cos \phi = 1$$

2. If $\alpha = \psi = 0$, then $1 + K$ is unity and the third term of equation A-6 is zero.

Since

$$\sin^2 \phi + \cos^2 \phi = 1$$

then

$$n \cos \phi = \cos \phi$$

ENERGY DIAGRAM PROGRAM

```

/* ENERGY MANEUVERABILITY HV DIAGRAM */
/* Input section */
PUT LIST('If n>21 and n<40, dcl line 19 x(m),an(n) ');
GET LIST(n,n);
k=0;
w=0;
DECLARE x(21), an(40);
IF alloca(f) THEN FREE f,ran;
ALLOCATE f(4,w),ran(2,w);
DECLARE f DEC(6) CONTROLLED, ran DEC(6) CONTROLLED;
DECLARE as30u EXT ENTRY;
GET LIST(rad,chor,blode,tapd,drag,weigh,if);
GET LIST(uat,eta);
GET LIST(vinc,vinit,hinc,hinit);
/* Calculation of ps at each grid point */
c2: DO j=1 TO n;
c1: DO i=1 TO n;
h=(i-1)*hinc+hinit;
dstd=(1-.0000007535*n)*5.2501;
tsl=uat*273.16;
thet=1-.0000007535*n;
s1gn=dstd/thet;
t=thet*tsl;
dvs=65.81106*sqrt(t);
drho=s1gn*.002378;
vel=vinc+j*vinit-vinc;
CALL as30u(rad,chor,blode,tapd,drag,weigh,vel,if,drho,dvs,dho);
IF h=3000 THEN GO TO c30;
hna=1100;
GO TO c31;
hna=.02*(h-3000)*1100;
c30: ps=300*(hna-dhn)/(eta*weigh);
c31: f(1,i)=ps;
END c1;
END c2;
/* find maximum value of ps at each velocity increments */
c9: DO j=1 TO n;
c7: DO i=1 TO n;
a(i)=f(i,j);
END c7;
CALL order(a,n);
ran(1,j)=a(n);
ran(2,j)=a(1);
END c9;
/* determination of range of ps */
c10: DO j=1 TO n;
an(j)=ran(1,j);
END c10;
CALL order(an,n);
psmax=an(n);
psmin=an(1);
c15: DO j=1 TO n;
xn(j)=ran(2,j);
END c15;
CALL order(xn,n);
psmin=an(1);
xmin=trunc(psmin*.5*sign(psmin));
xmax=trunc(psmax*.5*sign(psmax));
DO j=1 TO n;
xn(j)=ran(2,j);
END c15;
CALL order(xn,n);
psmin=an(1);
xmin=trunc(psmin*.5*sign(psmin));
xmax=trunc(psmax*.5*sign(psmax));
an=(xmax-xmin)/5;
an=an+1;
PUT LIST(an,xmax,xmin);
IF alloca(psc) THEN FREE psc,vc,hc;
ALLOCATE psc(an),vc(an,n),hc(an,n);
DECLARE psc DEC(6) CONTROLLED, vc DEC(6) CONTROLLED, hc DEC(6) CONTROLLED;
psc=0;
vc,hc=0;
psc(1)=xmax;
c16: DO i=2 TO an;
psc(i)=psc(i-1)-5;
END c16;
/* psc sweep */
c17: DO i=1 TO an;
/* velocity grid sweep */
a1: DO j=1 TO n;
i=1;
IF ran(1,j)>psc(i6) THEN GO TO d1;
IF ran(1,j+1)>psc(i6) THEN GO TO d2;
GO TO c18;
IF ran(1,j+1)>psc(i6) THEN GO TO d3;
vc(i6,j)=vinc*(j+1)+vinit-vinc;
hc(i6,j)=0;

```



```

      GO TO c18;
d3:  vc(16,j)=vnc*(psc(16)-f(1,j))/(f(1+1,j+1)-f(1,j))+vncj+vinit-vnc;
      hc(16,j)=0;
      GO TO c18;
d4:  IF ren(1,1)>psc(16) THEN GO TO d4;
      vc(16,j)=vncj+vinit-vnc;
      hc(16,j)=0;
      GO TO c18;
d5:  DO i=2 TO m;
      IF f(1,j)<psc(16) THEN GO TO d5;
      GO TO a2;
d6:  IF f(1,j)<psc(16) THEN GO TO d6;
      vc(16,j)=vncj+vinit-vnc;
      hc(16,j)=(i-1)*hinc+hinit;
      GO TO c18;
d7:  vc(16,j)=vncj+vinit-vnc;
      hc(16,j)=hinc*((i-1)-psc(16))/(f(1-1,j)-f(1,j))+hinc*(1-1)*hinit;
      GO TO c18;
a2:  END d4;
c18:  END d1;
      END c17;
c56:  DO i=1 TO n;
c57:  DO j=1 TO n-1;
      IF (psc(16)<f(1,j))&psc(16)>f(1,j+1) THEN GO TO c50;
      GO TO c51;
c50:  vc(16,j+1)=vnc*(f(1,j)-psc(16))/(f(1,j)-f(1,j+1))+vncj+vinit-vnc;
      GO TO c54;
c51:  IF (psc(16)>f(1,j))&psc(16)<f(1,j+1) THEN GO TO c52;
      GO TO c54;
c52:  vc(16,j)=vnc*(psc(16)-f(1,j))/(f(1,j)-f(1,j+1))+vncj+vinit-vnc;
c54:  END c57;
      END c56;
      /* output */
      PUT LIST(' ', na, vc, hc);
c24:  DO i=1 TO m;
c25:  DO j=1 TO n;
      IF vc(16,j)=0&hc(16,j)=0 THEN GO TO c11;
      PUT IMAGE(psc(16),vc(16,j),hc(16,j))(im2);
im2:  IMAGE;
-----
c11:  END c25;
      END c24;
      /* this subroutine arranges a column array into values of ascending order */
order: PROCEDURE (da, dm);
b6:  DO i2=1 TO dm;
      i5=i2+1;
b3:  DO d1=i5 TO dm;
      IF da(i2)<da(d1) THEN GO TO b4;
      temp=da(i2);
      da(i2)=da(d1);
      da(d1)=temp;
b4:  END d1;
b5:  END i2;
      END order;

as3010: PROCEDURE (r,c,b,wr,f1,gw1,v1,n1,rho,vs,hp);
/* THIS SUBROUTINE CALCULATES POWER REQUIRED FOR ENERGY MANEUVERABILITY */;
/* see constants for normal helicopters at sea level */;
s15: del0=.0075;
      del7=1;
      a=6.28;
      incp=.75;
      k1=1;
      k2=1;
      /* compute some constants */;
s0:  p1=3.1415926535;
      area=pi*r**2;
      sig=h*c/(p1*r);
      nondf=rho*area*wr**2;
      nondn=nondf*wr/550;
      ctg=7/(sig*a);
      f=f1;
      gw=gw1;
      v=vl=1.6878;
      mu=v/wr;
      k1=1-(mu-.34)*2.36;
      IF mu>.14 THEN k1=1;
      mu2=mu**2;
      x3=wr*(1+mu)/vs;
      n=n1;
      /* compute some more constants */;
      x4=5*rho*v**4;
      ctg=gw/nondf;
      ctn=sqrt(x4*x4/(nondf*nondf)*ct*ct);
      x1=x4*v/(ctn*nondf);

```



```

x2=ctn*nondf/(2*rho*area);
/* compute induced velocity from momentum theory equations */
count=0;
IF v>42.2 THEN GO TO s17;
v1=1.037*sqrt(x2);
IF v=0 THEN GO TO s11;
s17: v1n=x2/v;
s9: v1=x1*x2/(v+v*.866*v1n*v1n)**.5;
IF ABS(v1-v1n)>.001 THEN GO TO s11;
count=count+1;
IF count>40 THEN GO TO :0;
v1n=.866*v1+.4*v1n;
GO TO s9;
s10: PUT LIST('calculation non-convergent, induced velocity to 0');
v1=0;
GO TO s12;
s11: v1=v1-x1;
/* compute power required section */
/* flat plate drag power */
s12: hp1=x1*v/550;
/* induced power */
hp2=x1*ctn*nondf*v1/550;
/* blade profile drag power at zero lift */
hp3=del1*sig*nondp*(1+.6*mu2)/8;
/* blade profile drag power caused by angle of attack */
tc=2*ctn/sig;
tcrt=.1+.2/sqrt(1+.9*mu2);
hps=0;
hps=del12*sig*nondp*(1+.6*mu2)*(tc*tcrt)**2/8;
IF tc<tcrt THEN GO TO s19;
deltc=tc-tcrt;
hps=20000*deltc**1.5;
/* compressibility power */
s19: IF x3>ncro THEN GO TO s13;
dcp=0;
GO TO s14;
s13: del1=x3-ncro+.75*(2*ctn/sig);
dcp=delm**3*(.0033-del1*(.022-.11*del1));
s14: hp5=x2*dcp*nondp;
hp=hp1+hp2+hp3+hp4+hp5+hps;
END as3010;

```



ANF: FRABILITY MANEUVER DIAGRAM •/•

91



```

d3:  GO TO c18;
    vc(16,j)=vlnce(psc(16)-f(1,j))/(f(1+1,j+1)-f(1,j))+vlncej+vlnlt-vlnr;
    nc(16,j)=1;
d1:  GO TO c18;
    IF ran(1,j)>psc(16) THEN GO TO d4;
    vc(16,j)=vlncej+vlnlt-vlnr;
    nc(16,j)=1;
    GO TO c18;
d4:  DO i=1 TO m;
    IF f(i,j)=psc(16) THEN GO TO d5;
    GO TO a2;
d5:  IF f(1,j)<psc(16) THEN GO TO d6;
    vc(16,j)=vlncej+vlnlt-vlnr;
    nc(16,j)=1+(1-i)*vlnr;
    GO TO c18;
d6:  vc(16,j)=vlncej+vlnlt-vlnr;
    nc(16,j)=vlnce(f(1+1,j)-psc(16))/(f(1+1,j)-f(1,j))+vlnce(1-2)*1;
    GO TO c18;
a2:  END d4;
c18:  END a1;
END -7;
c39:  GO TO c1 TO a1;
c55:  DO j=1 TO n-1;
    IF psc(16)<=f(1,j)Apsc(16)>=f(1,j+1) THEN GO TO c50;
    GO TO c51;
c50:  vc(16,j+1)=vlnce(f(1,j)-psc(16))/(f(1,j)-f(1,j+1))+vlncej+vlnlt-vlnr;
    nc(16,j+1)=1;
    GO TO c54;
c51:  IF psc(16)>=f(1,j)Apsc(16)<=f(1,j+1) THEN GO TO c52;
    GO TO c54;
c52:  vc(16,j)=vlnce(psc(16)-f(1,j))/(f(1,j)-f(1,j+1))+vlncej+vlnlt-vlnr;
    nc(16,j)=1;
c54:  END c55;
END c39;
/* Output */;
PUT LIST(' ps   vc   nc   thd   pathd ');
c20:  DO i=1 TO m;
c23:  DO j=1 TO n;
    IF vc(16,j)=0Anc(16,j)<=1 THEN GO TO c11;
    thd=32.2+sqrt(nc(16,j)+nc(16,j+1))-63.3/(vc(16,j)+1.6873);
    pathd=psc(16)+thd/(57.3+32.2);
    IF nc(16,j)=1 THEN thd=0;
    PUT IMAGE(psc(16),vc(16,j),nc(16,j),thd,pathd)(1m3);
1m2:  IMAGE;
-----
c11:  END c23;
END c20;
GET LIST(t,tinc,tlnlt);
b8:  DO i=1 TO t+1;
    thd=tinc*(i-1)+tlnlt;
b7:  DO j=1 TO n+1;
    vel=vlnce(j-1)+vlnlt;
    IF ((thd+vel*.000915)**2+1)**.5;
    PUT IMAGE(thd,vel,t)(1m3);
1m3:  IMAGE;
-----
END b7;
END b8;
b10:  DO i=1 TO m+1;
b9:  DO j=1 TO n+1;
    IF i*(i-1)*vlnr;
    vel=vlnce(j-1)+vlnlt;
    thd=1092.1*(1+1/2-1)**.5/vel;
    PUT IMAGE(t,vel,thd,tinc);
1m4:  IMAGE;
-----
END b9;
END b10;
/* this subroutine arranges a column array into values of ascending order */;
ORDR:  PROCEDURE (dx,om);
b5:  DO i2=1 TO om;
    i5=i2+1;
b3:  DO i1=i5 TO om;
    IF dx(i2)<dx(i1) THEN GO TO b4;
    temp=dx(i2);
    dx(i2)=dx(i1);
    dx(i1)=temp;
b4:  END b3;
END b5;
END ORDR;

```




BELL HELICOPTER COMPANY

APPENDIX B



BELL HELICOPTER COMPANY

SIMPLIFIED THRUST MODEL

Below is a derivation of the equations used in the simplified math model.

The thrust for a given number of blades (b) can be calculated by

$$T = \int_0^R b q C_L c dr = \int_0^R \frac{b}{2} V_n^2 C_L c dr \quad (B-1)$$

where C_L is the section lift coefficient and V_n is the velocity normal to that section. The velocity normal to the blade is

$$V_n = \omega R x + V \sin \phi = (x + \mu \sin \phi) R \quad (B-2)$$

where $x = r/R$ and r is the distance out the blade and $\mu = V/\omega R$.

Substituting equation B-2 into B-1 and noting that $dr = R dx$, the expression for thrust becomes

$$T = \frac{b \omega R c (\omega R)^2}{2} \int_0^1 (x + \mu \sin \phi)^2 C_{L_x} dx \quad (B-3)$$

Expressing equation B-3 in terms of coefficient of thrust, we have:

$$C_T = \frac{T}{A (\omega R)^2} = \frac{b c R}{2A} \int_0^1 (x + \mu \sin \phi)^2 C_{L_x} dx \quad (B-4)$$

From equation B-4 we are ready to calculate the thrust coefficient as follows:

$$\begin{aligned} t_c &= \frac{2C_T}{\sigma} = \frac{\frac{2bcR}{2A}}{\frac{bcR}{A}} \int_0^1 (x + \mu \sin \phi)^2 C_{L_x} dx \\ &= \int_0^1 (x + \mu \sin \phi)^2 C_{L_x} dx \end{aligned} \quad (B-5)$$

Then to calculate $t_{c_{max}}$ for each μ we would use the maximum lift coefficient at each blade station. This can be expressed as follows:

$$t_{c_{max}} = \int_0^1 (x + \mu \sin \phi)^2 C_{L_{max_x}} dx \quad (B-6)$$



From Figure 21 the retreating side of the blade is partially in the reversed flow region. The locus of this region is defined by

$$x = -\mu \sin \phi \quad (180^\circ \leq \phi \leq 360^\circ) \quad (\text{B-7})$$

Then equation B-6 would be integrated from $x = -\mu \sin \phi$ to $x = 1$.

The effect of pitch rate on maximum rotor thrust is determined as follows:

$$M = 2I_b \mu q \sin \phi$$

or nondimensionally as

$$C_{M_q} = \frac{M}{I_b} = \frac{2q \sin \phi}{\omega} \quad (\text{B-8})$$

The total rotor moment of the advancing blade is expressed as follows:

$$C_{M_{\text{TOTAL}}} = \frac{\gamma}{2a} \left(\int_0^1 (x + \mu \sin \phi)^2 C_{L_{\text{max}}} x \, dx \right) + \frac{2q \sin \phi}{\omega} \quad (\text{B-9})$$

where $\gamma = \frac{C_{L_{\text{max}}} a R^4}{I_b}$, I_b is the blade inertia and a is the lift curve slope.



SIMPLIFIED MAXIMUM THRUST PROGRAM

```

/* TC-MU BY NUMERICAL INTEGRATION AND TABLE LOOK-UP FOR CL-P(MACH) */
DECLARE A(4), AH(4), I(8), CLM(21);
A(2),A(4)=0;
AH(1),AH(3)=1;
DPSI=.1765529251;
GET LIST(OPT);
IF OPT=0 THEN GO TO S2;
S1: GET LIST(CLM);
S2: GET LIST(MRMAX,PR,R,OMEGA,C,RHO,VS,E,IBLAD);
GET LIST(KK);
PUT LIST('');
IF KK=1 THEN PUT LIST('FULL UPLOAD IN REVERSE FLOW REGION');
IF KK=-1 THEN PUT LIST('FULL DOWNLOAD IN REVERSE FLOW REGION');
IF KK=0 THEN PUT LIST('NO LOAD IN REVERSE FLOW REGION');
PUT LIST('');
PUT LIST('THE FOLLOWING IS A LIST OF THE CL DATA TABLE USED FOR COMPUTATION');
PUT LIST('MACH NO. CLMAX');
Z1: DO Z=0 TO 20;
PUT IMAGE(Z*.05,CLM(Z+1))(IM);
IM: IMAGE;
---
END Z1;
PUT LIST('');
PUT LIST('');
Z2: INU=.;
G=CEILING(KK*IBLAD);
MUL=OMEGA/VS;
OMEGA=OMEGA/R;
PR=PR/57.3;
S3: DO I1=1 TO 11;
I1U=.1*(I1-1);
IF I1U>MRMAX THEN GO TO KK2;
TC=0;
S4: DO I2=1 TO 10;
PSI=DPSI*(I2-1);
NSID=10*(I2-1);
ISID=IN(SID(PSI));
KK=CEILING(NSID*(OMEGA*G));
A(1),A(2),A(3),A(4)=MAP;
DO I3=1 TO 4;
INT=0;
IF KK=0A13=2/I3=4 THEN GO TO S14;
A11=A(I3);
AH1=AH(I3);
S5: DX=.1*(AH1-A11);
DO I4=1 TO 11;
X=.1*(I4-1);
Q1=1;
IF I3>2 THEN Q1=X;
IF I3=2/I3=4 THEN Q1=Q1*KK;
Q2=X*ISID;
MACH=ABS(Q2)*MOR;
CALL TABLE(MACH,CL,CLM);
INT=INT+CL*DX*Q1*Q2*Q2;
END S5;
I(13)=INT;
END S4;
INT5=0;
INT6=0;
I34=I(3)*I(4)*K;
S6: DO I6=1 TO 11;
X=.1*(I6-1);
Q1=X*ISID;
MACH=ABS(Q1);
CALL TABLE(MACH,CL,CLM);
Q2=.1*CL*Q1*Q1;
INT5=INT5+Q2;
INT6=INT6+Q2*X;
IF INT6>I34 THEN GO TO S10;
END S6;
S10: INT5=INT5+Q2;
INT6=INT6+Q2*X;
Q3=I34-INT6;
S7: X=X-1;
XOLD=XU;
X=XU+Q3/(Q2*X+10);
IF X=XU THEN GO TO S13;
Q1=X*ISID;
MACH=ABS(Q1);
CALL TABLE(MACH,CL,CLM);
Q2=(X-XU)*CL*Q1*Q1;

```



```

s13:  t1nt6=Int6+q2*x;
      q3old=q3;
      q3=134-t1nt6;
      IF abs(q3)<.00001 THEN GO TO s12;
      q4=x;
      x=x-(x-xold)*q3/(q3-q3old);
      xold=q4;
      GO TO s11;
s12:  I(G)=Int6+q2*x;
      I(5)=Int5+q2;
      q4=2;
      IF I2=1||I2=10 THEN q4=1;
      tc=tc+q4*(I(1)+I(2)+I(5));
      IF IND=1 THEN PUT IMAGE(pold,x)(11);
      I1;
      IMAGE;
at pal=--,x=--,----- to balance
      IF I1=1 THEN GO TO s15;
      END s4;
      GO TO s16;
s15:  tc=tc+10;
s16:  tc=tc/36;
      PUT IMAGE(mu,tc)(12);
      I2;
      IMAGE;
at mu=--,--,max. tc=--,-----
      PUT LIST('');
      END s3;
      GO TO s2;
TABLE: PROCEDURE (dmach,dcl,dclm);
      I5=trunc(dmach-20+2);
      IF I5>21 THEN I5=21;
      I1=I5-1;
      dcl=dclm(I1)*(20-dmach-I1+1)+(dclm(I5)-dclm(I1));
      END TABLE;
      END ;

```



BELL HELICOPTER COMPANY

APPENDIX C



BELL HELICOPTER COMPANY

INPUT COEFFICIENT PROGRAM

```

/* INPUT COEFFICIENT DETERMINATION FOR AFSA CONTRACT */
DECLARE hp1(7), hp2(7), hp11(7), hp12(7), vc(7), hpc1(7), hpc2(7);
hp11=hp1,hpc1,hpc2=0;
GET LIST(i);
GET LIST(hp1,hp2,vc);
GET LIST(r,c,b,wr,fo,k3,k5);
GET LIST(h,uat);
GET LIST(gw1,gw2);
delta=(1.0000063333-h)*5.5561;
t=uat*273.16;
theta=t/288.16;
va=65.811366*cos(theta);
sig=delta/theta;
rho=sig*.002378;
pi=3.1415926535;
a=6.28;
area=pi*r**2;
sig=ho/(pi*area);
nondf=rho*area*wr**2;
nondp=nondf*wr/550;
ctc=k6/(sig**2);
ct1=gw1/nondf;
ct2=gw2/nondf;
/* CALCULATION OF INDUCED POWER */
e1: DO i=1 TO m;
vvc(i)=1.6878;
mu=v/wr;
CALL vind;
k1=1-(mu-.14)*k3;
IF mu>.14 THEN k1=1;
hp11(i)=k1*ctc*nondf*vi/550;
END e1;
e2: DO i=1 TO m;
vvc(i)=1.6878;
mu=v/wr;
CALL vind;
k1=1-(mu-.14)*k3;
IF mu>.14 THEN k1=1;
hp12(i)=k1*ctc*nondf*vi/550;
END e2;
e3: DO i=1 TO m;
hpcl(i)=hp11(i)-hp12(i);
hpc2(i)=hpc1(i)-hp12(i);
END e3;
/* CALCULATION OF DELTA 2 */
i=1;
dhp=hpc2(i)-hpc1(i);
vvc(i)=1.6878;
mu=v/wr;
mu2=mu*mu;
k1=sig*nondp*(1+.6*mu2)*(ctc*ct1)**2/8;
k2=sig*nondp*(1+.6*mu2)*(ctc*ct2)**2/8;
del2=dhp/(k2-k1);
/* CALCULATION OF HP STALL */
i=1;
vvc(m)=1.6878;
mu=v/wr;
mu2=mu*mu;
hpd=del2*sig*nondp*(1+.6*mu2)*(ct1*ctc)**2/8;
hpcl(m)=hpcl(m)-hpd;
hpd=del2*sig*nondp*(1+.6*mu2)*(ct2*ctc)**2/8;
hpc2(m)=hpc2(m)-hpd;
tc1=2*ct1/sig;
tc2=2*ct2/sig;
tcert=.1/.2/sqrt(1+.5*mu2);
IF tc1<tcert THEN GO TO e4;
deltc=tc1-tcert;
hps=20000*deltc**1.5;
hpcl(m)=hpcl(m)-hps;
GO TO e5;
e4: hps=0;
e5: IF tc2<tcert THEN GO TO e6;
deltc=tc2-tcert;
hps=20000*deltc**1.5;
hpc2(m)=hpc2(m)-hps;
GO TO e7;
e6: hps=0;
/* CALCULATION OF micro */
e7: hp=hpc2(m)-hpcl(m);
IF hp>0 THEN GO TO e23;
micro=.1

```



BELL HELICOPTER COMPANY

```

e23: GO TO e24;
      dno=.75*(tc2-tc1);
      dplm=100000/nondp;
      dndm=hp/dm;
      k=0;
      mcro=.74;
e2i: mcro=mcro+.005;
e3:  delm1=(1+mu)*wr/vs-mcro+.75*tc1;
      delm2=(1+mu)*wr/vs-mcro+.75*tc2;
      dcp1=delm1+.0033*delm1*(.022-.11*delm1);
      dcp2=delm2+.0033*delm2*(.022-.11*delm2);
      dcp1=delm1+100000;
      dcp2=delm2+100000;
      dcpdm=(dcp2-dcp1)/(delm2-delm1);
      IF k=1 THEN GO TO e4;
      IF dndm=dcpdm THEN GO TO e1;
      GO TO e2;
e1:  dcpdm1=dcpdm;
      mcro=mcro+.005;
      k=1;
      GO TO e3;
e4:  MCRO=delm1+dcpdm*.0033*(dcpdm1-dcpdm)*mcro;
      dcp1=delm1+nondp/100000;
      hpc1(m)=hpc1(m)-dcp1;
      /* CALCULATION OF d10 */
e24: v=vc(2)*1.6878;
      mu=vr/wr;
      x3=(1+mu)*wr/vs;
      IF x3>mcro THEN GO TO e21;
      delm=x3-mcro+.75*(2*ct2/slg);
      dcp=delm+.0033*delm*(.022-.11*delm);
      dhp=dcp+nondp;
      hpc1(2)=hpc1(2)-dhp;
e21: mu2=mu*mu;
      hpd2=del2*slg+nondp*(1+.6*mu2)*(ctc*ct2)*.2/8;
e8:  hpf=.5*rho*v*v*v/550;
      hpc=hpc1(2)-hpf-hpd2;
      k1=slg*nondp*(1+.6*mu2)/8;
      del1U=hpc/k1;
      /* CALCULATION OF Y */
      v=vc(m)*1.6878;
      mu=vr/wr;
      mu2=mu*mu;
      hpd=del10*slg+nondp*(1+.6*mu2)/8;
      hpf=hpc1(m)-hpd;
      k1=.5*rho*v*v*v/550;
      f=hpf/k1;
      /* CALCULATION OF TOTAL POWER */
e22: k=0;
      ct=ct1;
e8:  DO I=1 TO m;
      v=vc(I)*1.6878;
      mu=vr/wr;
      mu2=mu*mu;
      x4=.5*rho*v*v*v*f;
      ctp=sqrt(x4/(nondp*nondp)*ct*ct);
      hpd1=del10*slg+nondp*(1+.6*mu2)/8;
      hpd2=del2*slg+nondp*(1+.6*mu2)*(ctc*ct)*.2/8;
      hpf=x4/v/550;
      tc=2*ct/slg;
      tcrt=.1+.2/sqrt(1+.5*mu2);
      IF tc<tcrt THEN GO TO e11;
      deltc=tc-tcrt;
      hps=20000*deltc*.15;
      GO TO e12;
e11: hps=0;
e12: x3=(1+mu)*wr/vs;
      IF x3>mcro THEN GO TO e14;
      dcp=0;
      GO TO e15;
e14: delm=x3-mcro+.75*tc;
      dcp=delm+.0033*delm*(.022-.11*delm);
e15: hpc=dcp+nondp;
      CALL vmd;
      k1=1-(mu+.14)*k3;
      IF mu>.14 THEN k1=1;
      hp3=k1*ctp*nondp*v1/550;
      hpt=hpd1+hpd2+hp3+hp4+hps+hpc;
      IF k=1 THEN GO TO e16;
      error=hpl(1)-hpt;
      perc=error*100/hpl(1);
      PUT IMAGE(gw1,vc(1),hpl(1),hpt,e-for,perc)(IMI);
      IMAGE;
      gw1=-----,vc=-----,hpl=-----,hpc=-----,error=-----,perc=-----,
      GO TO e17;

```




```

a16: error=hp2(1)-hpt;
      perc=error*100/hp2(1);
      PUT IMAGE(gw2,vc(1),hp2(1),hpt,error,perc/(1m2));
      IMAGE;
      gw=-----, v=-----, hpc=-----, hpc=-----, error=-----, perc=-----,
a17:   ENDU a8;
      IF k=1 THEN GO TO a20;
      k=1;
      ct=ct2;
      GO TO a8;
a20:   PUT IMAGE(delo,del2)(1m3);
      IMAGE;
      delo=-----, del2=-----,
      PUT IMAGE(mcro,f)(1m4);
      IMAGE;
      mcro=-----, f=-----,
vind:  STOP;
      PRUCEDURE;
      count=0;
      IF v=0 THEN v=.6878;
      xh=.5*rho*v*v*fo;
      x1=xh*v/(ct*pnondf);
      x2=ct*pnondf/(2*rho*area);
      IF v>42.2 THEN GO TO a17;
      v1=1.037*sqrt(x2);
      IF v=0 THEN GO TO a11;
a17:   vin=x2/v;
a9:    v1=x1*x2/(v*v+.866*vin*vin)+.5;
      IF abs(v1-vin)<.001 THEN GO TO a11;
      count=count+1;
      IF count>40 THEN GO TO a10;
      vin=.86*vin+.14*v1;
      GO TO a9;
a10:   PUT LIST('CALCULATION NON CONVERGENT INDUCED VELOCITY TO 0');
      v1=0;
      GO TO a17;
a11:   v1=v1-x1;
      IF v=1.8878 THEN v=0;
a12:   ENDU vind;

```